AFCRL-63-29 3648-2-T

SCIENTIFIC REPORT NO. 5
STUDIES IN RADAR CROSS SECTIONS XLVIII - DIFFRACTION AND SCATTERING BY REGULAR BODIES II: THE CONE

by

R. E. Kleinman and T. B. A. Senior

January 1963

Report No. 3648-2-T

on

Contract AF 19(604)-6655

Project 5635

Task 563502

Prepared for

ELECTRONICS RESEARCH DIRECTORATE
AIR FORCE CAMBRIDGE RESEARCH LABORATORIES
OFFICE OF AEROSPACE RESEARCH
UNITED STATES AIR FORCE
BEDFORD, MASSACHUSETTS

Requests for additional copies by Agencies of the Department of Defense, their contractors, and other Government agencies should be directed to:

DEFENSE DOCUMENTATION CENTER (DDC)
ARLINGTON HALL STATION
ARLINGTON 12, VIRGINIA

Department of Defense contractors must be established for DDC services or have their "need-to-know" certified by the cognizant military agency of their project or contract.

All other persons and organizations should apply to:

U. S. DEPARTMENT OF COMMERCE
OFFICE OF TECHNICAL SERVICES
WASHINGTON 25, D. C.

PREFACE

This is the forty-eighth in a series of reports growing out of the study of radar cross sections at The Radiation Laboratory of The University of Michigan. Titles of the reports already published or presently in process of publication are listed on the following pages.

When the study was first begun, the primary aim was to show that radar cross sections can be determined theoretically, the results being in good agreement with experiment. It is believed that by and large this aim has been achieved.

In continuing this study, the objective is to determine means for computing the radar cross section of objects in a variety of different environments. This has led to an extension of the investigation to include not only the standard boundary-value problems, but also such topics as the emission and propagation of electromagnetic and acoustic waves, and phenomena connected with ionized media.

Associated with the theoretical work is an experimental program which embraces (a) measurement of antennas and radar scatterers in order to verify data determined theoretically; (b) investigation of antenna behavior and cross section problems not amenable to theoretical solution; (c) problems associated with the design and development of microwave absorbers; and (d) low and high density ionization phenomena.

R. E. Hiatt

STUDIES IN RADAR CROSS SECTIONS

I Scattering by a Prolate Spheroid. F. V. Schultz (UMM-42, Mar. 50). W33(038)-ac-14222. UNCLASSIFIED. 65 pgs.

II The Zeros of the Associated Legendre Functions $P_n^m(\mu')$ of Non-Integral Degree. K. M. Siegel, D. M. Brown, H. E. Hunter, H. A. Alperin and C. W. Quillen (UMM-82, Apr. 51). W33(038)-ac-14222. UNCLASSIFIED. 20 pgs.

III Scattering by a Cone. K. M. Siegel and H. A. Alperin (UMM-87, Jan. 52). AF30(602)9. UNCLASSIFIED. 56 pgs.

IV Comparison Between Theory and Experiment of the Cross Section of a Cone. K. M. Siegel, H. A. Alperin, J. W. Crispin, Jr., H. E. Hunter, R. E. Kleinman, W. C. Orthwein and C. E. Schensted. (UMM-92, Feb. 53). AF30(602)9. UNCLASSIFIED. 70 pgs.

V An Examination of Bistatic Early Warning Radars. K. M. Siegel (UMM-98, Aug. 52). W33(038)-ac-14222. SECRET. 25 pgs.

VI Cross Sections of Corner Reflectors and Other Multiple Scatterers at Microwave Frequencies. R. R. Bonkowski, C. R. Lubitz and C. E. Schensted (UMM-106, Oct. 53). AF30(602)9. UNCLASSIFIED 63 pgs.

VII Summary of Radar Cross Section Studies Under Project Wizard. K. M. Siegel, J. W. Crispin, Jr., and R. E. Kleinman (UMM-108, Nov. 52). W33(038)-ac-14222. SECRET. 75 pgs.

VIII Theoretical Cross Section as a Function of Separation Angle Between Transmitter and Receiver at Small Wavelengths. K. M. Siegel, H. A. Alperin, R. R. Bonkowski, J. W. Crispin, Jr., A. L. Maffett, C. E. Schensted and I. V. Schensted (UMM-115, Oct. 53). W33(038)-ac-14222. UNCLASSIFIED. 84 pgs.

IX Electromagnetic Scattering by an Oblate Spheroid. L. M. Rauch (UMM-116, Oct. 53). AF30(602)9. UNCLASSIFIED. 38 pgs.

X Scattering of Electromagnetic Waves by Spheres. H. Weil, M. L. Barasch and T. A. Kaplan (2255-20-T, July 56). AF30(602)1070. UNCLASSIFIED. 104 pgs.

XI The Numerical Determination of the Radar Cross Section of a Prolate Spheroid. K. M. Siegel, B. H. Gere, I. Marx and F. B. Sleator (UMM-126, Dec. 53). AF30(602)9. UNCLASSIFIED. 75 pgs.

XII Summary of Radar Cross Section Studies Under Project MIRO. K. M. Siegel, M. E. Anderson, R. R. Bonkowski and W. C. Orthwein (UMM-127, Dec. 53). AF30(602)9. UNCLASSIFIED. 90 pgs.

XIII Description of a Dynamic Measurement Program. K. M. Siegel and J. M. Wolf (UMM-128, May 54). W33(038)-ac-14222. CONFIDENTIAL 152 pgs.

XIV Radar Cross Section of a Ballistic Missile - I. K. M. Siegel, M. L. Barasch, J. W. Crispin, Jr., W. C. Orthwein, I. V. Schensted and H. Weil (UMM-134, Sept. 54). W33(038)-ac-14222. SECRET. 270 pgs.

XV Radar Cross Sections of B-47 and B-52 Aircraft. C. E. Schensted, J. W. Crispin, Jr., and K. M. Siegel (2260-1-T, Aug. 54). AF33(616)2531. CONFIDENTIAL. 155 pgs.

XVI Microwave Reflection Characteristics of Buildings. H. Weil, R. R. Bonkowski, T. A. Kaplan and M. Leichter (2255-12-T, May 55). AF30(602)1070. SECRET. 148 pgs.

XVII Complete Scattering Matrices and Circular Polarization Cross Sections for the B-47 Aircraft at S-Band. A. L. Maffett, M. L. Barasch, W. E. Burdick, R. F. Goodrich, W. C. Orthwein, C. E. Schensted and K. M. Siegel (2260-6-T, Jun 55). AF33(616)2531. CONFIDENTIAL 157 pgs.

XVIII Airborne Passive Measures and Countermeasures. K. M. Siegel, M. L. Barasch, J. W. Crispin, Jr., R. F. Goodrich, A. H. Halpin, A. L. Maffett, W. C. Orthwein, C. E. Schensted and C. J. Titus (2260-29-F, Jan. 56). AF33(616)2531. SECRET. 177 pgs.

XIX Radar Cross Section of a Ballistic Missile - II. K. M. Siegel, M. L. Barasch, H. Brysk, J. W. Crispin, Jr., T. B. Curtz and T. A. Kaplan (2428-3-T, Jan. 56). AF04(645)33. SECRET. 189 pgs.

XX Radar Cross Sections of Aircraft and Missiles. K. M. Siegel, W. E. Burdick, J. W. Crispin, Jr., and S. Chapman (ONR-ACR-10, Mar. 56). SECRET. 151 pgs.

XXI Radar Cross Section of A Ballistic Missile - III. K. M. Siegel, H. Brysk, J. W. Crispin, Jr., and R. E. Kleinman (2428-19-T, Oct. 56). AF04(645)33. SECRET. 125 pgs.

XXII Elementary Slot Radiators. R. F. Goodrich, A. L. Maffett, N. E. Reitlinger, C. E. Schensted and K. M. Siegel (2472-13-T, Nov. 56). AF33(038)28634, HA C-PO L-265165-F31. UNCLASSIFIED. 100pgs.

XXIII A Variational Solution to the Problem of Scalar Scattering by a Prolate Spheroid. F. B. Sleator (2591-1-T, Mar. 57). AF19(604)1949. UNCLASSIFIED. 67 pgs.

XXIV Radar Cross Section of a Ballistic Missile - IV. M. L. Barasch, H. Brysk, J. W. Crispin, Jr., B. A. Harrison, T. B. A. Senior, K. M. Siegel, H. Weil and V. H. Weston (2778-1-F, Apr. 59). AF30(602)1853. SECRET. 362 pgs.

XXV Diffraction by an Imperfectly Conducting Wedge. T. B. A. Senior (2591-2-T, Oct. 57). AF19(604)1949. UNCLASSIFIED. 71 pgs.

XXVI Fock Theory. R. F. Goodrich (2591-3-T, Jul. 58). AF19(604)1949. UNCLASSIFIED. 73 pgs.

XXVII Calculated Far Field Patterns from Slot Arrays on Conical Shapes. R. E. Doll, R. F. Goodrich, R. E. Kleinman, A. L. Maffett, C. E. Schensted and K. M. Siegel (2713-1-F, Feb. 58). AF33(038)28634, AF33(600)36192. UNCLASSIFIED. 115 pgs.

XXVIII The Physics of Radio Communication Via the Moon. M. L. Barasch, H. Brysk, B. A. Harrison, T. B. A. Senior, K. M. Siegel and H. Weil (2673-1-F, Mar. 58). AF30(602)1725. UNCLASSIFIED. 86 pgs.

XXIX The Determination of Spin, Tumbling Rates and Sizes of Satellites and Missiles. M. L. Barasch, W. E. Burdick, J. W. Crispin, Jr., B. A. Harrison, R. E. Kleinman, R. J. Leite, D. M. Raybin, T. B. A Senior, K. M. Siegel and H. Weil (2758-1-T, Apr. 59). SECRET 180 pgs.

XXX The Theory of Scalar Diffraction with Application to the Prolate Spheroid. R. K. Ritt (Appendix by N. D. Kazarinoff) (2591-4-T, Aug. 58). AF19(604)1949. UNCLASSIFIED. 66 pgs.

XXXI Diffraction by an Imperfectly Conducting Half-Plane at Oblique Incidence. T. B. A. Senior (2778-2-T, Feb. 59). AF30(602)1853. UNCLASSIFIED. 35 pgs.

XXXII On the Theory of the Diffraction of a Plane Wave by a Large Perfectly Conducting Circular Cylinder. P. C. Clemmow (2778-3-T, Feb. 59). AF30(602)1853. UNCLASSIFIED. 29 pgs.

XXXIII Exact Near-Field and Far-Field Solution for the Back Scattering of a Pulse from a Perfectly Conducting Sphere. V. H. Weston (2778-4-T, Apr. 59). AF30(602)1853. UNCLASSIFIED 61 pgs.

XXXIV An Infinite Legendre Integral Transform and Its Inverse. P. C. Clemmow (2778-5-T, Mar. 59). AF30(602)1853. UNCLASSIFIED 35 pgs.

XXXV On the Scalar Theory of the Diffraction of a Plane Wave by a Large Sphere. P. C. Clemmow (2778-6-T, Apr. 59). AF30(602)1853. UNCLASSIFIED. 39 pgs.

XXXVI Diffraction of a Plane Wave by an Almost Circular Cylinder. P. C. Clemmow and V. H. Weston (2871-3-T, Sept. 59). AF 19(604)4993. UNCLASSIFIED. 47 pgs.

XXXVII Enhancement of the Radar Cross Sections of Warheads and Satellites by the Plasma Sheath. C. L. Dolph and H. Weil (2778-2-F, Dec. 59). AF30(602)1853. SECRET (UNCLASSIFIED with Foreword removed). 42 pgs.

XXXVIII Nonlinear Modeling of Maxwell's Equations. J. E. Belyea, R. D. Low and K. M. Siegel (2871-4-T, Dec. 59). AF19(604)4993. UNCLASSIFIED. 39 pgs.

XXXIX Radar Cross Section of the B-70 Aircraft. R. E. Hiatt and T. B. A. Senior (3477-1-F, Feb. 60). NAA PO LOXO-XZ-250631. SECRET 157 pgs.

XL Surface Roughness and Impedance Boundary Conditions. R. E. Hiatt, T. B. A. Senior and V. H. Weston (2500-2-T, July 60). UNCLASSIFIED. 96 pgs.

XLI Pressure Pulse Received Due to an Explosion in the Atmosphere at an Arbitrary Altitude - Part I. V. H. Weston (2886-1-T, Aug. 60). AF19(602)5470. UNCLASSIFIED. 52 pgs.

XLII Microwave Bremsstrahlung From a Cool Plasma. M. L. Barasch (2764-3-T, Aug. 60). DA 36 039 SC-75041. UNCLASSIFIED. 39 pgs.

XLIII Plasma Sheath Surrounding a Conducting Spherical Satellite and the Effect on Radar Cross Section. K-M Chen (2764-6-T, Oct. 60). DA 36 039 SC-75041. UNCLASSIFIED. 38 pgs.

XLIV Integral Representations of Solutions of the Helmholtz Equation with Application to Diffraction by a Strip. R. E. Kleinman and R. Timman (3648-3-T, Feb. 61). AF19(604)6655. UNCLASSIFIED. 128 pgs.

XLV Studies in Nonlinear Modeling - II: Final Report. J. E. Belyea, J. W. Crispin, Jr., R. D. Low, D. M. Raybin, R. K. Ritt, O. Ruehr and F. B. Sleator (2871-6-F, Dec. 60). AF19(604)4993. UNCLASSIFIED 95 pgs.

XLVI The Convergence of Low Frequency Expansions in Scalar Scattering by Spheroids. T. B. A. Senior (3648-4-T, Aug. 61). AF19(604)6655 UNCLASSIFIED. 143 pgs.

XLVII Diffraction and Scattering by Regular Bodies - I: The Sphere. R. F. Goodrich, B. A. Harrison, R. E. Kleinman and T. B. A. Senior (3648-1-T, Dec. 61) AF19(604)6655. UNCLASSIFIED. 135 pgs.

XLVIII Diffraction and Scattering by Regular Bodies - II: The Cone. R. E. Kleinman and T. B. A. Senior (3648-2-T, Jan. 63) AF19(604)6655 UNCLASSIFIED. 143 pgs.

TABLE OF CONTENTS

I
INTRODUCTION

1.1 Preliminary Remarks

This is the second in a series of reports aimed at summarizing the available information about the electromagnetic scattering properties of selected bodies of simple shape. The first body considered was the sphere (Goodrich et al, 1961), which from the bibliographer's standpoint must certainly be the most popular of all scattering shapes. The present work is devoted to the cone which, while less abundantly represented in the literature, still presented a serious selection problem. In the case of the sphere it was immediately obvious that a large amount of related reference material would have to be omitted or discussed only briefly if a document of manageable size were to result. With the cone, the temptation to deal with the subject exhaustively is stronger, but still it was felt that such an attempt would jeopardize the objectives of the program which are to present in readily usable form available theoretical and experimental results in sufficient detail to satisfy most engineering needs and provide a useful guide to those who wish to delve more deeply into the subject. Hence a certain amount of arbitrariness was exercised not only in deciding what material was to be excluded but also in the relative emphasis given those topics which survived this editorial surgery.

The present work is mainly concerned with the scattering of time harmonic electromagnetic waves by a perfectly conducting cone, either finite or infinite in

extent, embedded in a homogeneous, isotropic medium. The corresponding scalar problem involving scattering of acoustic waves by "hard" and "soft" cones is also considered. The arbitrary but prevalent division into scattering and radiation problems, depending on whether the source of energy is off or on the cone surface, is observed. Thus in restricting attention to scattering problems, a large amount of work (e.g. Felsen, 1957c; Bailin and Silver, 1956; Goodrich et al, 1959) on the radiation from various slot configurations or dipole distributions on conical surfaces is omitted.

The choice of the cone as the second shape to be treated in this series was dictated by two reasons. In the first place the infinite cone is one of the few shapes for which an exact theoretical treatment is possible. Since the approximations which are introduced in order to make tractable the scattering problem for more complicated bodies either arise from or are tested in those few cases where exact solutions exist, familiarity with these cases seems essential for an understanding of the modern methods of handling scattering problems. The second reason for choosing the cone lies in the fact that the finite cone is a possible re-entry vehicle configuration, so that its scattering properties are of more than casual interest.

Unlike the sphere for which exact as well as approximate theoretical results can be compared with experiment, the infinite cone, for which an exact theory is also available, is clearly an untenable experimental shape; on the other hand, the finite cone, for which a considerable amount of experimental data is available, has

thus far resisted exact treatment. At one time it was felt that results for the infinite cone would be useful in predicting the finite cone behavior. While this is still true in a sense (tip scattering), it is now realised that the most vital scattering characteristic of the finite cone is its termination, which makes it fundamentally different from the infinite cone. Nevertheless, in keeping with the historical development of the problem, both finite and infinite cones will be treated here.

1.2 Historical Survey

Since the circular cone is a level surface ($\theta = \theta_o$) in spherical coordinates it was a natural step from the development of spherical harmonics of nonintegral order

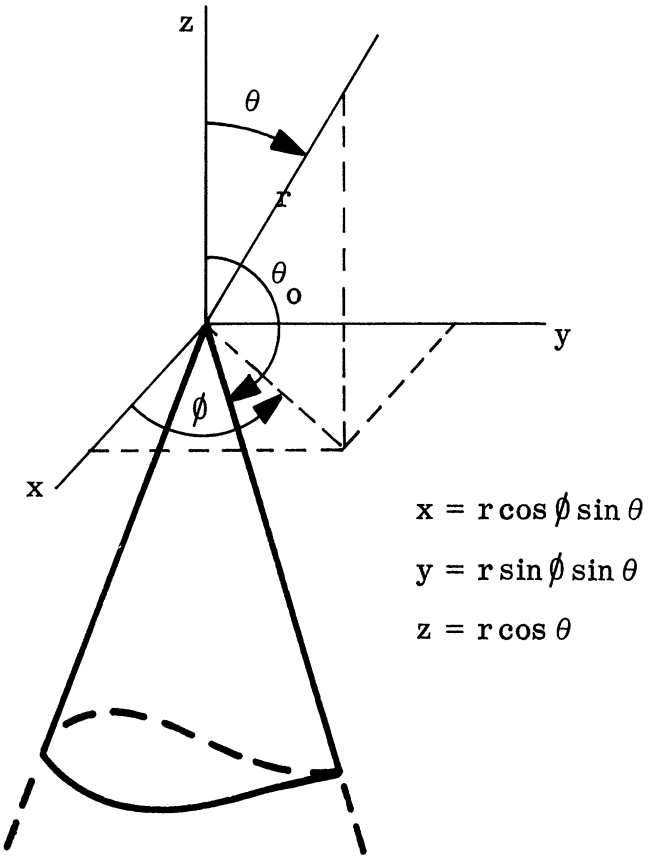

FIGURE 1

in the latter part of the nineteenth century to the investigation of potential problems for the cone. Although Green claimed to have found the potential near the vertex of a conducting cone in an electrostatic field as long ago as 1828 (Green, 1828; Macdonald, 1900a) this work was never published in detail and it was not until much later that the problem was adequately treated in the literature (Mehler, 1870; Heine, 1878; Hobson, 1889; Macdonald, 1900a). Work on the dynamic problem began more recently. Macdonald, in his aptly designated prize essay (Macdonald, 1902), discussed the problem of a perfectly conducting cone excited by what is now known as an axial (or vertical) electric dipole (dipole moment oriented along the axis of symmetry). With remarkable insight, Macdonald formulated and solved the problem as a series of spherical harmonics whose coefficients he determined from the known solution of the potential problem. Since he never worked directly with the Helmholtz equation but with a related partial differential equation which he derived from Maxwell's equations he apparently was unaware of (or at least unconcerned with) the fact that his work also held the solution of the scalar Dirichlet problem: a soft cone with an acoustic point source on the axis of symmetry. The fact that electromagnetic scattering problems for cones and spheres with axial dipole sources can be formulated in terms of Dirichlet and Neumann scalar scattering problems follows from the representation of an electromagnetic field in terms of radial Hertz vectors which are closely related to Debye potentials. This work, for the most part more recent than Macdonald's, is discussed in more detail in the next section where one of the resulting scalar problems is treated.

The solution of the scalar Dirichlet problem was presented by Carslaw (1910) in essentially the same form as Macdonald's although the applicability of Macdonald's result was apparently unknown to him. A few years later Carslaw (1914) published the solution of the scalar Neumann problem for the infinite cone. In this later paper Carslaw indicates awareness of Macdonald's work, calling attention to some weak points in the derivation (though the result is correct). The objection concerned Macdonald's argument that the coefficients in the series solution of the wave equation were the same as those for the corresponding potential problem, i.e. were independent of k. Subsequently Macdonald (1915) demonstrated the validity of his argument and this was acknowledged by Carslaw (1916). Nevertheless Carslaw's treatment is more elegant, if not more rigorous, and has since served as the classic work on the problem to the extent that Macdonald's work is apparently overlooked by modern writers on the subject.

Following Carslaw's thorough treatment of the scalar problem, it was not until the resurgence of interest in classical scattering problems occasioned by the development of radar that the cone received further study. In a series of reports, Hansen and Schiff (1948) discussed a number of scattering problems including that of finding the field scattered by a perfectly conducting cone when a plane electromagnetic wave is incident along the axis of symmetry. This is fundamentally a vector problem since the vector plane wave has no simple representation in terms of meaningful scalar sources. They constructed their solution in the form of infinite series

of Legendre functions of non-integral order using Hansen's vector wave functions (Stratton, 1941; Mentzer, 1955).

Evaluating the coefficients, however, involved a rather questionable use of asymptotic forms which makes the procedure subject to criticism even though the correct results are found. An additional difficulty is present when the source is at infinity (plane wave incidence), rather than at some finite distance from the vertex, since the far field expressions are divergent sums. This is also true in the scalar case for plane wave incidence (Siegel and Alperin, 1952). Special summation techniques were introduced by Schensted (1953) to obtain meaningful results for the back-scattering cross section in both vector and scalar cases for large and small cone angles. (See also Siegel et al 1953a, 1955b). These cases were treated independently by Felsen (1953, 1955, 1957a, b). He found the Green's functions for scalar and vector problems and based his calculations of back scattering cross section for small and large cone angles on these more general results. The calculations agreed with the results of Schensted (1953) and Siegel et al (1953a, 1955b) but by working with integral representations of the radial functions which occur, Felsen avoided the necessity of handling divergent sums. However, when the quantities of interest are the field components rather than the cross section, both series and integral expressions have drawbacks. In particular, any attempt to calculate the currents on the cone's surface meets with additional convergence problems in the series expression and a considerable complication of the integral expression.

A slightly different method of constructing the vector Green's function, using the Lorentz reciprocity theorem, was given by Bailin and Silver (1956), but calculations were carried out only for the radiation problem when the source is on the cone surface.

The above results are given explicitly in Section 3. Although approximations may be employed in evaluating the expressions for the field or the cross section, the formulae are exact in the sense that they are obtained from the unique solution of a well-set mathematical problem, and any particular calculation can be performed as accurately as time, money and patience will permit. This is borne out in the recent work of Goryanov (1961) who reports on extensive calculations of the scattered far field when a plane electromagnetic wave is incident along the axis of symmetry of the cone.

The preceding paragraphs just about complete the survey of existing exact treatments of scattering by a semi-infinite circular cone. A more general problem, scattering by an elliptic cone (of which the circular cone is a special case), has been solved by Kraus and Levine (1961). Although of special interest in the limiting case where the cone is a plane angular sector, their results are not particularly appropriate for the circular cone due to the extreme complexity of the series of products of Lamé functions in terms of which their solution is expressed.

Exact treatments of the finite cone problem are few indeed. Although there are uncountably many ways in which the cone can be terminated, what little exact

work that does exist deals almost exclusively with the spherically capped right circular cone[+]. This configuration is the intersection of two coordinate surfaces of the same spherical coordinate system (r = a and $\theta = \theta_o$ in Fig. 2). Since the wave equation is separable and solutions exist for each of the surfaces individually, it is possible to divide space into two distinct regions (see Fig. 2) in which different series

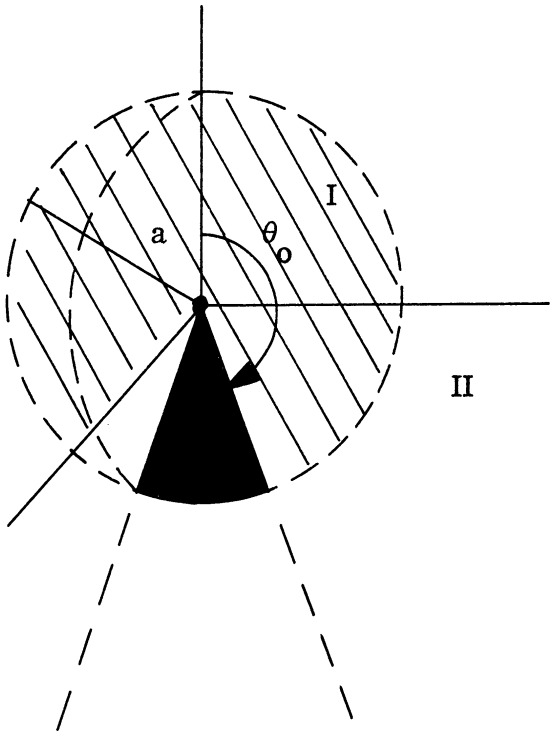

FIGURE 2

representations of the field are employed depending on the conditions at the boundaries of the regions. Thus in I the series is chosen to satisfy a condition on the

[+]Referred to in some circles as the "spherical sector".

cone whereas in II the representation must satisfy a condition on the relevant portion of the surface of the sphere. On that part of the boundary of the two regions which has no physical significance, the two representations must be equivalent. This manifests itself as a condition sufficient to determine an infinite set of constants, but the explicit determination usually requires the solution of an infinite system of linear equations. This procedure was followed by Northover (1962) who considered the problem of the scattering of electromagnetic energy when an electric dipole is oriented along the axis of symmetry of a perfectly conducting spherically-capped cone. A similar procedure was adopted by Rogers et al (1962) in considering the problem of a plane electromagnetic wave incident along the axis of symmetry. Since the plane wave is the limit of a transverse dipole, this problem is essentially different from the one treated by Northover. The big drawback in both cases is the necessity of dealing with infinite systems of equations. A possibly fruitful way to handle this problem was proposed by Plonus (1961, 1962) in his treatment of the closely related problem of calculating the radiation pattern of a biconical antenna.

A technique for finding the exact solution of the scalar wave equation satisfying Dirichlet boundary conditions on the intersection of two surfaces in terms of the solutions of the corresponding Dirichlet and Neumann potential problems for each surface has been developed by Darling (1960) and applied to the spherically-capped cone. The method is restricted to low frequencies since the solution is expressed in terms of an infinite series which converges only for frequencies in a bounded

range ($0 < k < k_0$). Within the radius of convergence, however, the series represents the exact solution.

Unfortunately, these exact treatments of the finite cone problem do not constitute a sufficient base from which significant quantitative results can be obtained. Since the finite cone, with various base terminations, is an object whose scattering properties are of practical importance, approximation methods have been developed and experiments performed in order to obtain the desired numerical results.

Experiments are limited in that they yield results at particular frequencies for particular models. The sensitivity of the field to small changes in frequency or model size is difficult to determine since it is impractical (to say the least) to try to provide a continuum of models or operating frequencies.

Theoretical approximations are also limited, though most often to a range of frequencies rather than a particular frequency. The frequency spectrum is divided roughly into three regions. The low frequency end of the spectrum (wavelength large with respect to any linear dimension of the scatterer) is usually referred to as the Rayleigh region. Clearly this has meaning only for finite bodies, for present purposes, finite cones. Following the work of Rayleigh (1897) the far zone scattered field is found to be proportional (to a first approximation) to the volume of the scatterer regardless of its detailed geometric configuration. Some refinements of this theory as well as explicit results for the scattering cross section of a finite cone have been given by Siegel (1959) and further extended by Siegel (1962, 1963).

The high frequency end of the spectrum (wavelength short with respect to the linear dimensions and radii of curvature of the scatterer) is generally referred to as the optics region since it is in this limit that the laws of geometric optics are applicable (see, for example, Born and Wolf, 1959). For many purposes, geometric optics is too gross an approximation and refinements are sought. One such is the physical optics approximation, which can be obtained from the integral representation of the field everywhere in space in terms of the field on the scatterer by using the geometric optics approximation of the field on the surface of the scatterer. This was applied to the cone by Spencer (1951) who attributes some of the work to P. M. Austin. Hansen and Schiff (1948) cite an earlier version of Spencer's work which also credits Crout, who worked with Austin at the M.I.T. Radiation Laboratory. A general discussion of geometric and physical optics as applied to the computation of back scattering (monostatic) radar cross sections is given by Kerr (1951). The physical optics result for back scattering from a semi-infinite cone viewed nose-on is given by Siegel and Alperin (1952). Although the applicability of physical optics when the scattering object has infinite length is subject to considerable question, the result was shown to be remarkably good when compared both with more exact theoretical results (Siegel et al, 1955b; Felsen, 1955) and experimental data (Sletten, 1952). More general results are given by Siegel et al (1955a) where bistatic physical optics cross sections are given for both finite and infinite cones when the transmitter is on the axis.

In the case of finite cones, the physical optics approximation is least reliable in determining the effect of the base, and since this is usually the dominant factor in determining what the field will be, the need for an improvement over physical optics is clear. This is provided for the flat-backed finite cone by the geometrical theory of diffraction (or modified geometric optics) of Keller (1957, 1958, 1960) which takes into account not only reflected rays but diffracted rays as well. Expressions for the back scattered field and cross section as a function of angle of incidence (plane wave excitation) are given by Keller (1960) for both Dirichlet and Neumann boundary conditions on the cone in the scalar case, and for the perfectly conducting cone in the electromagnetic case. This last result, in the case of nose-on incidence, was obtained independently by Siegel (1959) and Siegel et al (1959).

Keller also gives results for a cone with a smoothly joined spherical base (the "cone-sphere"), but these are not substantiated by experiment. In large measure the disagreement is attributable to Keller's omission of any contribution from the junction of the cone and sphere, where the radius of curvature is discontinuous. It is now believed that physical optics gives a reasonable estimate of the direct return from this region, but it is also true that no canonical problem which really bears on this question has yet been solved.

Between the Rayleigh and optics regions lies the resonance region, where the wavelength is comparable to some linear dimension of the scatterer. It is this region that offers the most difficulty to approximation methods. One approach to the

problem of finding approximations which are useful here is to refine the small and large wavelength approximations and effectively narrow the width of the resonance region. More terms can be calculated in both the quasi-static series (cf Senior and Darling, 1963) and the modified optics results of Keller (1960) but when, if ever, the regions of validity overlap is not known. Another attempt to bridge the resonance region gap based on physical reasoning is described by Siegel (1959) and Crispin et al (1963) in the case of nose-on back scattering from flat-backed finite cones.

Though subject to the limitations previously mentioned, the importance of experimental results should not be overlooked. Thus the work of Sletten (1952), Olte and Silver (1959), Keys and Primich (1959a, c, d) and Blore and Royer (1962) has served not only to increase knowledge of scattering by particular cones but has also played a valuable role in the development of approximate theoretical techniques.

It should be pointed out that some of the work referred to contains errors, some typographical and some more serious. Attention is called to these errors in the sections that follow and formulae presented explicitly have been corrected (wherever possible) and converted to the uniform notation used throughout this report.

In concluding this section the authors wish to extend appreciation to the many members of the Radiation Laboratory who assisted in the preparation of this report and especially to J. W. Crispin, Jr., formerly of the Radiation Laboratory, who prepared an earlier version.

II
EXACT SOLUTIONS

This section is devoted to the exact formulation and solution of the problems of scattering of electromagnetic energy by a cone. The relation between vector and scalar boundary value problems is examined.

In some cases, a single scalar function can be used to solve two meaningful physical problems, one scalar and one vector. One such case is treated in detail.

2.1 Precise Formulation

The problem with which this report is concerned is that of finding the electric and magnetic field vectors[+] $\underline{E}$ and $\underline{H}$ (and quantities derived from them) external to a perfectly conducting cone in the presence of various incident or primary fields. The cone is assumed embedded in a homogeneous, isotropic and perfectly dielectric medium of permeability μ and permittivity ϵ, which medium may be taken as free space. The propagation constant, k, is simply related to μ and ϵ as follows:

$$k = \omega \sqrt{\mu\epsilon} = \frac{2\pi}{\lambda} \tag{2.1}$$

where λ is the wavelength and ω the frequency. The harmonic time factor $e^{-i\omega t}$ is suppressed and MKS units are employed throughout. At all ordinary points in space the behavior of the field quantities is governed by Maxwell's equations

[+]The following vector notation is used throughout: vectors of arbitrary magnitude will be underlined, e.g. $\underline{E}$; unit vectors will be denoted by carets, e.g. $\hat{r}$; scalar products indicated by dots, e.g. $\hat{r} \cdot \underline{E}$; and vector products by wedges, e.g. $\nabla \wedge \underline{E}$.

$$\nabla \wedge \underline{E} - i\omega\mu\underline{H} = 0 , \tag{2.2}$$

$$\nabla \wedge \underline{H} + i\omega\epsilon\underline{E} = 0 , \tag{2.3}$$

$$\nabla \cdot \underline{E} = \nabla \cdot \underline{H} = 0 . \tag{2.4}$$

The homogeneous equations (2.2), (2.3) and (2.4) do not describe the field at source points. The sources treated here will be either dipoles or plane waves, both of which are defined below. The presence of the perfectly conducting cone is taken into account by requiring that on the cone the tangential component of $\underline{E}$ must vanish. With the addition of a radiation condition, which is necessary to ensure uniqueness, it is possible to formulate a well-set boundary value problem directly in terms of the electric field. It is customary, however, to introduce auxiliary functions from which the field quantities may be derived, and to formulate the problem in terms of these new functions. A very natural way of introducing both the Hertz vectors and Debye potentials stems from the derivation of the field quantities $\underline{E}$ and $\underline{H}$ in terms of a vector potential $\underline{A}$ (see Stratton, 1941). If $\underline{A}$ and f are vector and scalar functions of position such that

$$(\nabla^2 + k^2)\underline{A} = \nabla f \tag{2.5}$$

then $\underline{E}$ and $\underline{H}$ can be defined in terms of $\underline{A}$ by

$$\underline{H} = -i\omega\epsilon \nabla \wedge \underline{A} , \tag{2.6}$$

$$\underline{E} = -\frac{1}{i\omega\epsilon} \nabla \wedge H = \nabla \wedge \nabla \wedge \underline{A} . \tag{2.7}$$

It is simple to show that $\underline{E}$ and $\underline{H}$ so defined satisfy Maxwell's equations. The divergence condition (2.4) is satisfied because the divergence of a curl is identically zero. Equation (2.3) is clearly satisfied since it is taken as the defining equation for $\underline{E}$, (2.7). The remaining equation, (2.2), states, after substitution of (2.1), (2.6) and (2.7) that

$$\nabla_\wedge \nabla_\wedge \nabla_\wedge \underline{A} - k^2 \nabla_\wedge \underline{A} = 0 \ . \tag{2.8}$$

This can be rewritten, making use of well known vector identities, as

$$\nabla_\wedge (\nabla^2 + k^2) \underline{A} = 0 \tag{2.9}$$

which is satisfied by virtue of equation (2.5).

Any electromagnetic field can be so derived; that is, there exists a vector potential (in fact an equivalence class of potentials) for any field. In particular, there is a vector potential from which the field exterior to a conducting cone can be obtained. However, rather than investigate the restrictions imposed on this potential function by regularity, single valuedness, and other physically-based conditions on the field quantities, it is more customary to restrict the form of the potential and phrase the problem in terms of this smaller class of potentials. Of special interest is the construction of vector potentials from scalar potentials. In this regard if ψ is a scalar solution of the wave equation

$$(\nabla^2 + k^2) \psi = 0 \tag{2.10}$$

and the vector potential $\underline{A}$ is restricted to be of the form

$$\underline{A} = \psi \underline{\sigma} \tag{2.11}$$

where $\underline{\sigma}$ is a vector independent of ψ (but may be a function of position), then as shown by Senior (1960), $\underline{\sigma}$ must either be a constant or radial vector. (This seemingly preferred status enjoyed by rectangular and spherical coordinate systems results from the restrictions placed on $\underline{A}$ and does not pose any relativistic dilemmas.)

With the potential constructed in this way, the class of electromagnetic fields that can be obtained is limited, but by introducing a second, independent, vector potential subject to the same restrictions as the first it is possible to derive any electromagnetic field from these two potentials as follows:

$$\begin{aligned} \underline{E} &= \nabla \wedge \nabla \wedge \underline{A}_1 + i\omega\mu \nabla \wedge \underline{A}_2 \\ \underline{H} &= \nabla \wedge \nabla \wedge \underline{A}_2 - i\omega\epsilon \nabla \wedge \underline{A}_1 \end{aligned} \tag{2.12}$$

where either

$$\text{a)} \quad \underset{2}{\underline{A}_1} = \underset{2}{\underline{\mathcal{I}_1}} \underline{c}$$

or

$$\text{b)} \quad \underset{2}{\underline{A}_1} = \underset{2}{\psi_1} \underline{r} \, .$$

In case a) $\underline{c}$ is a constant vector (and may be taken to be of unit magnitude by redefining $\underset{2}{\underline{\mathcal{I}_1}}$), $\mathcal{I}_1$ and $\mathcal{I}_2$ are scalar wave functions, i.e. satisfying (2.10), and the

$\underline{A}_1$ and $\underline{A}_2$ so determined are electric and magnetic Hertz vectors, usually denoted by $\underline{\Pi}_e$ and $\underline{\Pi}_m$ respectively. If a rectangular cartesian coordinate system is oriented so that $\underline{c}$ lies along the z axis, i.e. $\underline{c} = \hat{i}_z$, then the rectangular field components defined by (2.12) are

$$E_x = \frac{\partial^2 \underline{\phi}_1}{\partial x \partial z} + i\omega\mu \frac{\partial \underline{\phi}_2}{\partial y} \qquad H_x = \frac{\partial^2 \underline{\phi}_2}{\partial x \partial z} - i\omega\epsilon \frac{\partial \underline{\phi}_1}{\partial y}$$

$$E_y = \frac{\partial^2 \underline{\phi}_1}{\partial y \partial z} - i\omega\mu \frac{\partial \underline{\phi}_2}{\partial x} \qquad H_y = \frac{\partial^2 \underline{\phi}_2}{\partial y \partial z} + i\omega\epsilon \frac{\partial \underline{\phi}_1}{\partial x}$$

$$E_z = \frac{\partial^2 \underline{\phi}_1}{\partial z^2} + k^2 \underline{\phi}_1 \qquad H_z = \frac{\partial^2 \underline{\phi}_2}{\partial z^2} + k^2 \underline{\phi}_2 \qquad (2.13)$$

In case b), $\underline{r}$ is the radius vector $\underline{r} = x\hat{i}_x + y\hat{i}_y + z\hat{i}_z$, and ψ_1 and ψ_2 are again scalar wave functions. The functions ψ_1 and ψ_2 are called Debye potentials and the $\underline{A}_1$ and $\underline{A}_2$ so defined are often referred to as radial Hertz vectors. The spherical polar field components defined in (2.12) are

$$E_r = \frac{\partial^2}{\partial r^2}(r\psi_1) + k^2 r\psi_1 \qquad H_r = \frac{\partial^2}{\partial r^2}(r\psi_2) + k^2 r\psi_2$$

$$E_\theta = \frac{1}{r}\frac{\partial^2 (r\psi_1)}{\partial r \partial \theta} + \frac{i\omega\mu}{\sin\theta}\frac{\partial \psi_2}{\partial \phi} \qquad H_\theta = \frac{1}{r}\frac{\partial^2 (r\psi_2)}{\partial r \partial \theta} - \frac{i\omega\epsilon}{\sin\theta}\frac{\partial \psi_1}{\partial \phi}$$

$$E_\phi = \frac{1}{r\sin\theta}\frac{\partial^2 (r\psi_1)}{\partial r \partial \phi} - i\omega\mu \frac{\partial \psi_2}{\partial \theta} \qquad H_\phi = \frac{1}{r\sin\theta}\frac{\partial^2 (r\psi_2)}{\partial r \partial \phi} + i\omega\epsilon \frac{\partial \psi_1}{\partial \theta} \qquad (2.14)$$

Note that if $\psi_1 \equiv 0$ then $E_r \equiv 0$, i.e. the electric field is transverse to any radius vector (TE case), whereas if $\psi_2 \equiv 0$ then $H_r \equiv 0$, i.e. the magnetic field is transverse (TM case).

Actually the statement that any electromagnetic field can be written in terms of two scalar functions using (2.12) with a) or b) is a bit too strong. Wilcox (1957) proves the validity of the Debye potential representation of any field defined everywhere in a region between two concentric spheres. Bouwkamp and Casimir (1954) establish a similar result for regions exterior to a sphere containing all currents and demonstrate the equivalence of the Hertz vector and Debye potential representations as well (cf Sommerfeld, 1935). Nisbet (1955) shows that ordinary points within the sphere containing sources admit of a representation by two scalar functions but not necessarily Debye potentials.

In cases which are not included in these rigorous treatments, it is usually assumed that such a representation is valid and the justification is found in the reasonableness of the consequences. Thus, in the case of the field scattered by an infinite cone (a body which cannot be enclosed in a sphere however large) Debye potentials still play an important role.

In formulating the boundary value problem in terms of scalar wave functions, it is clear from (2.14) that requiring either

$$\psi_1 \equiv 0, \quad \text{and} \quad \left.\frac{\partial \psi_2}{\partial \theta}\right|_{\theta = \theta_o} = 0$$

or

$$\psi_2 \equiv 0\,, \qquad \text{and} \qquad \psi_1\Big|_{\theta=\theta_o} = 0$$

is sufficient to ensure that the boundary conditions $E_r = E_\phi = 0$ at $\theta = \theta_o$ are satisfied. Wilcox (1957) proves that a condition sufficient to guarantee that $\underline{E}$ and $\underline{H}$ satisfy the Silver-Müller radiation condition, viz.

$$O \circ \underline{E} = O \circ \underline{H} = O \quad \text{uniformly in } \hat{r}$$

where

$$O = \lim_{r\to\infty} \left\{ \underline{r} \wedge (\nabla \wedge) + ikr \right\},$$

is that $\underline{E}$ and $\underline{H}$ be formed from Debye potentials ψ_1 and ψ_2 as shown in (2.14) and that these satisfy the scalar Sommerfeld radiation condition

$$\lim_{r\to\infty} r\left(\frac{\partial\psi_{1,2}}{\partial r} - ik\psi_{1,2}\right) = 0 \qquad \text{uniformly in } \hat{r}.$$

In the usual formulation of a scattering problem, the total field is considered as consisting of two terms, an incident or primary field (i.e. the field which would exist were there no scattering object present) and a scattered field, which can be thought of as a perturbation or correction term accounting for the presence of the scatterer. It is therefore necessary to discuss the kinds of primary fields which are of interest. In most radar scattering problems, the target is assumed to be illuminated by an incoming plane wave with $\underline{E}$ and $\underline{H}$ transverse to the direction of propa-

gation. In the mathematical formulation, however, it is often preferable to treat sources at a finite distance from the scatterer even though it involves introducing singularities (of a prescribed nature) into the field expressions. This is particularly true when the scatterer is infinite in extent, as is the circular cone treated in the next section. In the first place, the radiation condition is imposed uniformly on all field quantities when all sources are a finite distance from the origin, whereas with plane wave excitation only the scattered field or perturbation term obeys the radiation condition, and if the scatterer is not finite in extent, this term must be further separated into a reflected term which does not satisfy the radiation condition and a diffracted term which does. Secondly, by considering sources at finite distances, it is sometimes possible with the help of Debye potentials, to solve a meaningful scalar (acoustic) scattering problem and a vector (electromagnetic) scattering problem at the same time. This is not true with plane wave incidence and the attractive prospect of solving two problems with one function is not to be overlooked. Lastly, with the general solution of a scattering problem for an arbitrary dipole source (essentially finding the Green's functions for the particular scatterer) it is possible by superposition to construct solutions for any source distribution and, by passing to a limit, the plane wave case can also be derived. Of the various sources only dipoles will be considered since more complicated sources can be represented as a distribution of dipoles.

Let (r, θ, ϕ) and (r_1, θ_1, ϕ_1) denote the field and source points respectively and R the distance between them (see Fig. 3). A scalar source at the point r_1, θ_1, ϕ_1 is then given by

$$\psi = \frac{e^{ikR}}{R}$$

We note in passing that ψ can also represent an acoustic velocity potential.

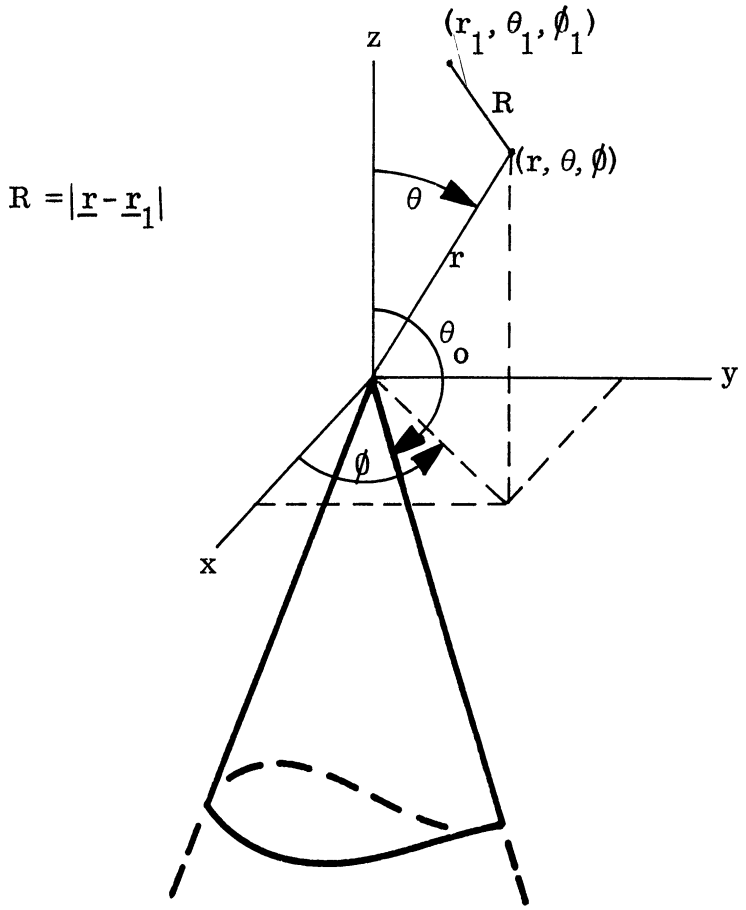

FIGURE 3

An electromagnetic source at the point r_1, θ_1, ϕ_1 can be derived from ψ in a variety of ways:

a) In equation (2.13), let $\underline{\Phi}_1 = \frac{e^{ikR}}{R}$ and $\underline{\Phi}_2 = 0$, or alternatively, $\underline{\Phi}_1 = 0$, $\underline{\Phi}_2 = \frac{e^{ikR}}{R}$. In the first case the field components given by (2.13) are those of a Hertzian electric dipole at (r_1, θ_1, ϕ_1) with $\underline{\Pi}_e = \frac{e^{ikR}}{R}\hat{i}_z = \underline{\Phi}_1\hat{i}_z$. In the second case the equations (2.13) define the field components of a Hertzian magnetic dipole at (r_1, θ_1, ϕ_1) with $\underline{\Pi}_m = \frac{e^{ikR}}{R}\hat{i}_z = \underline{\Phi}_2\hat{i}_z$. Expressed in the notation of Stratton (1941) $\underline{\Pi}_e$ and $\underline{\Pi}_m$ are electric and magnetic dipoles of moment $\underline{p}^{(1)} = 4\pi\epsilon\hat{i}_z$ and $\underline{m}^{(1)} = 4\pi\hat{i}_z$, respectively.

b) In similar fashion, the equations (2.14) can be used to define electromagnetic sources by taking either $\psi_1 = \frac{e^{ikR}}{R}$ and $\psi_2 = 0$ or $\psi_1 = 0$ and $\psi_2 = \frac{e^{ikR}}{R}$. The equations (2.14) then represent the field components of a radial Hertzian electric dipole (first case) or a radial Hertzian magnetic dipole (second case). At first sight it would appear that in order to treat these dipoles in the same manner as the dipoles described in a) (which will be designated axial to distinguish them) it is necessary to define the dipole moments as

$$\underline{p}^{(1)} = 4\pi\epsilon\underline{r} \quad \text{and} \quad \underline{m}^{(1)} = 4\pi\underline{r}\,. \tag{2.15}$$

One would be hard put to give a physical interpretation to a dipole moment which varied with field point. However it is a relatively simple matter to show that if the constant vector $\underline{r}_1$ replaces the variable vector $\underline{r}$ in the definitions of dipole

moment there is no change in the field quantities. That is,

$$\nabla \wedge \left(\underline{r} \frac{e^{ikR}}{R} \right) \equiv \nabla \wedge \left(\underline{r}_1 \frac{e^{ikR}}{R} \right) \tag{2.16}$$

and, of course, this remains true if one operates on both sides with a curl. To verify (2.16), we first note that

$$R = |\underline{r} - \underline{r}_1| \qquad \text{which implies} \qquad \nabla R = \frac{\underline{r} - \underline{r}_1}{|\underline{r} - \underline{r}_1|} ,$$

(∇ operates on field variables)

and also $\nabla \wedge \underline{r} = \nabla \wedge \underline{r}_1 = 0$. With these facts in mind it is clear that

$$\nabla \wedge (\underline{r} - \underline{r}_1) \frac{e^{ikR}}{R} = \nabla \frac{e^{ikR}}{R} \wedge (\underline{r} - \underline{r}_1) = \frac{d}{dR} \left(\frac{e^{ikR}}{R} \right) \nabla R \wedge (\underline{r} - \underline{r}_1)$$

$$= \frac{d}{dR} \left(\frac{e^{ikR}}{R} \right) \frac{(\underline{r} - \underline{r}_1)}{|\underline{r} - \underline{r}_1|} \wedge (\underline{r} - \underline{r}_1) = 0 .$$

Hence (2.16) is an identity and the dipole moments can be defined as

$$\underline{p}^{(1)} = 4\pi\epsilon \underline{r}_1 \qquad \text{and} \qquad \underline{m}^{(1)} = 4\pi \underline{r}_1$$

which are truly radial dipoles at (r_1, θ_1, ϕ_1) though admittedly normalized in a peculiar way.

Because of the convenience of the Debye potentials or radial Hertzian vectors, scattering problems with radial Hertzian dipole sources are often encountered in the literature.

In one special case, of course, the relation between radial and axial dipoles is particularly simple. This occurs when the source is on the z-axis ($\theta_1 = 0$) but not at the origin. Since the rectangular coordinate system employed here is oriented so that the z-axis is co-linear with the axial Hertz vectors, we then have $\underline{r}_1 = r_1 \hat{i}_z$. Consequently, the field components defined by (2.13) when

$$\underline{\Pi}_e = \underline{\phi}_1 \hat{i}_z = \frac{e^{ik\sqrt{x^2+y^2+(z-r_1)^2}}}{\sqrt{x^2+y^2+(z-r_1)^2}} \hat{i}_z \qquad (2.17)$$

$$\underline{\Pi}_m = \underline{\phi}_2 \hat{i}_z = 0$$

are the same as those defined by (2.14) when

$$\psi_1 = \frac{e^{ikR}}{r_1 R} \qquad \text{and} \qquad \psi_2 = 0 \qquad (2.18)$$

The factor $1/r_1$ normalizes the dipole moment to be $4\pi\epsilon\hat{r}_1$, or in this case $4\pi\epsilon\hat{i}_z$. (An analogous relation holds between axial and radial Hertz magnetic dipoles.)

Explicitly

$$H_x = -i\omega\epsilon\, y\, e^{ikR}\left(\frac{ik}{R^2} - \frac{1}{R^3}\right) \qquad E_x = -x(z-r_1)\, e^{ikR}\left(\frac{k^2}{R^3} + \frac{3ik}{R^4} - \frac{3}{R^5}\right)$$

$$H_y = i\omega\epsilon\, x\, e^{ikR}\left(\frac{ik}{R^2} - \frac{1}{R^3}\right) \qquad E_y = -y(z-r_1)\, e^{ikR}\left(\frac{k^2}{R^3} + \frac{3ik}{R^4} - \frac{3}{R^5}\right)$$

$$H_z = 0 \qquad E_z = e^{ikR}\left(\frac{ik}{R^2} + \frac{k^2\left[x^2+y^2\right]-1}{R^3} - \frac{3ik(z-r_1)^2}{R^4} + \frac{3(z-r_1)^2}{R^5}\right)$$

(2.19)

where $R = \sqrt{x^2 + y^2 + (z - r_1)^2}$.

In terms of spherical coordinates these become

$$H_r = 0 \qquad E_r = e^{ikR}(r_1 f - \cos\theta g)$$

$$H_\theta = 0 \qquad E_\theta = e^{ikR}(-r \sin\theta f + \sin\theta g)$$

$$H_\phi = i\omega\epsilon r \sin\theta\, e^{ikR}\left(\frac{ik}{R^2} - \frac{1}{R^3}\right) \qquad E_\phi = 0 \qquad (2.20)$$

where

$$f = \frac{k^2 r}{R^3} + \frac{3ikr}{R^4} - \frac{3r}{R^5}$$

$$g = \frac{2ik}{R^2} + \frac{k^2 r r_1 \cos\theta - 2}{R^3} + \frac{3ikrr_1\cos\theta}{R^4} - \frac{3rr_1\cos\theta}{R^5} \quad .$$

When $r_1 = 0$, the case invariably treated in standard texts (e.g. Stratton, 1941), it is easily seen that $r = R$ and the above components then reduce to

$$H_r = 0 \qquad E_r = -2\cos\theta\, e^{ikr}\left(\frac{ik}{r^2} - \frac{1}{r^3}\right)$$

$$H_\theta = 0 \qquad E_\theta = -\sin\theta\, e^{ikr}\left(\frac{k^2}{r} + \frac{ik}{r^2} - \frac{1}{r^3}\right)$$

$$H_\phi = i\omega\epsilon \sin\theta\, e^{ikr}\left(\frac{ik}{r} - \frac{1}{r^2}\right) \qquad E_\phi = 0. \qquad (2.21)$$

There is some difficulty with the radial dipole formulation when $r_1 = 0$ due to the presence of the factor r_1 in the definition of the dipole moment. The radial elec-

tric dipole of moment $4\pi\epsilon\underline{r}_1 = 4\pi\epsilon r_1 \hat{i}_z$ (θ_1 is still zero) has zero moment when $r_1 = 0$ and therefore cannot radiate, i.e. the field components are all zero. If, on the other hand, the dipole moment is normalized to be $4\pi\epsilon\hat{i}_z$, then (see equation 2.18) ψ_1 is apparently singular when $r_1 = 0$ for all r. Of course, if the field components are computed first, the limit $r_1 \to 0$ presents no difficulty, but in spite of this it is more convenient to avoid the radial dipole formulation for sources at the origin. In many important examples, indeed all the problems discussed in this report, the source will not lie at the origin, it being more convenient to choose the coordinate system so that the scattering surface rather than the source is simply described, and the radial dipole formulation no longer presents a difficulty.

It is now possible to formulate simultaneously in terms of Debye potentials both vector and scalar scattering problems involving a cone in the presence of elementary excitations. First define the ranges of field and source variables to be

$$r_1 > 0 \qquad 0 \leqslant \theta_1 < \theta_o \qquad 0 \leqslant \phi_1 \leqslant 2\pi$$

$$r \geqslant 0 \qquad 0 \leqslant \theta \leqslant \theta_o \qquad 0 \leqslant \phi \leqslant 2\pi \ .$$

If a single valued function ψ_1^s of all six variables, twice-differentiable in each except (possibly) at the boundary $\theta = \theta_o$, can be found such that

$$(\nabla^2 + k^2)\psi_1^s = 0 \qquad (2.22)$$

$$\lim_{r \to \infty} r \left(\frac{\partial \psi_1^s}{\partial r} - ik\psi_1^s \right) = 0 \quad \text{uniformly in } \hat{r}, \tag{2.23}$$

and

$$\left(\frac{e^{ikR}}{R} + \psi_1^s \right) \Bigg|_{\theta = \theta_o} = 0 \ , \tag{2.24}$$

then

a) the velocity potential of the field scattered by a perfectly soft cone in the presence of a source $\frac{e^{ikR}}{R}$ is given by ψ_1^s;

b) the electromagnetic field scattered by a perfectly conducting cone in the presence of a radial electric dipole (with moment $4\pi\epsilon \underline{r}_1$) is given by equations (2.14) with $\psi_1 = \psi_1^s + \frac{e^{ikR}}{R}$, $\psi_2 = 0$;

and c) the field components of b) in the particular case when $\theta_1 = 0$ also represent the electromagnetic field scattered by a perfectly conducting cone in the presence of an axial electric dipole of moment $\underline{p}^{(1)} = 4\pi\epsilon r_1 \hat{i}_z$.

If a function ψ_2^s can be found which fulfills all of the conditions required of ψ_1^s except that the boundary condition (2.24) is replaced by

$$\frac{\partial}{\partial \theta} \left(\frac{e^{ikR}}{R} + \psi_2^s \right) \Bigg|_{\theta = \theta_o} = 0 \tag{2.25}$$

then d) the velocity potential of the field scattered by a perfectly rigid cone in the presence of a source $\frac{e^{ikR}}{R}$ is given by ψ_2^s;

e) the electromagnetic field scattered by a perfectly conducting cone in the presence of a radial magnetic dipole (with moment $4\pi \underline{r}_1$) is given by equations (2.14) with $\psi_1 = 0$, $\psi_2 = \psi_2^s + \frac{e^{ikR}}{R}$,

and f) the field components of e) in the particular case when $\theta_1 = 0$ also represent the electromagnetic field scattered by a perfectly conducting cone in the presence of an axial magnetic dipole of moment $4\pi r_1 \hat{i}_z$.

A detailed derivation of the functions ψ_1^s and ψ_2^s is carried out in the next section for the cases when the source is on the axis of symmetry of the cone, so that $\theta_1 = 0$.

This section is brought to a close with a brief word on the important case of plane wave incidence. The plane wave, either scalar or vector can be thought of as a limiting case of a point source: namely as a point source removed to infinity with all field quantities appropriately renormalized. For example, consider the scalar source $\frac{e^{ikR}}{R}$ when $\theta_1 = 0$. We then have $R = \sqrt{r^2 + r_1^2 - 2rr_1\cos\theta}$, and for sufficiently large values of r_1

$$\frac{e^{ikR}}{R} \sim \frac{e^{ikr_1 - ikr\cos\theta}}{r_1} = \frac{e^{ikr_1 - ikz}}{r_1}$$

Deleting the factor $\frac{e^{ikr_1}}{r_1}$, i.e. renormalizing the source strength, now leaves only e^{-ikz}, which is a plane wave propagating in the direction of the negative z-axis. Unfortunately, however, letting $\psi_1 = e^{-ikz}$ and $\psi_2 = 0$ (or $\psi_1 = 0$, $\psi_2 = e^{-ikz}$) in

the equations (2.14) will never produce a plane electromagnetic wave, and consequently for plane wave incidence the scalar and vector problems must be treated separately. Although it is possible to find two scalar functions which, through the equations (2.14), produce a vector plane wave, these functions have no meaningful interpretation in the scalar sense, since to produce the plane wave $\underline{E} = \hat{i}_x e^{-ikz}$, $\underline{H} = -\hat{i}_y \sqrt{\frac{\epsilon}{\mu}}\, e^{-ikz}$ using (2.14), it is necessary that

$$\psi_1 = \frac{x e^{-ikz}}{k^2(x^2+y^2)} \qquad \text{and} \qquad \psi_2 = \frac{-y\, e^{-ikz}}{k\omega\mu(x^2+y^2)}$$

which exhibit a delta function behavior at all points on the z-axis.

The vector plane wave is the limiting case of a dipole when the dipole goes to infinity in a direction normal to its moment. Thus the above example of a plane wave propagating down the z-axis is the limit of an electric dipole $\underline{\Pi}_e = \frac{e^{ikR}}{k^2 R}\hat{i}_x$ where the limit and renormalization are as in the scalar case. For this source, and indeed for a transverse dipole in general, there is no meaningful scalar problem which can be formulated simultaneously. Though Debye potentials may still be employed, they have meaning only together with the equations (2.14) which define the field quantities, whereas for radial dipoles the appropriate Debye potentials are meaningful in themselves.

The problem of finding the electric field scattered by a perfectly conducting cone in the presence of a dipole of arbitrary location and orientation is one of deter-

mining a single-valued, non-singular, twice-differentiable vector function $\underline{E}^s$ such that

$$
\begin{aligned}
&(1)\quad (\nabla^2 + k^2)\,\underline{E}^s = 0 \\
&(2)\quad \nabla \cdot \underline{E}^s = 0 \\
&(3)\quad \lim_{r\to\infty}\left\{\underline{r}\wedge(\nabla\wedge\underline{E}^s) + ikr\underline{E}^s\right\} = 0 \\
&(4)\quad (E_r^s + E_r^i)\Big|_{\theta=\theta_o} = 0 = (E_\phi^s + E_\phi^i)\Big|_{\theta=\theta_o}
\end{aligned}
\qquad (2.26)
$$

where either

$$\underline{E}^i = \nabla\wedge\nabla\wedge\left(\frac{e^{ikR}}{R}\,\underline{p}\right) \quad \text{(electric dipole of moment } 4\pi\epsilon\underline{p})$$

or

$$\underline{E}^i = i\omega\mu\,\nabla\wedge\left(\frac{e^{ikR}}{R}\,\underline{m}\right) \quad \text{(magnetic dipole of moment } 4\pi\underline{m})$$

with

$$R = |\underline{r} - \underline{r}_1| \ .$$

The most important cases are those where $\underline{r}_1 \cdot \underline{p} = 0$ or $\underline{r}_1 \cdot \underline{m} = 0$ (transverse dipoles). When $\underline{r}_1\wedge\underline{p} = 0$ or $\underline{r}_1\wedge\underline{m} = 0$ there is the alternate formulation in terms of Debye potentials (equations (2.22) through (2.25)), and any arbitrary moment can be decomposed into a transverse component and a radial component.

2.2 Particular Solution

Consider a point source of radiation located on the axis of a semi-infinite right circular cone at a distance r_1 from the vertex. In terms of spherical polar

coordinates (r, θ, ϕ) with origin at the vertex, the cone is defined by the equation

$$\theta = \theta_o > \pi/2$$

so that $\pi - \theta_o$ is the half cone angle, and the source is assumed situated in the exterior region.

Attention will be confined to the scalar problem (and appropriate vector problems as described in the previous section) in which the boundary condition at the surface of the cone is either $\psi = 0$ or $\frac{\partial \psi}{\partial \theta} = 0$ where ψ is the total field, and in the neighborhood of the source ψ has the prescribed behavior

$$\frac{e^{ikR}}{kR} ,$$

with $R = \sqrt{r^2 + r_1^2 - 2rr_1 \cos\theta}$. The Dirichlet condition, $\psi = 0$, is appropriate to both an acoustically "soft" surface and an electromagnetically perfectly conducting surface in the presence of an electric dipole (axial or radial) whilst the Neumann condition ($\frac{\partial \psi}{\partial \theta} = 0$) corresponds to both a "hard" acoustic surface and a perfectly conducting surface in the presence of a magnetic dipole (axial or radial). The task which then confronts us is the determination of a solution ψ of the scalar wave equation which is free of singularities in the region $0 \leqslant \theta \leqslant \theta_o$ except at the source but including the cone vertex, which satisfies the boundary condition on the cone surface, and which has the appearance of an outgoing wave at infinity (see equations (2.22) through (2.25)).

The form of the solution is suggested by the representation of the source function in cylindrical polar coordinates. From Stratton (1941), we have

$$\frac{e^{ikR}}{kR} = i \sum_{n=0}^{\infty} (2n+1)\, j_n(kr_<)\, h_n(kr_>)\, P_n(\mu) \tag{2.27}$$

where $\mu = \cos\theta$, $j_n(x)$ and $h_n(x)$ are the spherical Bessel and Hankel functions of the first kind defined in terms of the corresponding cylinder functions by the equation

$$z_n(x) = \sqrt{\frac{\pi}{2x}}\, Z_{n+1/2}(x). \tag{2.28}$$

$r_<$ stands for r when $r<r_1$, but for r_1 when $r>r_1$, and conversely for $r_>$. Following Carslaw (1914) the sum is now expressed as an integral over a contour C in the complex ν plane:

$$\frac{e^{ikR}}{kR} = \frac{1}{2} \int_C \frac{(2\nu+1)\, j_\nu(kr_<)\, h_\nu(kr_>)\, P_\nu(-\mu)}{\sin\nu\pi}\, d\nu \tag{2.29}$$

and because of the behavior of the integrand for large $|\nu|$, the contour can be taken as a parabolic path running from $\nu = (1+ix)\infty$ to $\nu = (1-ix)\infty$, where x is a real positive number, and intersecting the real ν axis between $\nu = -1/2$ and $\nu = 0$.

The above representation of the source function suggests that for the total (incident plus scattered) field we write

$$\psi = \frac{1}{2} \int_C \frac{(2\nu+1)\, j_\nu(kr_<)\, h_\nu(kr_>)\, f_\nu(\mu)}{\sin\nu\pi}\, d\nu,$$

where $f_\nu(\mu)$ is a linear combination of $P_\nu(\mu)$ and $P_\nu(-\mu)$ chosen so as to satisfy the various boundary conditions. Taking first the problem of the hard cone ($\frac{\partial \psi}{\partial \theta} = 0$ at the surface) we observe that if

$$f_\nu(\mu) = P_\nu(-\mu) - \frac{\frac{d}{d\mu_o} P_\nu(-\mu_o)}{\frac{d}{d\mu_o} P_\nu(\mu_o)} P_\nu(\mu) \tag{2.30}$$

the boundary condition at $\theta = \theta_o$ is satisfied automatically. In addition the solution is finite in $0 \leqslant \theta \leqslant \theta_o$ except at the source, where it has the desired infinity, satisfies the scalar wave equation, and has the appearance of an outgoing wave as $r \rightarrow \infty$. Inasmuch as all the conditions are now satisfied, the solution for the Neumann problem is therefore

$$\psi_2 = \frac{1}{2} \int_C \frac{(2\nu+1)\, j_\nu(kr_<)\, h_\nu(kr_>)}{\sin \nu\pi} \left\{ \frac{P_\nu(-\mu) \frac{d}{d\mu_o} P_\nu(\mu_o) - P_\nu(\mu) \frac{d}{d\mu_o} P_\nu(-\mu_o)}{\frac{d}{d\mu_o} P_\nu(\mu_o)} \right\} d\nu \tag{2.31}$$

This solution may also be expressed as an infinite sum. To this end we note that since

$$P_n(-\mu) = (-1)^n P_n(\mu)$$

the bracketed terms in the integrand of (2.31) are zero for integer ν, and consequently the only singularities of the integrand are poles at the zeros of $\frac{d}{d\mu_o} P_\nu(\mu_o)$.

As a function of ν, these are real and distinct (see Carslaw, 1914) and are non-integral except for $\nu = 0$. This last is a zero because of the identity

$$P_o(\mu) \equiv 1$$

and since $\nu = 0$ is also a zero of $\sin\nu\pi$, the residue at this point requires special consideration.

From the definition of the Legendre function, we have

$$P_\nu(\mu) = {}_2F_1(-\nu, \nu+1; 1; \frac{1-\mu}{2}) \tag{2.32}$$

(see for example, Magnus and Oberhettinger, 1949) and hence for small ν

$$P_\nu(\mu) = 1 + \nu \log\frac{1+\mu}{2} + O(\nu^2) . \tag{2.33}$$

The residue of the integrand in (2.31) at $\nu = 0$ is therefore

$$\frac{1}{\pi} j_o(kr_<) h_o(kr_>) \cdot \frac{2}{1-\mu_o} \tag{2.34}$$

and if the contour is now closed in the right hand half plane, we have[+]

$$\psi_2 = \frac{2i}{1-\mu_o} j_o(kr_<) h_o(kr_>) - i\pi \sum_\nu \frac{(2\nu+1) j_\nu(kr_<) h_\nu(kr_>)}{\sin\nu\pi} \frac{\frac{d}{d\mu_o} P_\nu(-\mu_o)}{\frac{d^2}{d\nu d\mu_o} P_\nu(\mu_o)} P_\nu(\mu) \tag{2.35}$$

[+]We remark in passing that Carslaw's formula corresponding to (2.35) is in error by virtue of his failure to separate out the residue at $\nu = 0$, though his result corresponding to (2.37) is correct.

where the summation is over all the zeros of $\frac{d}{d\mu_o} P_\nu(\mu_o)$ for $\nu>0$.

The above expression can be further simplified by using the fact that for ν real

$$(1-\mu^2)\left\{P_\nu(\mu)\frac{d}{d\mu}P_\nu(-\mu) - P_\nu(-\mu)\frac{d}{d\mu}P_\nu(\mu)\right\} = -\frac{2}{\pi}\sin\nu\pi \tag{2.36}$$

(Carslaw, 1914). If ν is a zero of $\frac{d}{d\mu_o} P_\nu(\mu_o)$, then

$$(1-\mu_o^2)P_\nu(\mu_o)\frac{d}{d\mu_o}P_\nu(-\mu_o) = -\frac{2}{\pi}\sin\nu\pi$$

which can be substituted into equation (2.35) to give

$$\psi = \frac{2i}{1-\mu_o} j_o(kr_<) h_o(kr_>) + 2i \sum_\nu (2\nu+1) j_\nu(kr_<) h_\nu(kr_>) \frac{P_\nu(\mu)}{(1-\mu_o^2)P_\nu(\mu_o)\frac{d^2}{d\nu d\mu_o}P_\nu(\mu_o)}.$$

This can be written somewhat more compactly as

$$\psi_2 = 2i \sum_\nu (2\nu+1) j_\nu(kr_<) h_\nu(kr_>) \frac{P_\nu(\mu)}{(1-\mu_o^2)P_\nu(\mu_o)\frac{d^2}{d\nu d\mu_o}P_\nu(\mu_o)} \tag{2.37}$$

where the summation is over all the zeros of $\frac{d}{d\mu_o} P_\nu(\mu_o)$ for $\nu>-1/2$. Since

$$P_\nu(\mu_o) = P_{-\nu-1}(\mu_o),$$

all the zeros of the derivative are included in this summation.

For the case in which the cone is soft rather than hard, the treatment is analogous to that given above. Corresponding to (2.31) we have

$$\psi_1 = \frac{1}{2} \int_C \frac{(2\nu+1) j_\nu(kr_<) h_\nu(kr_>)}{\sin \nu\pi} \left\{ \frac{P_\nu(-\mu) P_\nu(\mu_o) - P_\nu(\mu) P_\nu(-\mu_o)}{P_\nu(\mu_o)} \right\} d\nu \tag{2.38}$$

which can be written as

$$\psi_1 = -i\pi \sum_\nu \frac{(2\nu+1) j_\nu(kr_<) h_\nu(kr_>)}{\sin \nu\pi} \frac{P_\nu(-\mu_o)}{\frac{d}{d\nu} P_\nu(\mu_o)} P_\nu(\mu) \tag{2.39}$$

(cf equation 2.35), where the summation is over the zeros of $P_\nu(\mu_o)$ for $\nu > -1/2$. Since $\nu = 0$ is not a zero, the difficulty which was found for the hard cone does not now appear, and using equation (2.36) the above result can be expressed directly as

$$\psi_1 = -2i \sum_\nu (2\nu+1) j_\nu(kr_<) h_\nu(kr_>) \frac{P_\nu(\mu)}{(1-\mu_o^2) \frac{d}{d\nu} P_\nu(\mu_o) \frac{d}{d\mu_o} P_\nu(\mu_o)} \tag{2.40}$$

(cf equation 2.37). We note the omission of a factor $\nu + 1/2$ in the equations corresponding to (2.39) and (2.40) in Carslaw (1910).

With all the above formulae computation of numerical results is laborious for two reasons. In the first place it is difficult to obtain sufficiently precise values for the zeros of the Legendre functions and their derivatives, and secondly the infinite series converges very slowly under most circumstances of practical interest.

Deferring until later a discussion of the first point, attention is now focussed on the convergence properties.

That the series actually do converge can be seen by considering the behavior of the elements of the summation for large ν. Taking first the radial functions we have

$$j_\nu(x) = \frac{1}{2}\sqrt{\pi}\,\frac{(x/2)^\nu}{\Gamma(\nu+3/2)}\left\{1+O(x^2/\nu)\right\} \tag{2.41}$$

$$h_\nu(x) = \frac{-i}{2\sqrt{\pi}}\,\frac{\Gamma(\nu+1/2)}{(x/2)^{\nu+1}}\left\{1+O(x^2/\nu)\right\} \tag{2.42}$$

valid for $\nu \gg x^2$. Also

$$P_\nu(\mu) \sim \sqrt{\frac{2}{\nu\pi\sin\theta}}\,\sin\left\{(\nu+1/2)\theta+\frac{\pi}{4}\right\} \tag{2.43}$$

(see, for example, Carslaw, 1914), giving

$$\frac{dP_\nu(\mu)}{d\mu} \sim -\sqrt{\frac{2}{\nu\pi\sin^3\theta}}\,(\nu+1/2)\cos\left\{(\nu+1/2)\theta+\frac{\pi}{4}\right\} \tag{2.44}$$

and

$$\frac{d^2P_\nu(\mu)}{d\nu d\mu} \sim \sqrt{\frac{2}{\nu\pi\sin^3\theta}}\,(\nu+1/2)\theta\sin\left\{(\nu+1/2)\theta+\frac{\pi}{4}\right\}. \tag{2.45}$$

Hence, in equation (2.37) the terms for which ν is sufficiently large can be written as

$$-i\sqrt{\frac{\pi}{2\nu\sin\theta}}\left(\frac{kr_<}{kr_>}\right)^\nu \frac{1}{kr_>\theta_o}\,\frac{\sin\left\{(\nu+1/2)\theta+\frac{\pi}{4}\right\}}{\sin^2\left\{(\nu+1/2)\theta_o+\frac{\pi}{4}\right\}} \tag{2.46}$$

which tends to zero as $\nu \to \infty$, and does so with a rapidity which increases as $r_</r_>$ decreases. A glance at equation (2.43) reveals that the zeros of $P_\nu(\mu_o)$ are approximated by $\nu \sim \pi/\theta_o(m - 1/4) - 1/2$ (m integer) wherever (2.43) obtains (for ν, hence m, large). Similarly the zeros of $\frac{dP_\nu(\mu_o)}{d\mu_o}$ are approximated by $\pi/\theta_o(m+ 1/4) - 1/2$, (m integer) when ν (and m) are large. Substituting this last value in (2.46) yields

$$\frac{-i}{kr_>}\sqrt{\frac{1}{\theta_o \sin\theta\,(2m+\frac{1}{2}-\frac{\theta_o}{\pi})}}\left(\frac{kr_<}{kr_>}\right)^{\frac{\pi}{4\theta_o}-\frac{1}{2}+\frac{m\pi}{\theta_o}} \sin\left[(m+1/4)\frac{\pi\theta}{\theta_o}+\frac{\pi}{4}\right], \tag{2.47}$$

which in absolute value can be shown to be less than $\frac{c}{\sqrt{m}}\left(\frac{kr_<}{kr_>}\right)^{m\pi/\theta_o}$, where c is independent of m and bounded, so that by the comparison test the series (2.37) appears to converge absolutely when $\frac{kr_<}{kr_>} < 1$. A similar result also applies to the sums in equations (2.35), (2.39) and (2.40). A completely rigorous proof of convergence would also show that this convergence is unaltered when all higher order terms in $1/\nu$ in the expressions for the Bessel and Legendre functions (2.41) - (2.43) are included. Such a proof, to the best of the authors' knowledge, has never been given.

Assuming that these higher order terms are truly negligible, a study of (2.46) or (2.47) indicates that the convergence is improved if the source (or the receiver) is moved off to infinity, and since this case has considerable practical

interest it will be considered next. To this end, let us assume that in equation (2.37) the sum can be truncated at some value $\nu = \nu_1$, say. For sufficiently large $kr_>$ the spherical Hankel function can then be replaced by its asymptotic expansion for large argument, viz

$$h_\nu(kr_>) \sim \frac{-i}{kr_>} e^{i(kr_> - \nu\frac{\pi}{2})} \left\{1 - i\frac{\nu(\nu+1)}{kr_>} - \ldots\right\} \qquad (2.48)$$

and if only the first term is employed, the expression for ψ_2 becomes

$$\psi_2 = 2\frac{e^{ikr_>}}{kr_>} \sum_\nu e^{-i\nu\frac{\pi}{2}} (2\nu+1) j_\nu(kr_<) \frac{P_\nu(\mu)}{(1-\mu_o^2)P_\nu(\mu_o)\frac{d^2}{d\nu d\mu_o}P_\nu(\mu_o)}, \qquad (2.49)$$

valid for $kr_> \gg \nu_1(\nu_1+1)$. Providing that the truncation of the original series can be justified, equation (2.49) gives the solution for either a receiver at a large distance from the vertex or the point source at a large distance. For the limiting case of the source at infinity (plane wave incidence) it is necessary to re-normalize ψ_2 by multiplying through by $kr_> e^{-ikr_>}$ before taking the limit $kr_> \to \infty$. This is equivalent to deleting the factor $(kr_>)^{-1} e^{-ikr_>}$ in (2.49).

To obtain an estimate for ν_1 it is sufficient to apply to the sum in (2.49) the same analysis used in regard to equation (2.37). For ν sufficiently large that the Bessel and Legendre functions can be replaced by their approximations for large order (equations 2.41 through 2.45), the corresponding term in (2.49) then becomes

$$\pi\, e^{-i\nu\frac{\pi}{2}} \sqrt{\frac{\nu}{2\sin\theta}}\, \frac{(kr_<)^\nu}{\Gamma(\nu+3/2)}\, \frac{\sin\left\{(\nu+1/2)\theta+\pi/4\right\}}{\theta_o}$$

which can be written as

$$e^{-i\nu\frac{\pi}{2}+\frac{3}{2}} \sqrt{\frac{\pi}{\sin\theta}} \left(\frac{kr_< e}{2\nu+3}\right)^\nu \frac{\sqrt{\nu}}{2\nu+3}\, \frac{\sin\left\{(\nu+1/2)\theta+\pi/4\right\}}{\theta_o} \qquad (2.50)$$

by using Stirling's formula for the gamma function. This tends to zero rapidly as $\nu \to \infty$ and to judge from its form it would appear that a sufficient criterion on ν_1 is

$$\nu_1 \gg kr_< \,. \qquad (2.51)$$

Accordingly, the introduction of the asymptotic expansion for $h_\nu(kr_>)$ is justified if

$$kr_> \gg (kr_<)^2 \,, \qquad (2.52)$$

and in the limiting case of plane wave excitation the total field is (from equation 2.49)

$$\psi_2 = 2 \sum_\nu e^{-i\nu\frac{\pi}{2}} (2\nu+1) j_\nu(kr)\, \frac{P_\nu(\mu)}{(1-\mu_o^2) P_\nu(\mu_o) \frac{d^2}{d\nu d\mu_o} P_\nu(\mu_o)} \,. \qquad (2.53)$$

where ν is such that $\frac{dP_\nu(\mu_o)}{d\mu_o} = 0$. The corresponding plane wave result for the soft cone (equation 2.40) is

$$\psi_1 = -2 \sum_\nu e^{-i\nu\frac{\pi}{2}}\, \frac{(2\nu+1) j_\nu(kr) P_\nu(\mu)}{(1-\mu_o^2) \frac{dP_\nu(\mu_o)}{d\nu} \frac{dP_\nu(\mu_o)}{d\mu_o}} \qquad (2.54)$$

where ν is such that $P_\nu(\mu_o) = 0$.

It is easily demonstrated (e.g. Siegel and Alperin, 1952) that when ν is such that $\frac{dP_\nu}{d\mu_o}(\mu_o) = 0$, then

$$\frac{(1-\mu_o^2)}{2\nu+1}\,\frac{d^2P_\nu(\mu_o)}{d\mu_o\,d\nu}\,P_\nu(\mu_o) = \int_{\mu_o}^{1}\left[P_\nu(\mu)\right]^2 d\mu = \frac{1}{\nu(\nu+1)}\int_{\mu_o}^{1}\left[P_\nu^1(\mu)\right]^2 d\mu \qquad (2.55)$$

and when ν is such that $P_\nu(\mu_o) = 0$, then

$$\frac{(1-\mu_o^2)}{2\nu+1}\,\frac{dP_\nu(\mu_o)}{d\mu_o}\,\frac{dP_\nu(\mu_o)}{d\nu} = \int_{1}^{\mu_o}\left[P_\nu(\mu)\right]^2 d\mu = \frac{1}{\nu(\nu+1)}\int_{1}^{\mu_o}\left[P_\nu^1(\mu)\right]^2 d\mu \qquad (2.56)$$

If these expressions are used in (2.53) and (2.54) the total field for both boundary conditions for plane wave excitation can be expressed as

$$\psi = 2\sum_\nu e^{-i\nu\frac{\pi}{2}}\,\frac{j_\nu(kr)P_\nu(\mu)}{\int_{\mu_o}^{1}\left[P_\nu(\mu)\right]^2 d\mu} \qquad (2.57)$$

where $\psi = \psi_1$ (soft cone) with the summation over ν such that $P_\nu(\mu_o) = 0$ and $\psi = \psi_2$ (hard cone) when $\frac{dP_\nu(\mu_o)}{d\mu_o} = 0$. Note that a uniform expression can also be obtained for the point source solutions (equations 2.37 and 2.40), namely

$$\psi = 2i\sum_\nu \frac{j_\nu(kr_<)h_\nu(kr_>)P_\nu(\mu)}{\int_{\mu_o}^{1}\left[P_\nu(\mu)\right]^2 d\mu} \qquad (2.58)$$

where the same convention is observed; namely ψ is the solution of the Dirichlet problem when the ν's are zeros of $P_\nu(\mu_o)$ and ψ the solution of the Neumann problem when the ν's are the zeros of $\frac{dP_\nu(\mu_o)}{d\mu_o}$.

The solution required in most calculations associated with the cross section is given by (2.57) but unfortunately its form is not convenient. In the first place, the sum represents the total field, whereas the incident and scattered fields are individually necessary in order to compute a cross section, and the separation of (2.57) is a not too easy task. In addition, the definition of the cross section, viz

$$\sigma = \lim_{r \to \infty} 4\pi r^2 \left| \psi^s / \psi^i \right|^2$$

implies that the receiver is placed at such a distance from the body that the scattered field has acquired the characteristics of a spherical wave; and avoiding the question of whether this definition is applicable when the body is infinite in the transverse direction (Brysk, 1960) the consideration of equation (2.57) for large values of kr is fraught with difficulties.

If the Bessel function $j_\nu(kr)$ in (2.53) and (2.54) is replaced by the first term of its asymptotic expansion for large kr the resulting series diverge. However, in the case of back scattering, Schensted (1953) and Siegel et al (1953a, 1955b) use special summation methods to obtain expressions for the cross section. The difficulty inherent in treating divergent series is avoided by Felsen (1955) who replaces the Bessel function not by an asymptotic form but by its Sommerfeld integral repre-

sentation, and obtains by steepest descents analysis an approximate evaluation of both the field and the cross section for large and small angle cones. The results of these analyses are presented in Section 3.

This section is brought to a close with a brief discussion of the computational problem of finding precise values for the zeros of the Legendre functions and their first derivatives (those values of ν for which $P_\nu(\cos\theta)$ or $\frac{d}{d\theta} P_\nu(\cos\theta)$ vanish for fixed values of θ). In addition, the zeros of $\frac{d}{d\theta} P_\nu^1(\cos\theta)$ are of interest in the vector problem (see section 3.1.3).

For large values of ν, these zeros can be simply approximated, as was mentioned earlier in the discussion of convergence. However, the dominant contribution to the series (2.57) and (2.58) (or any of the alternate forms given) comes from the early terms and consequently the small zeros (small values of ν for which $P_\nu^m(\cos\theta) = 0$) are quite important in any computation of the field or the cross section.

Obtaining accurate values for these small zeros and increasing the accuracy of the large zero approximation are not trivial problems. Hobson (1931) summarizes the work of Macdonald (1900b) and Pal (1918, 1919) who find approximations to the zeros as a function of argument. These expressions were employed by Carrus and Treuenfels (1951) who tabulated the first 50 zeros of $P_\nu^1(\cos\theta)$ every 5^o for $90^o < \theta < 175^o$ and the first 50 zeros of $\frac{d}{d\theta} P_\nu^1(\cos\theta)$ every 5^o for $90^o < \theta < 130^o$.

Also tabulated were the integrals $\int_0^{\mu_0} \left[P_\nu^1(\mu)\right]^2 d\mu$ for these ν's. Errors in these tables were noted by Siegel et al (1951). For the special value $\theta_0 = 165^\circ$ the first twenty zeros and normalizing integrals were recomputed by Siegel et al (1952, 1953b). These last were again recomputed with even more accuracy by the Institute of Numerical Analysis (see Siegel et al, 1953a).

Even if the zeros were tabulated, however, the calculation of the field or cross section would still present a formidable computational problem. Some of the difficulties inherent in the representation as infinite sums over appropriate zeros are avoided in the integral representations. Appropriate integral expressions, if available, should be used in any extensive computational program [see Section 3 and Felsen (1953, 1955, 1957a,b,d, 1958)]. This is especially true in the light of present day high speed computing techniques, as is borne out by the work of Goryanov (1961) (see section 3.3).

III

SUMMARY OF SEMI-INFINITE CONE FORMULAE

This section presents a systematic listing of existing expressions for the scattering properties of semi-infinite cones with either plane wave or point source excitation. Various approximations are given, together with the restrictions on the parameters under which the approximations are valid. All formulas have been transformed to the notation employed throughout this report. Thus ψ^i represents a scalar source (either point source or plane wave), ψ_1^s represents the field scattered by a soft cone (Dirichlet boundary condition) and $\psi_1 = \psi^i + \psi_1^s$ is the total field. ψ_2^s represents the field scattered by a hard cone (Neumann boundary condition) and $\psi_2 = \psi^i + \psi_2^s$. In general these ψ will be functions of six variables, viz. 3 field coordinates and 3 source coordinates. When ψ^i is a plane wave, the number is reduced to five and in the important case when the plane wave is incident along the axis of symmetry, the field is a function only of the three field coordinates.

When the scattered field is observed far from the vertex, it is convenient to introduce the scattering amplitude S_j where $\psi_j^s \sim \frac{e^{ikr}}{kr} S_j(\theta, \phi)$ and $j = 1$ or 2. For general plane wave incidence the scattering amplitude is also a function of θ_1, ϕ_1, the angles specifying the direction of incidence. The scalar scattering cross sections will be denoted by σ_j where

$$\sigma_j = \lim_{r \to \infty} 4\pi r^2 \left| \psi_j^s / \psi^i \right|^2$$
$$= \frac{\lambda^2}{\pi} \left| S_j \right|^2 \quad .$$

In general σ_j will be a function of four angular variables, but most of the results available are for the case $\theta_1 = 0$ (incidence along the z-axis) so that the number is reduced to two. The back scattered far field for plane wave incidence along the z-axis is an oft-computed quantity and will be denoted by $S_j(0)$ and $\sigma_j(0)$. The electromagnetic results will all be given in terms of the electric field $\underline{E}$, and the same superscript convention will be observed as described above. Thus, $\underline{E}^i$ is the incident field, $\underline{E}^s$ the scattered field, and $\underline{S}$ the far zone scattering amplitude (now a vector). σ (without subscript) will denote cross section, defined as

$$\sigma = \lim_{r \to \infty} 4\pi r^2 \left| \underline{E}^s / \underline{E}^i \right|^2$$
$$= \frac{\lambda^2}{\pi} \left| \underline{S} \right|^2$$

and $\sigma(0)$ is the back scattered cross section for incidence along the z-axis.

In the presentation of formulae, the natural division into vector and scalar problems, with the latter further split into Dirichlet and Neumann boundary conditions, will be observed. With each formula will appear the appropriate conditions for applicability.

3.1 Dirichlet Boundary Condition.

For an arbitrarily located scalar source $\frac{e^{ik|\underline{r}-\underline{r}_1|}}{k|\underline{r}-\underline{r}_1|}$ in the presence of a soft ($\psi|_{\theta=\theta_o} = 0$) semi-infinite cone of half angle $\pi - \theta_o$ (equivalent to a radial electric dipole of moment $\frac{4\pi\epsilon\underline{r}_1}{k}$ and a perfectly conducting cone) the total field is given by Felsen (1957a, b) as

$$\psi_1 = \frac{1}{2}\sum_{m=o}^{\infty} \epsilon_m \cos m(\phi - \phi_1) \int_c d\nu \left\{ (2\nu+1)\frac{\Gamma(\nu+m+1) j_\nu(kr_<) h_\nu(kr_>)}{\Gamma(\nu-m+1)\sin(\nu-m)\pi} \cdot \right.$$

$$\left. \cdot \frac{P_\nu^{-m}(\cos\theta_<)}{P_\nu^{-m}(\cos\theta_o)} \left[P_\nu^{-m}(\cos\theta_>) P_\nu^{-m}(-\cos\theta_o) - P_\nu^{-m}(-\cos\theta_>) P_\nu^{-m}(\cos\theta_o) \right] \right\}, \tag{3.1}$$

where

$$j_\nu(x) = \sqrt{\pi/2x}\ J_{\nu+1/2}(x), \quad h_\nu(x) = \sqrt{\pi/2x}\ H^{(1)}_{\nu+1/2}(x),$$

$$\epsilon_o = 1, \ \epsilon_m = 2 \text{ for } m = 1, 2, 3, \ldots,^{+}$$

$$r_< = r \text{ for } r < r_1, \qquad r_> = r \text{ for } r > r_1,$$

$$= r_1 \text{ for } r_1 < r \qquad = r_1 \text{ for } r_1 > r$$

$$\theta_< = \theta \text{ for } \theta < \theta_1 \qquad \theta_> = \theta \text{ for } \theta > \theta_1$$

$$= \theta_1 \text{ for } \theta_1 < \theta \qquad = \theta_1 \text{ for } \theta_1 > \theta,$$

and the contour c is shown in Fig. 4.

+ These definitions of ϵ_m and the spherical Bessel functions agree with those in Magnus and Oberhettinger (1949) but differ from those in Felsen (1957b).

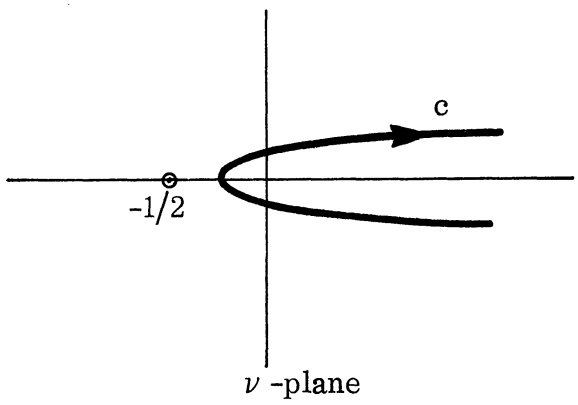

FIGURE 4

When the source is on the axis of symmetry ($\theta_1 = 0$) equation (3.1) simplifies considerably, and only one of the many alternative forms for the resulting expression is given here. Alternate expressions can be found in Section II of this report, Felsen (1955), Carslaw (1910) and Macdonald (1902), though care is necessary to make sure that the source normalization and time dependence are consistent before comparisons are drawn. An additional problem is present in the older references (Carslaw and Macdonald) because their notation is usually different from that employed by modern writers; e.g. Macdonald's (α, β, γ), and (x, y, z) are the components of $4\pi \underline{H}$ and $\frac{4\pi}{\mu} \underline{E}$ respectively, and Carslaw's $K_\nu(ikr)$ is $\frac{-i\pi}{2} e^{\frac{-i\nu\pi}{2}} H_\nu^{(2)}(kr)$.

The total field for a source $\frac{e^{ikR}}{kR}$, with $R = \sqrt{r^2 + r_1^2 - 2 r\, r_1 \cos\theta}$, is

$$\psi_1 = 2i \sum_{\nu} \frac{j_\nu(kr_<)h_\nu(kr_>)P_\nu(\cos\theta)}{\int_{\mu_o}^{1} \left[P_\nu(\mu)\right]^2 d\mu} \tag{3.2}$$

where $\mu_o = \cos\theta_o$ and the summation is over the positive zeros of $P_\nu(\mu_o)$, that is, over the set of ν such that $\nu > -1/2$ and $P_\nu(\mu_o) = 0$.

A symmetric distribution of electric dipoles about the z-axis is discussed by Macdonald (1902) and a simply varying circular source is treated by Felsen (1959).

When a plane wave is incident from an arbitrary direction the total far field is given by Felsen (1957b) as

$$\psi_1 = e^{-ikr\left[\sin\theta\,\sin\theta_1\cos(\phi-\theta_1)+\cos\theta\cos\theta_1\right]} \frac{i\,e^{ikr}}{2kr(\cos\theta+\cos\theta_1)\log\frac{2}{\pi-\theta_o}} \tag{3.3}$$

subject to the restriction $kr >> 1$, $\theta+\theta_1 < 2\theta_o-\pi$, and $\theta_o \sim \pi$ (thin cone).

When a plane wave is incident along the axis of symmetry, $\psi^i = e^{-ikz}$, the total field is given in Section II [also Felsen (1955)] as

$$\psi_1 = 2 \sum_{\nu} e^{-i\nu\,\pi/2} \frac{j_\nu(kr)P_\nu(\cos\theta)}{\int_{\mu_o}^{1} \left[P_\nu(\mu)\right]^2 d\mu}. \tag{3.4}$$

The backscattered far field for plane wave incidence along the z-axis is given approximately by Felsen (1953, 1955) as

$$\psi_1^s(0) = \frac{-i\, e^{ikz}}{4kz \log \frac{2}{\pi - \theta_o}} \tag{3.5}$$

when $\frac{1}{\pi-\theta_o} >> kz >> 1$,

$$\psi_1^s(0) = -\frac{\left(\frac{\pi}{\theta_o}\right)^2 \exp\left(i\frac{\pi^2}{4\theta_o}\right)}{4\sin^2\left(\frac{\pi^2}{2\theta_o}\right)} \left[\frac{3}{4} + \frac{1}{4}\exp\left(-i\frac{\pi^2}{\theta_o}\right)\right] \frac{e^{ikz}}{kz} \tag{3.6}$$

$$\sim -\frac{i\, e^{ikz}}{4\left(\theta_o - \frac{\pi}{2}\right)^2 kz} \tag{3.7}$$

when $\theta_o \sim \frac{\pi}{2}$, $kz >> 1$ and $\left|\sqrt{kz}\cos\theta_o\right| >> 1$, and

$$\psi_1^s(0) = -e^{ikz}\sin\theta_o \left\{1 - 2\sqrt{2}\,\xi\, e^{-i\frac{\pi}{4} - 2i\xi^2} \int_{(1-i)\xi}^{\infty} e^{-y^2}\, dy\right\} \tag{3.8}$$

when $\theta_o \sim \frac{\pi}{2}$ and $\sqrt{kz} >> 1$, where $\xi = \sqrt{kz}\,\left|\cos\theta_o\right|$.

Note that equation (3.7) can be rewritten in terms of ξ as

$$\psi_1^s(0) \sim \frac{-i\, e^{ikz}}{4\xi^2}, \qquad \xi >> 1. \tag{3.9}$$

The coefficients of $-e^{ikz}$ in equations (3.8) and (3.9) are plotted in Fig. 5 where it is seen that the two coincide for $\xi \sim 4$ [+]; hence (3.8) must be used for $\xi < 4$ while the simpler expression (3.9) suffices for $\xi > 4$ (Felsen, 1958).

Corresponding to (3.5) and (3.7) the following expressions for the back scattering cross section obtain:

$$\sigma_1(0) = \frac{\lambda^2}{16\pi \left(\log \frac{2}{\pi-\theta_0}\right)^2} \tag{3.10}$$

when $\theta_0 \sim \pi$, and

$$\sigma_1(0) = \frac{\lambda^2}{16\pi(\theta_0-\frac{\pi}{2})^4} \tag{3.11}$$

when $\theta_0 \sim \frac{\pi}{2}$.

The cross sections given in (3.10) and (3.11) are plotted in Fig. 6 as a function of θ_0.

3.2 The Neumann Boundary Condition.

For an arbitrarily located scalar source $\frac{e^{ik|\underline{r}-\underline{r}_1|}}{k|\underline{r}-\underline{r}_1|}$ in the presence of a hard $\left(\left.\frac{\partial\psi}{\partial\theta}\right|_{\theta=\theta_0} = 0\right)$ semi-infinite cone of half-angle $\pi-\theta_0$ (equivalent to a radial magnetic dipole of moment $\frac{4\pi}{k}\underline{r}_1$ and a perfectly conducting cone) the total field is given by Carslaw (1914) [see also Felsen, 1957b] as

$$\psi_2 = 2i \sum_{m=o}^{\infty} \epsilon_m \cos m(\phi-\phi_1) \sum_{\nu} \frac{(2\nu+1) j_\nu(kr_<) h_\nu(kr_>) P_\nu^{-m}(\cos\theta) P_\nu^{-m}(\cos\theta_1)}{(1-\mu_o^2) P_\nu^{-m}(\cos\theta_o) \frac{d^2}{d\nu\, d\mu_o} P_\nu^{-m}(\mu_o)} \tag{3.12}$$

[+] The amplitude curves coincide at $\xi \sim 2$ but the phases differ.

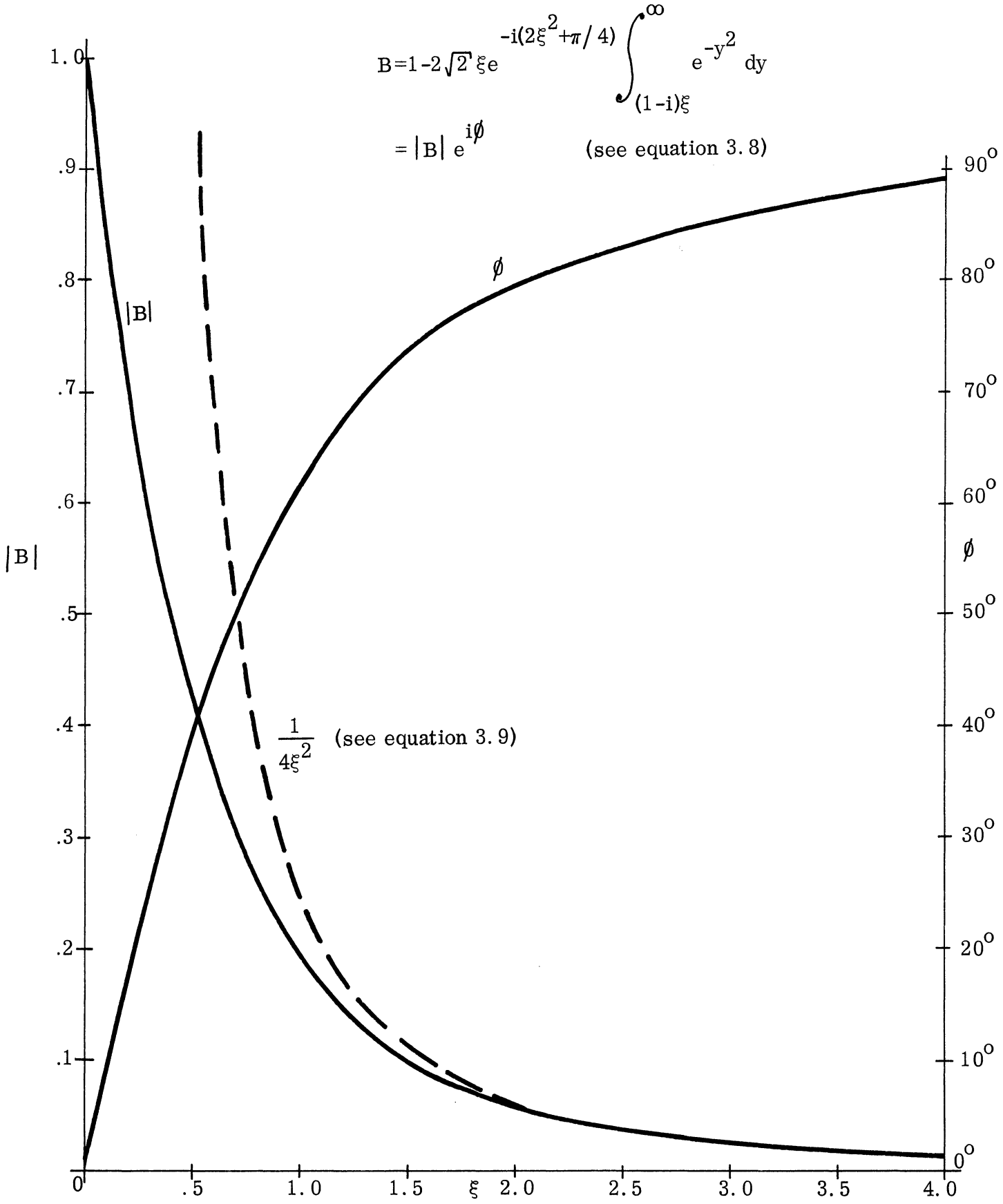

FIGURE 5: FAR FIELD COEFFICIENTS FOR THICK CONES

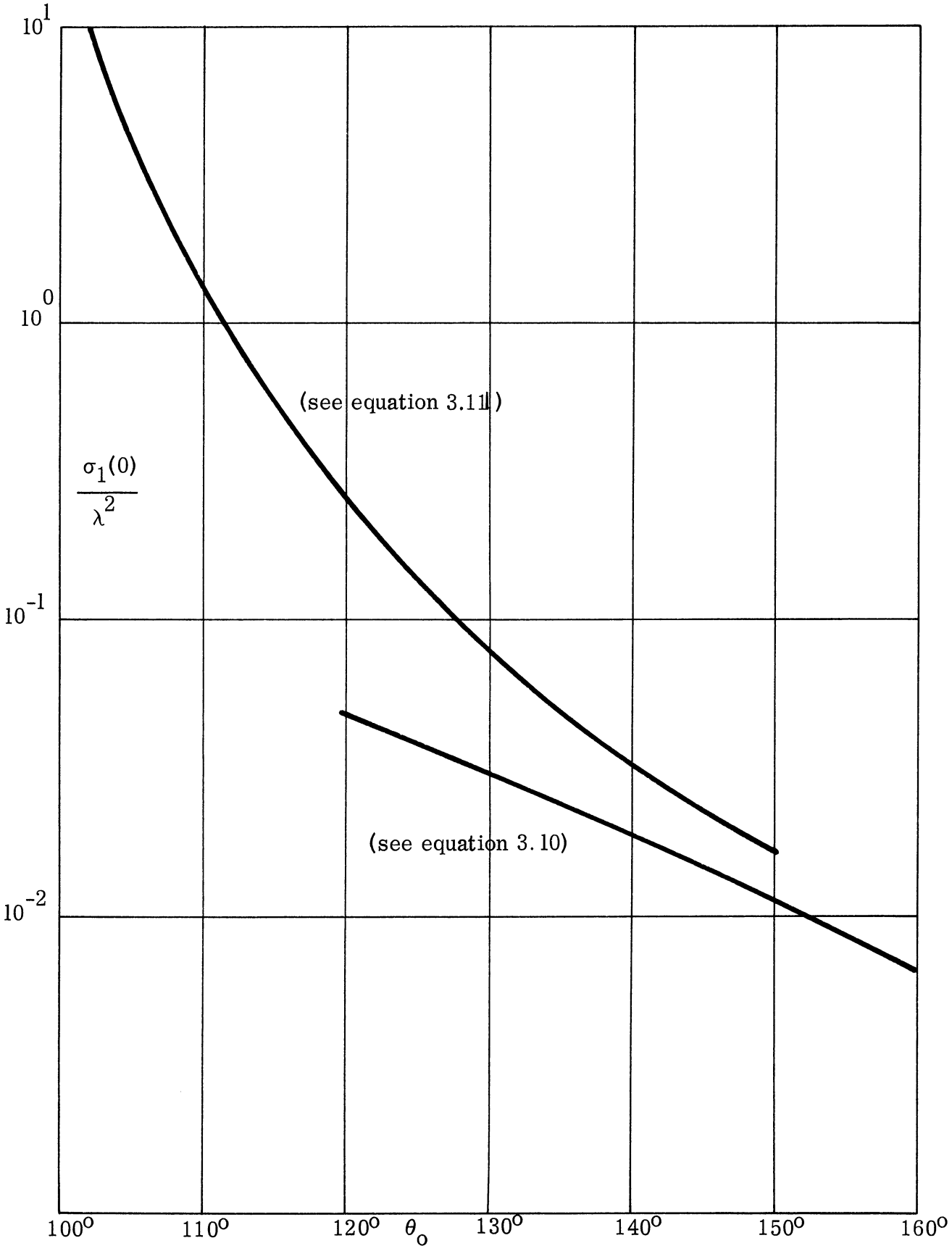

FIGURE 6: NOSE-ON BACK SCATTERING CROSS SECTION OF A SOFT CONE

where the notation is the same as defined under equation (3.1) except that the summation is over the non-negative zeros of $\frac{dP_\nu^{-m}}{d\theta_o}(\cos\theta_o)$. That is, the set of ν's for each m consists of those ν for which $\nu > -1/2$ and $\frac{dP_\nu^{-m}}{d\theta_o}(\cos\theta_o)=0$. Note that when m=0, $\nu=0$ is an element of the set.

When the source is on the axis of symmetry ($\theta_1=0$) the field expression is given more simply (see Section II) as

$$\psi_2=2i\sum_\nu \frac{j_\nu(kr_<)h_\nu(kr_>)P_\nu(\cos\theta)}{\int_{\mu_o}^1 \left[P_\nu(\mu)\right]^2 d\mu} \tag{3.13}$$

where the ν are now such that $\nu > -1/2$, $\frac{dP_\nu}{d\theta_o}(\cos\theta_o)=0$. Alternate expressions can be found in Carslaw (1914) and Felsen (1955, 1957a,b).

When a plane wave is incident from an arbitrary direction so that

$$\psi^i = e^{-ikr\left[\sin\theta\sin\theta_1\cos(\phi-\phi_1)+\cos\theta\cos\theta_1\right]},$$

the scattered field is given by Felsen (1957b) for thin cones as

$$\psi_2^s = -\pi^2\left(\frac{\pi-\theta_o}{2}\right)^2\sqrt{\frac{1}{2\pi kr}}\,e^{-i\frac{\pi}{4}}\left(\frac{1}{2}I_o+\cos(\phi-\phi_1)I_1\right) \tag{3.14}$$

where

$$I_o = \int_{-\infty}^{\infty} dx \left\{ x \frac{e^{x\frac{\pi}{2}}}{\cosh^2 \pi x} H_{ix}^{(1)}(kr)(1/4+x^2) P_{ix-1/2}(\cos\theta) P_{ix-1/2}(\cos\theta_1) \right\}$$

$$I_1 = \int_{-\infty}^{\infty} dx \left\{ x \frac{e^{x\frac{\pi}{2}}}{\cosh^2 \pi x} H_{ix}^{(1)}(kr) P_{ix-1/2}^{1}(\cos\theta) P_{ix-1/2}^{1}(\cos\theta_1) \right\}$$

and

$$\theta_o \sim \pi, \quad \theta+\theta_1 < 2\theta_o - \pi .$$

In the far zone, equation (3.14) can be simplifed (Felsen 1957b) to read

$$\psi_2^s = \frac{i(\pi-\theta_o)^2}{2(\cos\theta+\cos\theta_1)^3} \frac{e^{ikr}}{kr} \left[1+\cos\theta\cos\theta_1+2\sin\theta\sin\theta_1\cos(\phi-\phi_1)\right] \qquad (3.15)$$

for $kr >> 1$, $\theta_o \sim \pi$, and $\theta+\theta_1 < 2\theta_o-\pi$. Higher order approximations are discussed by Felsen (1957d).

When a plane wave is incident along the axis of symmetry, $\psi^i = e^{-ikz}$, the total field is given in Section II (see also Siegel and Alperin, 1952 and Felsen, 1955) as

$$\psi_2 = 2\sum_{\nu} e^{-i\nu\pi/2} \frac{j_\nu(kr)P_\nu(\cos\theta)}{\int_{\mu_o}^{1} \left[P_\nu(\mu)\right]^2 d\mu} \qquad (3.16)$$

where ν is such that $\nu > -1/2$ and $\dfrac{dP_\nu(\mu_o)}{d\mu} = 0$.

The back scattered far field for plane wave incidence along the z-axis is given approximately by Felsen (1953, 1955, 1958) as

$$\psi_2^s(0) = \frac{i}{2}\left(\frac{\pi-\theta_o}{2}\right)^2 \frac{e^{ikz}}{kz} \tag{3.17}$$

when $\dfrac{1}{\pi-\theta_o} >> kz >> 1$;

$$\psi_2^s(0) = -\frac{\left(\frac{\pi}{\theta_o}\right)^2 \exp(3i\pi^2/4\theta_o)}{4\sin^2(\pi^2/2\theta_o)}\left[\frac{1}{4}+\frac{3}{4}e^{-i\pi^2/\theta_o}\right]\frac{e^{ikz}}{kz} \tag{3.18}$$

$$\sim \frac{i}{4(\theta_o-\pi/2)^2}\frac{e^{ikz}}{kz}$$

when $\theta_o \sim \pi/2$, $kz >> 1$ and $\left|\sqrt{kz}\cos\theta_o\right| >> 1$; and

$$\psi_2^s(0) = e^{ikz}\sin\theta_o\left(1-2\sqrt{2}\,\xi\, e^{-i\pi/4-2i\xi^2}\int_{(1-i)\xi}^{\infty} e^{-y^2}\,dy\right) \tag{3.19}$$

when $\theta_o \sim \pi/2$, $kz >> 1$, where $\xi = \sqrt{kz}\left|\cos\theta_o\right|$. Note that (3.18) can be rewritten in terms of ξ as

$$\psi_2^s(0) \sim \frac{ie^{ikz}}{4\xi^2}, \qquad \xi >> 1 \tag{3.20}$$

and that (3.19) and (3.20) differ only in sign from the corresponding soft cone results (3.8 and 3.9) plotted in Fig. 5.

Corresponding to (3.17) and (3.18), the following expressions for the back scattering cross section obtain:

$$\sigma_2(0) = \frac{\lambda^2(\pi-\theta_o)^4}{64\pi} \tag{3.21}$$

when $\theta_o \sim \pi$, and

$$\sigma_2(0) = \frac{\lambda^2}{16\pi(\theta_o-\pi/2)^4} \tag{3.22}$$

when $\theta_o \sim \pi/2$.

A more general expression for the back scattering cross section is given by Schensted (1953) and Siegel et al (1953a, 1955b) as

$$\sigma_2(0) = \frac{\lambda^2}{\pi}\left|\sum_\nu \frac{e^{-i\nu\pi}\,\nu(\nu+1)}{\int_{\mu_o}^1 \left[P_\nu^1(\mu)\right]^2 d\mu}\right|^2 = \frac{\lambda^2}{\pi}\left|\sum_\nu \frac{e^{-i\nu\pi}}{\int_{\mu_o}^1 \left[P_\nu(\mu)\right]^2 d\mu}\right|^2 \tag{3.23}$$

where the summation is over the non-negative zeros of $\frac{dP_\nu}{d\theta_o}(\cos\theta_o)$, but only a finite number of terms must be included since the infinite series diverges. (See remarks following equation 3.32). Despite this drawback, the expression was used (Schensted, 1953; Siegel et al 1953a, 1955b) to yield the next order in the large and small cone angle approximations (3.21) and (3.22). These are

$$\sigma_2(0)=\frac{\lambda^2}{16\pi}(1+\cos\theta_o)^2\left[1+(2\log\frac{2}{1+\cos\theta_o}-1)(1+\cos\theta_o)\right] \tag{3.24}$$

for $\theta_o \sim \pi$, and

$$\sigma_2(0)=\frac{\lambda^2(1-4\cos^2\theta_o)}{16\pi\cos^4\theta_o} \tag{3.25}$$

for $\theta_o \sim \pi/2$.

The cross sections given in (3.24) and (3.25), as well as the first order approximations (3.21) and (3.22), are plotted in Fig. 7 as functions of θ_o.

3.3 Vector Boundary Condition.

The field of a transverse electric dipole of moment $4\pi\epsilon\underline{p}_t$ and arbitrary location is given by

$$\underline{E}^i=\nabla_\wedge\nabla_\wedge\left(\underline{p}_t\frac{e^{ik|\underline{r}-\underline{r}_1|}}{|r-r_1|}\right) \tag{3.26}$$

where $\underline{p}_t=p_{\theta_1}\hat{\theta}_1+p_{\phi_1}\hat{\phi}_1$. When this source is in the presence of a perfectly conducting semi-infinite cone, Felsen (1957b) gives the total field as

$$\underline{E}=\nabla_\wedge\nabla_\wedge\left\{\hat{r}\left(\frac{p_{\theta_1}}{r_1}\frac{\partial^2 S_1}{\partial\theta_1\partial r_1}+\frac{p_{\phi_1}}{r_1\sin\theta_1}\frac{\partial^2 S_1}{\partial\phi_1\partial r_1}\right)\right\}$$
$$-k^2\nabla_\wedge\left\{\hat{r}\left(\frac{p_{\phi_1}}{r_1}\frac{\partial S_2}{\partial\theta_1}-\frac{p_{\theta_1}}{r_1\sin\theta_1}\frac{\partial S_2}{\partial\phi_1}\right)\right\}, \tag{3.27}$$

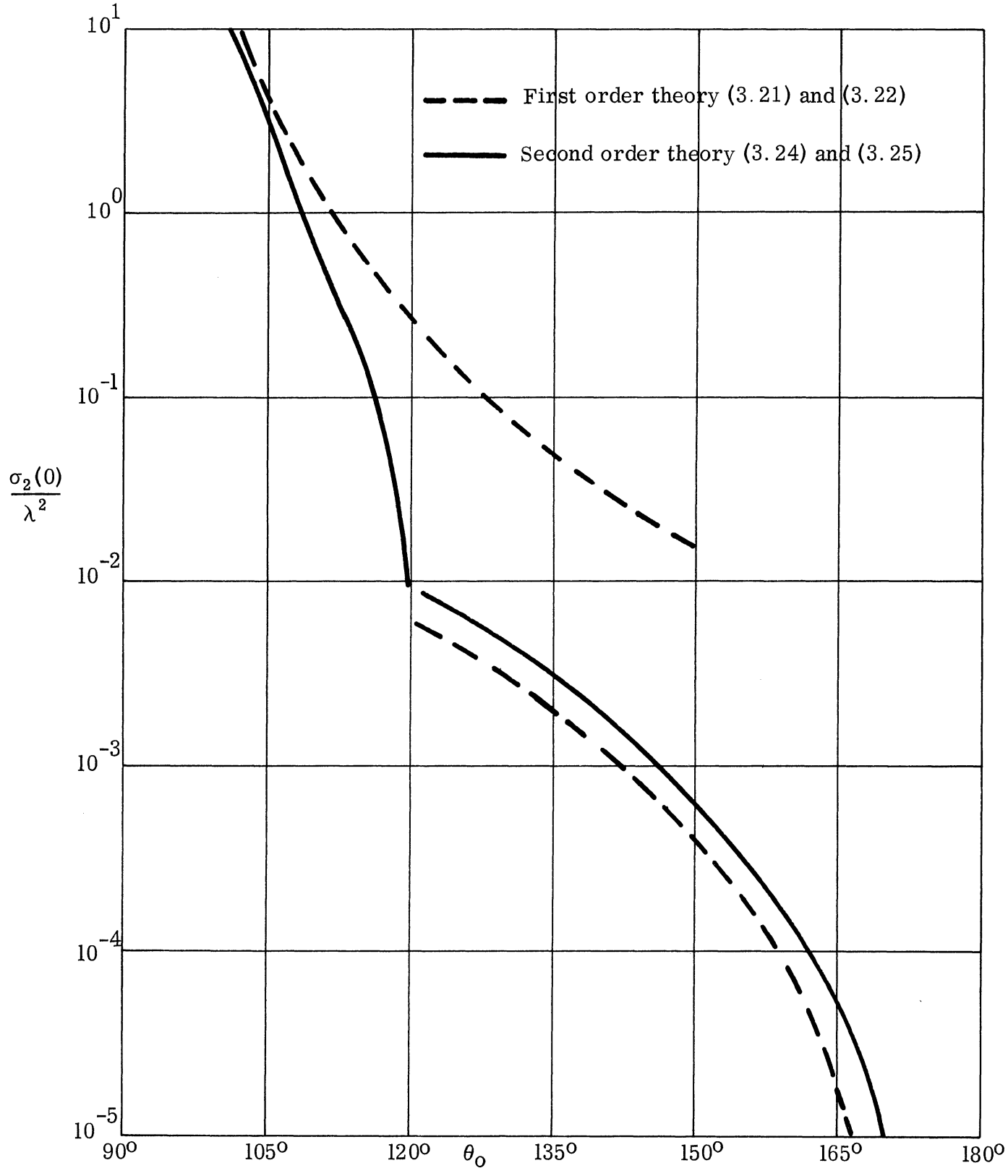

FIGURE 7: NOSE-ON BACK SCATTERING CROSS SECTION OF A HARD CONE

where

$$S_1 = -\frac{krr_1}{2}\sum_{m=o}^{\infty} \epsilon_m \cos m(\phi-\phi_1)\int_c d\nu \frac{(2\nu+1)j_\nu(kr_<)h_\nu(kr_>)\Gamma(\nu+m+1)P_\nu^{-m}(\cos\theta_<)}{\nu(\nu+1)\Gamma(\nu-m+1)\sin(\nu-m)\pi P_\nu^{-m}(\cos\theta_o)}$$

$$\cdot\left[P_\nu^{-m}(\cos\theta_>)P_\nu^{-m}(-\cos\theta_o)-P_\nu^{-m}(-\cos\theta_>)P_\nu^{-m}(\cos\theta_o)\right]$$

$$S_2 = -\frac{krr_1}{2}\sum_{m=0}^{\infty} \epsilon_m \cos m(\phi-\phi_1)\int_c d\nu \frac{(2\nu+1)j_\nu(kr_<)h_\nu(kr_>)\Gamma(\nu+m+1)P_\nu^{-m}(\cos\theta_<)}{\nu(\nu+1)\Gamma(\nu-m+1)\sin(\nu-m)\pi\frac{\partial}{\partial\theta_o}P_\nu^{-m}(\cos\theta_o)}$$

$$\cdot\left[P_\nu^{-m}(\cos\theta_>)\frac{\partial}{\partial\theta_o}P_\nu^{-m}(-\cos\theta_o)-P_\nu^{-m}(-\cos\theta_>)\frac{\partial}{\partial\theta_o}P_\nu^{-m}(\cos\theta_o)\right]$$

(3.28)

and the contour c encloses all positive zeros of the denominators of the integrands (but not $\nu = 0$) as shown in Fig. 8.

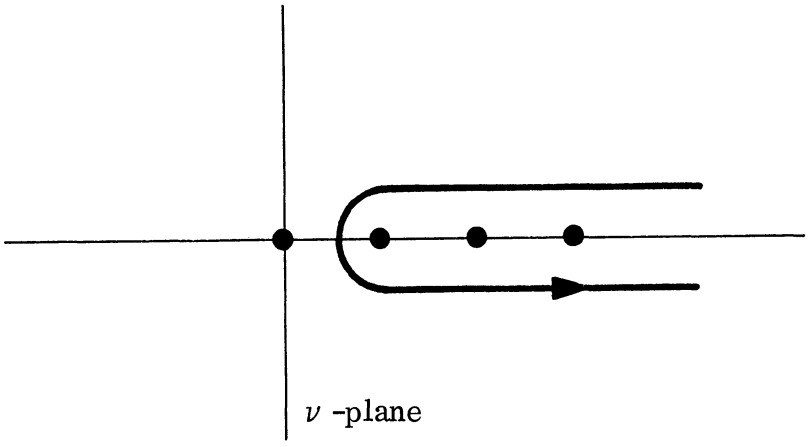

FIGURE 8

The notation is that defined under equation (3.1). Arbitrarily-oriented electric dipoles may always be decomposed into transverse and radial components, so that equation (3.27) together with (3.1) is sufficient to describe the field exterior to a perfectly conducting cone in the presence of an electric dipole, regardless of its location or orientation. An alternative representation, in terms of the tensor Green's function, is contained in Felsen (1957a), which also provides a comparable expression for an arbitrary magnetic dipole source.

When

$$\underline{E}^i = \hat{\phi}_1 \, e^{-ikr(\sin\theta \sin\theta_1 \cos(\phi - \phi_1) + \cos\theta \cos\theta_1)}$$

the scattered far field is given by Felsen (1957b) as

$$E^s_\theta = \frac{e^{ikr}}{ikr} \sin(\phi - \phi_1) \left(\frac{\pi - \theta_o}{2}\right)^2 \left[\frac{\sec^2\frac{\theta}{2} + \sec^2\frac{\theta_1}{2}}{\cos\theta + \cos\theta_1} + \frac{\sin^2\theta + \sin^2\theta_1}{2\cos^2\frac{\theta}{2}\cos^2\frac{\theta_1}{2}(\cos\theta + \cos\theta_1)^2} \right]$$

$$E^s_\phi = \frac{e^{ikr}}{ikr} \left(\frac{\pi - \theta_o}{2}\right)^2 \left\{ \frac{2\sin\theta\sin\theta_1}{(\cos\theta + \cos\theta_1)^3} + \cos(\phi - \phi_1) \left[\frac{\sec^2\frac{\theta}{2} + \sec^2\frac{\theta_1}{2}}{\cos\theta + \cos\theta_1} \right.\right.$$

$$\left.\left. + \frac{\sin^2\theta + \sin^2\theta_1}{2\cos^2\frac{\theta}{2}\cos^2\frac{\theta_1}{2}(\cos\theta + \cos\theta_1)^2} + \frac{16\sin^2\frac{\theta}{2}\sin^2\frac{\theta_1}{2}}{(\cos\theta + \cos\theta_1)^3} \right] \right\} \qquad (3.29)$$

under the restrictions

$$kr >> 1, \quad \theta_o \sim \pi, \quad \theta + \theta_1 < 2\theta_o - \pi \, .$$

Note that $\hat{\phi}_1 = \hat{i}_x$ when $\phi_1 = -\pi/2$.

In the particular case of back scattering ($\theta=\theta_1, \phi=\phi_1$) the above expressions for the field components reduce to

$$\underline{E}^i=\hat{\phi}_1 e^{-ikr}$$

$$E_\theta^s=0$$

and

$$E_\phi^s=\frac{e^{ikr}}{ikr}\left(\frac{\pi-\theta_o}{2}\right)^2\frac{3+\cos^2\theta}{4\cos^3\theta} \quad . \tag{3.30}$$

When a plane wave is incident along the axis of symmetry, that is,

$$\underline{E}^i=\hat{i}_x e^{-ikz} \tag{3.31}$$

the scattered far field is given by Hansen and Schiff (1948) (see also Mentzer, 1955) as

$$E_\theta^s=-\frac{ie^{ikr}}{kr}\cos\phi\left\{\sum_{\nu_\beta}\frac{e^{-i\nu_\beta\pi}P^1_{\nu_\beta}(\cos\theta)}{\sin\theta\int_{\mu_o}^1\left[P^1_{\nu_\beta}(\mu)\right]^2 d\mu}-\sum_{\nu_\alpha}\frac{e^{-i\nu_\alpha\pi}\frac{\partial}{\partial\theta}P^1_{\nu_\alpha}(\cos\theta)}{\int_{\mu_o}^1\left[P^1_{\nu_\alpha}(\mu)\right]^2 d\mu}\right\}$$

$$E_\phi^s=\frac{ie^{ikr}}{kr}\sin\phi\left\{\sum_{\nu_\beta}\frac{e^{-i\nu_\beta\pi}\frac{\partial}{\partial\theta}P^1_{\nu_\beta}(\cos\theta)}{\int_{\mu_o}^1\left[P^1_{\nu_\beta}(\mu)\right]^2 d\mu}-\sum_{\nu_\alpha}\frac{e^{-i\nu_\alpha\pi}P^1_{\nu_\alpha}(\cos\theta)}{\int_{\mu_o}^1\left[P^1_{\nu_\alpha}(\mu)\right]^2 d\mu}\right\} \tag{3.32}$$

where ν_α is such that $P^1_{\nu_\alpha}(\mu_o)=0$, $\nu_\alpha>-1/2$, ν_β is such that $\frac{\partial}{\partial\mu_o}P^1_{\nu_\beta}(\mu_o)=0$, $\nu_\beta>-1/2$,

and $kr >> 1$.

No upper limit is given for the sums. This omission stems from the fact that the ν_α and ν_β are infinite sets and if all the terms are included, the sums diverge. Siegel et al (1953a) estimate that when $\theta = 0$ (back scattering) approximately $\left[\frac{\sqrt{kr}}{100}\right]$ terms are of the form shown but the remaining terms (infinite in number) are negligible. This complication is avoided in the integral representation of the scattered field given by Felsen (1957b, d). Goryanov (1961) explicitly gives the integral representations corresponding to (3.32) as

$$E_\theta^s = -\frac{ie^{ikr}}{kr}\cos\phi\left\{-\frac{\partial}{\partial\theta}\int_0^\infty \nu \sinh(\nu\pi)F_1(\nu)d\nu + \frac{1}{\sin\theta}\int_0^\infty \nu \sinh(\nu\pi)F_2(\nu)d\nu + \frac{\cot^2\frac{\theta_o}{2}}{2\cos^2\frac{\theta}{2}}\right\} \tag{3.33}$$

$$E_\phi^s = \frac{ie^{ikr}}{kr}\sin\phi\left\{-\frac{1}{\sin\theta}\int_0^\infty \nu \sinh(\nu\pi)F_1(\nu) + \frac{\partial}{\partial\theta}\int_0^\infty \nu \sinh(\nu\pi)F_2(\nu)d\nu + \frac{\cot^2\frac{\theta_o}{2}}{2\cos^2\frac{\theta}{2}}\right\}$$

where

$$F_1(\nu) = \frac{P^1_{i\nu-1/2}(-\cos\theta_o)P^1_{i\nu-1/2}(\cos\theta)}{P^1_{i\nu-1/2}(\cos\theta_o)\cosh\nu\pi(\nu^2+1/4)}$$

$$F_2(\nu) = \frac{\frac{\partial}{\partial\theta_0} P^1_{i\nu-1/2}(-\cos\theta_0) P^1_{i\nu-1/2}(\cos\theta)}{\frac{\partial}{\partial\theta_0} P^1_{i\nu-1/2}(\cos\theta_0)\cosh(\nu\pi)(\nu^2+1/4)}$$

and

$$kr >> 1.$$

Equation (3.33) is valid only for $\theta < 2\theta_0 - \pi$, that is for field points exterior to the cone formed by the specularly reflected rays. For this range Goryanov (1961) reports extensive calculations of the bracketed terms in (3.33). Although his numerical results are presented only qualitatively, he concludes that the difference between the true far field and that predicted by physical optics (see below) increases uniformly with angle away from the back scattered direction and that the difference never exceeds 10 percent of the value computed with (3.33) for $\theta \leqslant 2\theta_0 - \pi - \pi/90$.

The far field components for the plane wave (3.31) incident along the axis of symmetry, as computed by physical optics (see section IV) are given by Goryanov in the form

$$E^s_\theta = -\frac{ie^{ikr}}{kr}\cos\phi\, L, \qquad E^s_\phi = \frac{ie^{ikr}}{kr}\sin\phi\, L$$

where

$$L = \left| \frac{\sin^2\theta_0\cos\theta_0}{4\cos\theta/2\left[\cos(\theta_0-\theta/2)\cos(\theta_0+\theta/2)\right]^{3/2}} \right| . \qquad (3.34)$$

The back scattered far field for this same incident field (3.31) has been approximated by Felsen (1953, 1955) as follows:

$$\underline{E}^s(0,0,z) = -\hat{i}_x e^{ikz} \sin^3\theta_o \left(1 - 2\sqrt{2}\,\xi\, e^{-i(2\xi^2+\pi/4)} \int_{(1-i)\xi}^{\infty} e^{-y^2}\, dy\right) \tag{3.35}$$

where

$$\xi = \left|\sqrt{kz}\,\cos\theta_o\right|$$

and $\theta_o \sim \pi/2, \quad kz >> 1, \quad \xi < 4\,;$

$$\underline{E}^s(0,0,z) = -\hat{i}_x \frac{ie^{ikz}}{4kz(\theta_o - \pi/2)^2} \tag{3.36}$$

for $\theta_o \sim \pi/2, \quad kz >> 1, \quad \xi > 4;$

and

$$\underline{E}^s(0,0,z) = -\hat{i}_x \frac{ie^{ikz}}{kz} \left(\frac{\pi-\theta_o}{2}\right)^2 \tag{3.37}$$

when $\dfrac{1}{\pi-\theta_o} >> kr >> 1.$

Note that the magnitudes of E^s given in (3.35) and (3.36) are plotted in Fig. 5.

Although all the field expressions given above can be used to calculate radar cross sections, the calculations which have been carried out explicitly invariably deal with plane wave incidence along the axis of symmetry. The physical optics result is then independent of ϕ and is given by Siegel et al (1955a) as

$$\sigma(\theta) = \frac{\lambda^2 \tan^4\theta_o}{16\pi} \cdot \frac{2(1+\cos 2\theta_o)^3}{(1+\cos\theta)(\cos\theta+\cos 2\theta_o)^3} \tag{3.38}$$

When $\theta = 0$ this reduces to the widely-quoted back scattering physical optics cross section, given first[+] by Spencer (1951) as

$$\sigma(0) = \frac{\lambda^2}{16\pi} \tan^4(\pi - \theta_o) \quad . \tag{3.39}$$

The small cone angle approximation of Felsen (1955) (equation 3.37) yields substantially the same cross section:

$$\sigma(0) = \frac{\lambda^2}{16\pi} (\pi - \theta_o)^4 \tag{3.40}$$

for $$\frac{1}{\pi - \theta_o} >> kr >> 1 \; .$$

The large cone angle approximation (3.36) also gives essentially the same result as physical optics, namely

$$\sigma(0) = \frac{\lambda^2}{16\pi} (\theta_o - \pi/2)^4 \tag{3.41}$$

for $$\theta_o \sim \pi/2, \qquad kr >> 1, \qquad \sqrt{kr} \cos\theta_o >> 1 \; .$$

The back scattering cross section obtained from the field expressions (3.32) is given by Hansen and Schiff (1948) (see also Siegel et al, 1953a, 1955b; and Mentzer, 1955) as

$$\sigma(0) = \frac{\lambda^2}{4\pi} \left| \sum_{\nu_\alpha} \frac{\nu_\alpha(\nu_\alpha+1) e^{-i\nu_\alpha \pi}}{\int_{\mu_o}^{1} \left[P^1_{\nu_\alpha}(\mu)\right]^2 d\mu} - \sum_{\nu_\beta} \frac{\nu_\beta(\nu_\beta+1) e^{-i\nu_\beta \pi}}{\int_{\mu_o}^{1} \left[P^1_{\nu_\beta}(\mu)\right]^2 d\mu} \right|^2 \tag{3.42}$$

[+] Hansen and Schiff(1948) quote an earlier version of Spencer's work, now unavailable.

where ν_α and ν_β are the zeros of $P^1_{\nu_\alpha}(\mu_o)$ and $\frac{\partial}{\partial \mu_o} P^1_{\nu_\beta}(\mu_o)$ respectively and the same convergence difficulties mentioned under (3.32) are still present. Despite these difficulties the expression was successfully employed by Schensted (1953) (see also Siegel et al, 1953a, 1955b; and Felsen, 1955) to yield second order corrections to equations (3.40) and (3.41). These are

$$\sigma(0) = \frac{\lambda^2}{16\pi \cos^4\theta_o}(1-2\cos^2\theta_o) \tag{3.43}$$

for $\theta_o \sim \pi/2$, and

$$\sigma(0) = \frac{\lambda^2}{4\pi}(1+\cos\theta_o)^2\left[1+3(1+\cos\theta_o)\right] \tag{3.44}$$

for $\theta_o \sim \pi$.

The cross sections given by equations (3.39), (3.40), (3.41), (3.43) and (3.44) are plotted in Fig. 9 as functions of θ_o.

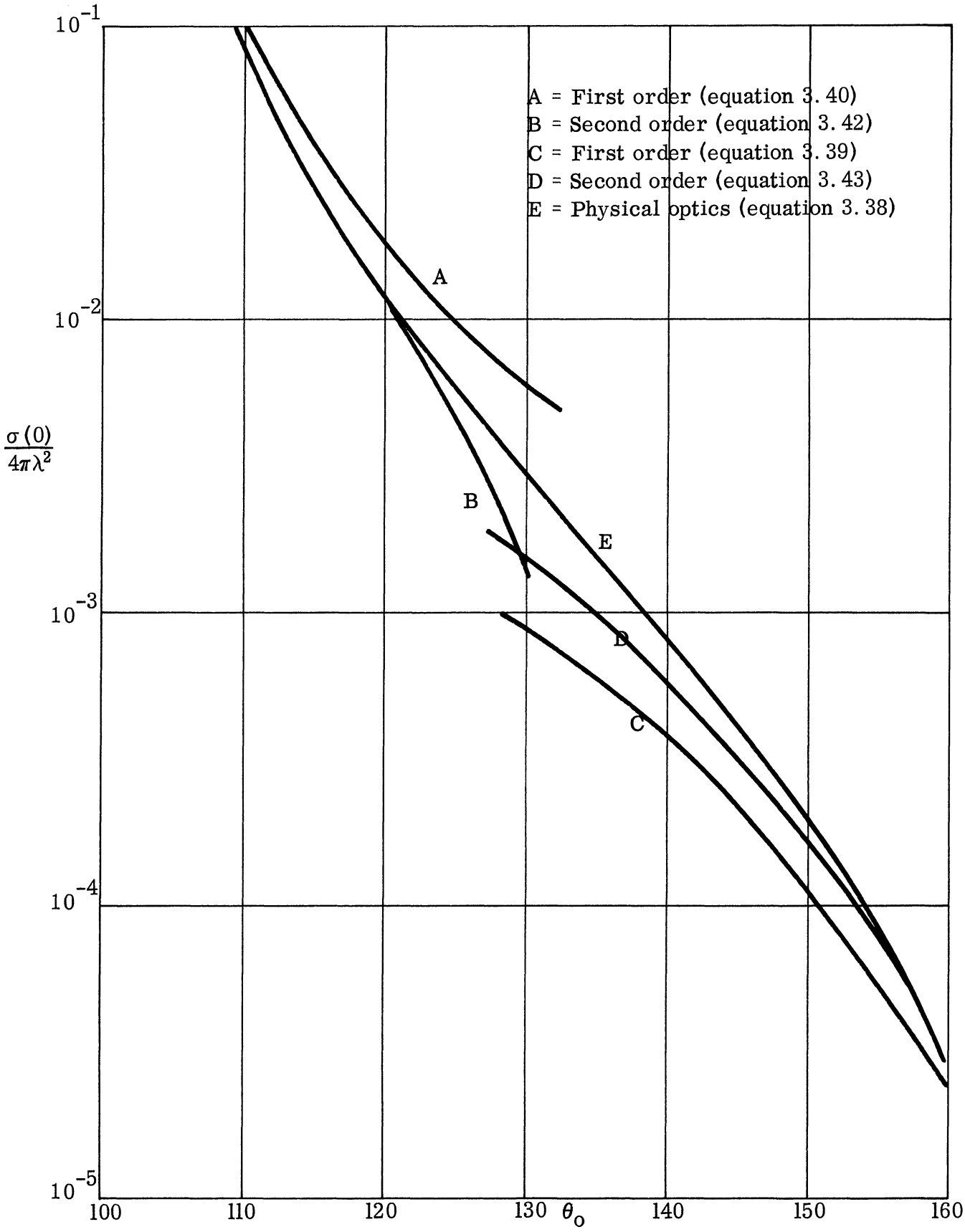

FIGURE 9: NOSE-ON BACK SCATTERING CROSS SECTION OF A PERFECTLY CONDUCTING CONE

IV
APPROXIMATE RESULTS FOR A FINITE CONE

Even for the semi-infinite cone the complexity of the exact solution is such that detailed computations are extremely difficult, and some approximation is almost essential if the physical content of the solution is to be apparent. For the finite cone the situation is still worse. The only exact solution available is for a spherically capped cone (Northover, 1962; Rogers et al, 1962) and the results are not yet amenable to computation. It is therefore appropriate to investigate the extent to which approximate techniques are applicable to this type of body.

In this section we shall be concerned exclusively with the back scattering cross section for plane wave incidence on a circular cone with any of several different types of terminations. The low frequency behavior is discussed in Section 4.1 and in the next section the physical optics method is used to derive the scattered field at high frequencies. The intermediate range of frequencies is again the difficult one, but in Section 4.3 some of the methods for extending the high frequency results into this range are presented.

4.1 Low Frequency Scattering

Consider a plane electromagnetic wave incident upon a body all of whose dimensions are finite. At sufficiently low frequencies, the complex amplitude of the scattered electric field in the far zone can be expanded in a series of increasing positive powers of k, where k is the wave number. If this amplitude is denoted

by $\underline{S}$, and is defined as the coefficient of e^{ikr}/kr where (r, θ, ϕ) are spherical polar coordinates referred to an origin in a neighborhood of the body, then

$$\underline{S} = k^3 \sum_{n=0}^{\infty} k^n \underline{f}_n \tag{4.1}$$

where the $\underline{f}_n$ are vector functions of the angular variables θ and ϕ, the body parameters and the characteristics of the incident field, but are independent of k. Since $\underline{S}$ is a dimensionless function, it is clear that each power of k must have associated with it a like power of some body dimension ℓ, and for sufficiently small values of $k\ell$ the series in (4.1) is convergent. The leading term corresponds to Rayleigh scattering and when substituted into the formula for the cross section (see introduction to Section 3), we have

$$\sigma = 4\pi k^4 \left| \underline{f}_o \right|^2 \tag{4.2}$$

which depends on the wavelength through the inverse fourth power. This is the well known Rayleigh law and holds for all angles of scattering including forward. For practical purposes, however, the case of back scattering is of most interest and attention will be confined to this for the remainder of the section.

The simplest body is the sphere and for this it is a straightforward matter to determine as many of the $\underline{f}_n$ as desired by appropriate expansion of the Mie series (Goodrich et al, 1961). In particular, the leading coefficient $\underline{f}_o$ is made up of contributions from an electric and a magnetic dipole with relative magnitudes 1

and 1/2 respectively, giving a net contribution $3a^2/2$ where a is the radius of the sphere. Hence

$$\sigma = 9\pi k^4 a^6 \tag{4.3}$$

which can be written as

$$\sigma = \frac{81}{16\pi} k^4 V^2 , \tag{4.4}$$

where V is the volume, and we remark that to this order in k any material of non-zero conductivity appears perfectly conducting.

Since exact results (such as the Mie series) are known for very few bodies it is fortunate that the $\underline{f}_n$ can be obtained in an alternative manner by solving certain scalar problems in potential theory. The technique is described in Senior and Darling (1963) and has been applied to the spherically capped cone by Darling (1960), leading to an expression for $\underline{f}_o$ in terms of infinite matrices. The method is formally applicable to any body which is the intersection of a finite number of regions within each of which the electrostatic Green's function is known, and can therefore be used in the treatment of cones with other types of termination.

For general bodies of revolution with on-axis excitation an approximate method for the determination of $|f_o|$, and hence of σ, has been proposed by Siegel (1959). The theory has its origin in the fact that as regards f_o, the body appears only as a singularity to the wave, and the structure of the body is in the nature of a second order correction. Since the return is also insensitive to changes in polarization, f_o can be a function only of the geometric properties of the shape, and the

obvious first choice for a function of dimension ℓ^3 is to take it proportional to the volume. Accordingly, we write

$$\sigma = C_1 k^4 (VF)^2 , \tag{4.5}$$

where C_1 is a pure number and F is a dimensionless correction factor that takes into account the approximate dependence of the cross section on the shape. From a study of the exact expression for $|f_o|$ for a spheroid of semi-major and semi-minor axes a and b respectively, Seigel deduced an expression for F of the form

$$F = 1 + \frac{1}{\pi y} e^{-y} , \tag{4.6}$$

where $y = b/a$, and with $C_1 = 4/\pi$ the resulting formula for σ is in agreement with the exact spheroid answer (Rayleigh, 1897) to within a few percent for all ellipticities. For the particular case of the sphere, $y = 1$ and equations (4.5) and (4.6) then imply

$$\sigma = 1.5889\, k^4 V^2 ,$$

compared with the correct result (equation 4.4)

$$\sigma = 1.6114\, k^4 V^2 .$$

If it is now assumed that (4.5) and (4.6) are a valid approximation for all bodies of revolution under symmetrical excitation with y taken as a measure of the elongation (the ratio of a characteristic dimension along the axis to one in the perpendicular direction), the formula can be used to derive the Rayleigh scattering cross section of a finite cone. Inasmuch as the nature of the termination is unlikely

to be important to this order of approximation[+] it is sufficient to confine attention to a right circular cone of altitude h and base radius a. The volume is then $\pi a^2 h/3$, and from the definition of y it would seem natural to choose $y = h/2a$. A better approximation, however, is to require that the cross section approach that of a disc as $h \rightarrow 0$, from which we have $y = h/4a$ (Siegel, 1959). The cross section of the cone in the low frequency limit is therefore

$$\sigma = \frac{4\pi}{9} k^4 a^4 h^2 \left\{ 1 + \frac{4a\, e^{-h/4a}}{\pi h} \right\}^2 \qquad (4.7)$$

The above formula is in good agreement with experiment (Brysk et al, 1959), though care is necessary to ensure that the frequency is low enough to justify its use. Since the cross section is determined by the volume and the maximum dimensions, the upper extremity of the Rayleigh region for most right circular cones is dictated by the slant length and not the base diameter even at nose-on incidence, which implies that for a cone of fixed diameter the Rayleigh region recedes with decreasing cone angle. In order to use equation (4.7) we therefore need

$$k \sqrt{h^2 + r^2} \ll 1$$

and this is the reason the experimental data of Keys and Primich (1959a) failed to display the anticipated wavelength dependence. We also observe that equations (4.5) and (4.6) are the same whether we view the object from the front or the rear, and

[+] Except for the extent to which the volume is then changed; but see Siegel (1963).

consequently for a cone in the Rayleigh region the nose-on and base-on cross sections should be identical. This was first pointed out by Siegel et al (1959) and has since been verified experimentally.

So far we have considered only electromagnetic scattering but a few words are necessary about the corresponding scalar problems associated with hard and soft bodies. The hard body (Neumann boundary condition at the surface) is the one of interest in acoustics and for this the low frequency expansion is similar to that shown in equation (4.1) except that the coefficients f_n are now scalar functions. Only a single dipole contributes to f_o, however, and the exact Rayleigh cross section for a hard sphere is

$$\sigma = \frac{25}{16\pi} k^4 V^2 \qquad (4.8)$$

which is smaller that the electromagnetic result by a factor 81/25. Siegel's approximate method leads to a value $C_1 = 1/\pi$ (a single dipole effect rather than two equal in-phase contributions) so that for a hard cone the cross section given in (4.7) must be reduced by a factor 4. For a soft body, on the other hand, the expansion for the far field amplitude S is quite different. The leading term is proportional to k with a coefficient which is simply the electrostatic capacity of the body (Senior and Darling, 1963), and the entire scattering behavior now differs accordingly.

4.2 High Frequency Scattering

At high frequencies the scattering behavior is more intimately related to the geometrical properties of the body, and if the wavelength is small in comparison

with all the major dimensions, an accurate approximation to the scattering cross section can be obtained by the method of physical optics. In many cases the method gives good results even when there are singularities on the surface, such as edges and points (as, for example, the vertex of the cone), and we shall begin by using it to calculate the back scattering cross section for a plane wave ($\underline{E}^i = e^{-ikz}\hat{i}_x$) at nose-on incidence on a cone with various types of termination.

The method is based on an approximation to the field distribution induced on the surface of the object. On the illuminated side of the surface each element is assumed to possess the field it would have possessed had it been part of an infinite tangent plane, whereas on the shadowed portion the field is taken to be zero. This leads to a current distribution which is zero in the shadow and twice the tangential component of the incident magnetic field in the lit region, and the calculation of the scattered field is now reduced to quadratures.

The general expression for the scattered field under this approximation is given in Crispin et al (1959). This simplifies considerably for the case of back scattering from a body of revolution at nose-on incidence. If such a surface is defined by the equation

$$z = g(\rho) \quad , \qquad \rho = \sqrt{x^2 + y^2}$$

then the scattered electric vector in the far field can be written as

$$\underline{E}^s = E^s \hat{i}_x, \qquad E^s = \frac{e^{ikr}}{kr}\left(ik^2 \int_a^b e^{-2ikg}\,\rho d\rho\right) \tag{4.9}$$

where the integration is carried out over the illuminated portion of the body (for a smooth convex body $a = 0$, $b = \rho_{shadow}$). The bracketed quantity in (4.9) is simply the far field amplitude and if this is denoted by S then

$$S = \frac{4\pi^2 i}{\lambda^2} \int_a^b e^{-2ikg}\,\rho d\rho \tag{4.10}$$

in terms of which the cross section is given by

$$\sigma = \frac{\lambda^2}{\pi} |S|^2 . \tag{4.11}$$

For a flat-backed cone of height h and semi-vertex angle $\pi - \theta_o$,

$$S = \frac{4i\pi^2}{\lambda^2} \tan^2\theta_o \int_o^h e^{2iku}\,u du$$

$$= -\frac{i}{4} \tan^2\theta_o \left\{1 + e^{2ikh}(2ikh - 1)\right\} , \tag{4.12}$$

which implies a scattering amplitude

$$-\frac{i}{4} \tan^2\theta_o \tag{4.13}$$

associated with the tip, and a scattering amplitude

$$-\frac{i}{4}\tan^2\theta_o(2ikh - 1)e^{2ikh} \tag{4.14}$$

corresponding to the edge singularity at the base. For large (but finite) kh the latter is approximately

$$\frac{\pi h}{\lambda}\tan^2\theta_o\, e^{2ikh} \tag{4.15}$$

which dominates the overall return at high frequencies due to its wavelength dependence. In practice, however, a more accurate estimate of the base return is required, and this is considered later.

In the limit of a semi-infinite cone ($h = \infty$) no return can come from the "termination" and the second of the above contributions must be ignored. This is usually justified on a mathematical basis by attributing a non-zero conductivity to the surrounding medium (giving k a positive imaginary part), so that the second term in (4.12) is exponentially attenuated through the factor e^{2ikh}. The only return is now provided by the tip, and from (4.13) we have

$$\sigma = \frac{\lambda^2}{16\pi}\tan^4\theta_o \tag{4.16}$$

which is the well known "tip" answer.

With terminations other than a flat back the physical optics result will only be affected if a portion of the cap is in the illuminated region, and consequently for a spherically-capped cone with the origin of the sphere at the apex of the cone (or,

indeed, on the axis of the cone at any distance X from the apex with $0 \leqslant X \leqslant h$) the predicted return is identical to that in equation (4.12). But if the sphere is chosen to have its origin at a distance $h + X$ $(X > 0)$ from the apex, with radius $\left\{(h\tan\theta_o)^2 + X^2\right\}^{1/2}$ (so as to achieve a join to the cone with a discontinuity in at most the first derivative of the profile[+]), a part of the sphere is visible, and the physical optics cross section is changed accordingly. The far field amplitude is now

$$S = -\frac{i}{4}\left\{\tan^2\theta_o + e^{2ikh}\left[2ik(h\tan^2\theta_o - X) - \sec^2\theta_o\right] + e^{2ik(X+h)}\right\} \quad (4.17)$$

The first term arises from the tip and is as before. The second group of terms represents the scattering amplitude associated with the join, and can be written approximately as

$$S = \frac{i}{4}\sec^2\theta_o\left\{1 - 2ikh\tan\theta_o\tan\delta\right\} e^{2ikh} \quad (4.18)$$

where δ is the angle between the tangents to the cone and the sphere at their junction. Hence, for the cone-sphere ($\delta = 0$) the scattering amplitude attributable to the join is

$$S = \frac{i}{4}\sec^2\theta_o\, e^{2ikh} \quad , \quad (4.19)$$

which has the same wavelength dependence as the tip contribution, but is of a much larger magnitude for all cones except those of largest angle. It is believed that this

[+]The profile is simply the curve $z = g(\rho)$ which defines the body.

is an accurate estimate of the return when the first derivatives[+] of the profile are matched. Inasmuch as the surface in the neighborhood of the singularity is entirely in the illuminated region, the assumed current distribution should not be appreciably in error, and the most accurate experimental data available in the Radiation Laboratory is consistent with a scattering amplitude having this wavelength dependence, and a magnitude differing from that in (4.19) by less than 20 percent.

On the other hand, if the kink angle δ is not zero, the second term in (4.18) is present, and will dominate the return at high frequencies. The corresponding far field amplitude is

$$S = \frac{a\pi}{\lambda} \sec^2\theta_o \tan\delta \; e^{2ikh}, \qquad (4.20)$$

where a is the radius of the singularity, and this is almost identical to the result obtained by Dawson et al (1960) using circular wedge theory (see later discussion). It is therefore obvious that in any experimental measurement of cone-sphere cross sections extreme care must be taken to ensure accurate modeling of the surface profile near to the cone-sphere join.

The third term in equation (4.17) originates at the shadow boundary of the sphere and is known to be spurious. It arises because of the discontinuity in the current distribution introduced by the physical optics approximation, and is independent

[+] The wavelength dependence of the physical optics contribution from a junction between two surfaces is λ^{n-1}, where n is the order of the first discontinuous derivative.

of the presence of the cone. From an analysis of the field scattered by a sphere (see, for example, Goodrich et al, 1961), it is seen that the only contribution from the shadow boundary is produced by a set of creeping waves which have traversed the back of the sphere. The associated scattering amplitude decreases exponentially with increasing frequency, and is small compared with the specular return for all spheres more than a few wavelengths in radius. With the cone-sphere, however, the specular return is not present, and since the contributions from the tip and join are quite small in magnitude (and certainly so when compared with a specular signal) the creeping waves continue to provide a significant effect until the wavelength has decreased to a very small fraction of the sphere radius. Nevertheless, at sufficiently high frequencies the creeping waves can be ignored, and there is some slight evidence (Turner and Dawson[+], 1960; unpublished Radiation Laboratory data) to suggest that the best estimate of the cone-sphere return is then obtained by ignoring the spurious term in (4.17). The resulting high frequency cross section is

$$\sigma = \frac{\lambda^2}{16\pi} (\tan^4\theta_o + \sec^4\theta_o) \qquad (4.21)$$

and since the term produced by the phase factor e^{2ikh} has been omitted, (4.21) should be interpreted as an average over a small frequency band. For small cone angles the cross section is of order $0.02\lambda^2$, which is approximately one-half that which would have been found if the spurious term had been retained

[+] who also use the physical optics method to calculate the return due to a termination produced by the rotation of an off-set spherical arc about the cone axis.

Before leaving this discussion of the nose-on behavior, a final point of interest is the transition of the cross section for the flat-backed cone to the disc answer. As the half-cone angle $\pi - \theta_o$ approaches $\pi/2$, with the base radius a held constant, the cone degenerates into a disc whose far field amplitude is inversely proportional to λ^2. The manner in which this transition occurs can be seen from equation (4.12) if $\tan\theta_o$ is replaced by $-a/h$. We then have

$$S = -\frac{i}{4}(a/h)^2 \left\{1 + e^{2ikh}(2ikh - 1)\right\} \qquad (4.22)$$

and by expanding the exponential function for small argument it is found that as $h \to 0$ the bracketed terms decrease in just such a way as to cancel the infinity produced by the first factor. In the limit $h = 0$ the far field amplitude is simply

$$S = 2i\left(\frac{\pi a}{\lambda}\right)^2 \qquad (4.23)$$

which is the known result for a disc of radius a. We note in passing that this is also the appropriate expression for rear-on incidence on a flat-backed cone.

For angles of incidence away from nose-on the calculation of the back scattering cross section by the physical optics method is again straightforward, though more tedious owing to the asymmetrical illumination and (possibly) the varying position of the shadow boundary as a function of aspect. Moreover, because of the inaccuracy in the prediction of the shadow boundary effect, the usefulness of the method is mainly limited to the determination of the specular return from the cone sides and its side lobes. For such a calculation it is generally sufficient to assume that the

cone has a flat back, though the type of termination will affect the manner in which the return falls off at aspects beyond the specular direction.

If the plane wave is incident at an angle α to the negative z axis, the optics integral can be obtained from the general expression in section 4.3 of Crispin et al (1959). When this is particularized to the problem of a right circular cone and the notation changed to that presently in use, the expression for the far field amplitude becomes

$$S = -\frac{2i\pi}{\lambda^2}\tan\theta_o \iint \left\{\sin\alpha\cos\phi - \cos\alpha\tan\theta_o\right\} \cdot e^{2ikz'(\cos\alpha + \sin\alpha\tan\theta_o\cos\phi)} z'dz'd\phi \tag{4.24}$$

where z' is measured along the axis of the body and the integration is over the illuminated portion. The result is independent of whether the electric vector lies in the plane containing the axis and the direction of propagation (horizontal polarization) or in the plane perpendicular thereto (vertical polarization).

When the direction of incidence lies within the backward cone, i.e. $0 \leqslant \alpha \leqslant \pi - \theta_o$, the whole of the surface is illuminated and the z' integration can be carried out immediately to give

$$S = \frac{i}{8\pi}\tan\theta_o \int_{-\pi}^{\pi} \frac{\sin\alpha\cos\phi - \cos\alpha\tan\theta_o}{(\cos\alpha + \sin\alpha\tan\theta_o\cos\phi)^2} \left[1 - \left\{1 - 2ikh(\cos\alpha + \sin\alpha\tan\theta_o\cos\phi)\right\} e^{2ikh(\cos\alpha+\sin\alpha\tan\theta_o\cos\phi)}\right] d\phi . \tag{4.25}$$

In the special case of nose-on incidence ($\alpha = 0$) the ϕ integration is trivial, leading to the result shown in equation (4.12), but otherwise the validity of (4.25) is limited to angles α away from the specular direction $\theta_o - \pi/2$ (which lies within the backward cone only for half angles $\pi - \theta_o > \pi/4$). The integration of the first term in (4.25) gives[+]

$$-\frac{i}{4}\ \frac{\tan^2\theta_o}{(1 - \sin^2\alpha \sec^2\theta_o)^{3/2}} \tag{4.26}$$

which is the required generalization of the tip return (4.13). If in addition $kh \sin\alpha \tan(\pi - \theta_o) \ll 1$, the second group of terms in (4.25) can be treated by expanding the exponential for small argument, leading to a simple multiple of (4.26) but with a phase corresponding to a contribution from the base of the cone. Hence, for incidence in the backward cone with $kh \sin\alpha \tan(\pi - \theta_o) \ll 1$,

$$S \simeq -\frac{i}{4} \tan^2\theta_o (1 + 3 \sin^2\alpha \sec^2\theta_o) \left[1 + e^{2ikh\cos\alpha}(2ikh\cos\alpha - 1)\right] \tag{4.27}$$

which should be compared with the expression for nose-on incidence shown in equation (4.12). On the other hand, if $kh \sin\alpha \tan(\pi - \theta_o) \gg 1$ the integration of the second group of terms in (4.25) can be carried out by the stationary phase method, and the resulting far field amplitude is

$$S = \frac{1}{4} e^{i\pi/4} \sqrt{\frac{kh \tan(\pi - \theta_o)}{\pi \sin\alpha}}\ \tan(\alpha - \theta_o)\ e^{2ikh\cos(\alpha - \theta_o)\sec\theta_o} \tag{4.28}$$

[+]A result first obtained by Spencer (1951).

The phase is now appropriate to a contribution from the base end of the nearest generator of the cone, and because of the restriction on kh under which the above expression was obtained, the tip contribution is negligible by comparison.

For angles of incidence outside the backward cone only a portion of the surface is illuminated, but this fact is of no concern if the stationary phase method is applied to the ϕ integral in (4.24). We then have

$$S = -e^{-i\pi/4} k \sqrt{\frac{\tan(\pi - \theta_o)}{2\lambda \sin\alpha}} \sin(\alpha - \theta_o) \sec\theta_o \int_o^h e^{2ikz'\cos(\alpha - \theta_o)\sec\theta_o} \sqrt{z'}\, dz'$$

which can be written as

$$S = \frac{1}{4} e^{i\pi/4} \sqrt{\frac{kh\tan(\pi - \theta_o)}{\pi \sin\alpha}} \tan(\alpha - \theta_o)\, e^{2ikh\cos(\alpha - \theta_o)\sec\theta_o} \cdot \left\{1 - F\left(\sqrt{2kh\cos(\alpha - \theta_o)\sec\theta_o}\right)\right\} \tag{4.29}$$

where

$$F(\tau) = \frac{e^{-i\tau^2}}{\tau} \int_o^\tau e^{ir^2}\, dr,$$

and is related to the Fresnel integral (see, for example, Jahnke and Emde, 1945). If $|\tau| \gg 1$, $F(\tau) = O(\tau^{-1})$ and can be neglected in comparison with the first term in (4.29), in which case we recover the expression shown in (4.28). For small $|\tau|$, however,

$$F(\tau) = 1 - \frac{2}{3} i\tau^2 + O(\tau^4)$$

and consequently as α approaches $\theta_o - \pi/2$, the far field amplitude reduces to

$$S = -\frac{kh}{3} e^{-i\pi/4} \sqrt{\frac{kh \sin\theta_o}{\pi}} \sec^2\theta_o . \qquad (4.30)$$

This is the specular contribution. It is equivalent to the broadside return from a thick cylinder whose length is the slant length of the cone and whose radius is $4/9\, a \sec(\pi - \theta_o)$, where $a = h\tan(\pi - \theta_o)$ is the base radius of the cone, but this choice of dimension is not unique, nor is it sufficient for computing the side lobes. Indeed, the far side lobes must be calculated from equation (4.28) and to investigate the transition from (4.28) to (4.30) it is necessary to determine S from (4.29) using the available tabulations of the Fresnel integral. The asymmetrical nature of the side lobes is then apparent[+] even for the flat-backed cone, and can be observed in the experimental data of Keys and Primich (1959c, d).

As previously remarked, one of the limitations of the physical optics approach is the inaccuracy of its prediction of the return from a shadow boundary. If a flat-backed cone (or any finite cone whose termination leads to a "positive" discontinuity in the first derivative of the surface profile at the join) is viewed at or near nose-on, the shadow boundary coincides with the base of the cone, and the physical optics result for the scattering from the base is suspect. Moreover, at high frequencies the

[+] This is also evident from equation (4.29) if the Fresnel integral is approximated for small values of its argument.

base has the appearance of a ring singularity at these aspects, suggesting that the corresponding contribution will be dominant; even physical optics displays this fact (see equation 4.15), but before any reliance is placed upon the magnitude which it predicts an alternative method of derivation is desirable. This is particularly so since (4.15) can be written as

$$S = \frac{\pi a}{\lambda} \tan(\pi - \theta_o)\, e^{2ika\cot(\pi - \theta_o)} ; \qquad (4.31)$$

for fixed a, the far field amplitude tends to zero with decreasing cone angle, whereas the analogy with the ring would suggest a limit which is finite but non-zero.

To provide a more accurate estimate of the base return at high frequencies, a method was proposed by Siegel in 1957 (see Siegel, 1959) which is similar to one employed by Artmann (1950) in his analysis of the thick half-plane. Taking, for example, a flat-backed cone at nose-on incidence, the idea is to treat every element of the edge formed by the sides of the cone and the base as a portion of an infinite wedge on which the field is incident at an appropriate angle. By using the known solution for such a wedge, and regarding every element as scattering independently of the rest, the net return can be obtained by simple integration providing due account is taken of the varying polarization for the different elements. The solution originally developed was in error because of an incorrect interpretation of the polarization effect. The error was pointed out by Keller (1959) and duly corrected (Siegel et al, 1959). Simultaneously, Keller (1959; but see 1960) published an alternative

derivation based on his geometrical theory of diffraction (Keller, 1957), and presented the solutions[+] for all aspects, hard and soft scalar cases as well as vector. For the electromagnetic problem with nose-on incidence the far field amplitude associated with the base return is

$$S = -\frac{\pi a}{n\lambda} \operatorname{cosec} \frac{2\pi}{n} e^{2ika \cot(\pi - \theta_o)} \tag{4.32}$$

where

$$n = \frac{5}{2} - \frac{\theta_o}{\pi} , \tag{4.33}$$

and compared with the physical optics solution (4.31) which tends to zero as $\theta_o \to \pi$ (cone of vanishing angle), (4.32) is non-zero at this limit.

A graphical comparison of the two solutions as a function of cone angle is given in Siegel et al (1959) and clearly shows the increasing discrepancy as $\theta_o \to \pi$. For small cone angles, the previous estimates of the base return must therefore be abandoned in favor of that obtained by wedge theory. Accordingly, (4.15) and (4.31) must be replaced by (4.32), but for a termination which produces only a slight kink in the profile (or no kink at all), wedge theory and physical optics are in agreement, and consequently the results for the cone-sphere are unaffected.

[+] Two errors in Keller (1959, 1960) were noted in 1960 (see Crispin et al, 1963) and corrected by Keller (1961). The second term in equation (29) of Keller's papers should be $(\cos \pi/n - \cos 3\pi/n)^{-1}$, and the legends attached to the two curves in Fig. 4 should be interchanged.

As $\theta_o \rightarrow \pi/2$ (the disc), both (4.31) and (4.32) tend to infinity, and do so at the same rate. Neither of them now provides a satisfactory estimate of the base return. On the other hand, we have already seen that the three-term optics approximation (4.12) is successful in reproducing the correct transitional behavior, and for wide angle cones (4.12) should be used in place of either (4.31) or (4.32). As of the moment one must arbitrarily choose the cone angle at which to switch from (4.32) to (4.12), but it has been suggested (Crispin et al, 1963) that if $h \gg a$, (4.32) should be used; if $kh \ll 1 \ll ka$, (4.12); and if h and a are comparable, the mean of the two results.

In an attempt to predict the high frequency scattering with an accuracy greater than that which can be achieved by physical optics, the cylindrical current method has been proposed by Dawson and Turner (1960). This also is based on an approximation to the current distribution excited on the surface, and as such is similar to physical optics, but whereas the latter assumes that each element scatters as though part of an infinite tangent plane, the new approach postulates a current which is the same as for an infinite cylinder having axis and radius identical to those of the body at the point in question. It is therefore limited to bodies of revolution, but formally at least it is "valid" for a much wider range of radius to wavelength ratios providing that the cylinder solution is used in its exact form. If the incident electric vector is normal to the plane containing the direction of propagation and the axis of the body (vertical polarization), the far field amplitude obtained by this method is

$$S = \frac{2i}{\lambda} \int S_1 \, e^{2ikz'\cos\alpha} \, dz' \tag{4.34}$$

where

$$S_1 = \sum_{-\infty}^{\infty} (-1)^n \frac{J_n'(kR\sin\alpha)}{H_n^{(1)'}(kR\sin\alpha)} \tag{4.35}$$

and R is the radius of the body at a distance z' along its axis. For horizontal polarization the solution differs only in having S_1 replaced by S_2, the corresponding sum over the undifferentiated functions.

With all except the most trivial bodies, an exact analytical evaluation of the above integral is impossible, and a digital computer is almost essential if the full advantages of the method are to be realized. Nevertheless, if $kR\sin\alpha \gg 1$, $-S_1$ and S_2 can both be approximated by the function

$$\frac{1}{2} \sqrt{\pi kR\sin\alpha} \; e^{i(\pi/4 - 2kR\sin\alpha)} ,$$

and when expressed in terms of the electric vector the scattering amplitudes for vertical and horizontal polarization are now identical. This is the same type of polarization independence displayed by the physical optics method. The resulting expression for S is

$$S = -\frac{i}{\lambda} \sqrt{\pi k\sin\alpha} \; e^{i\pi/4} \int \sqrt{R} \, e^{2ik(z'\cos\alpha - R\sin\alpha)} \, dz' \tag{4.36}$$

with $R = R(z')$, and this has been evaluated by Dawson and Turner (1960), Turner (1960) for bodies of various shapes. In particular, for the flat-backed cone

$R = -z' \tan\theta_o$, $0 \leqslant z' \leqslant h$, and the far field amplitude associated with the return from the cone sides is then of the same form as that shown in equation (4.29), but is smaller[+] by a factor $(1 - \tan\theta_o \cot\alpha)$. This implies a reduction in the specular contribution by a factor $\sec^2\theta_o$. Analogous results for the cone-sphere have also been given by Dawson and Turner (1960), and these reveal a similar discrepancy with the physical optics predictions.

In spite of the functional differences between the two sets of formulae, the differences in their numerical values are only significant for wide angle cones, and the experimental data available at the moment is not sufficient to show which of the two methods is more accurate. For a body of revolution the cylindrical current method would seem to have the greater potential, but is possible that the intrinsic accuracy is lost in the approximation to S_1 and S_2. Certainly this approximation prevents any consideration of nose-on incidence, and for this range of aspects we are forced to rely on physical optics, or the other high frequency approximations described in this section.

[+]For a body of revolution whose dimensions are greater than a wavelength or so and whose surface is half in shadow, Turner (1960) claims that the two methods are, in fact, equivalent. However, the proof appears to assume that R is independent of z', and since the body is then a cylinder of constant radius, this is the one case for which the conclusion is obvious.

4.3 The Resonance Region

The resonance region can be regarded as the frequency range for which the wavelength is comparable to a major dimension of the body. It is intermediate to the ranges for which the Rayleigh and optical (high frequency) laws apply, and is usually characterized by the presence of large oscillations in the back scattering cross section as a function of wavelength. It also poses one of the severest challenges to the theoretician since it is here the the transition between two contrasting types of scattering behavior takes place.

In attempting to investigate this region it is natural to consider the possibility of extending the techniques appropriate to the neighboring frequency ranges. By including more terms in the low frequency expansion (4.1) it may be feasible to penetrate the region to some small extent, but since the series has a finite radius of convergence (Senior and Darling, 1963) this procedure is strictly limited both in theory and in practice. On the other hand, no formal restriction of this type exists at the high frequency end, and at least a partial coverage of the resonance region can be achieved by applying the pseudo asymptotic techniques available at high frequencies.

In the case of a flat-backed cone the necessary extension can be obtained using the geometrical theory of diffraction, and for nose-on incidence the appropriate formulae have been derived by Keller (1960). Whereas the wedge solution (4.32) corresponds to those rays which are scattered by the base and return directly to the receiver, the second order term is produced by rays which traverse the base of the

cone, and are therefore diffracted twice before being observed. The far field amplitude correct to this order is now

$$S = -\frac{\pi a}{n\lambda}\,\mathrm{cosec}\frac{2\pi}{n}\,e^{2ika\cot(\pi-\theta_o)}\left\{1+\frac{1}{n}\sin\frac{\pi}{n}\,\frac{e^{2ika-i\pi/4}}{(\pi ka)^{1/2}}\,\frac{\cos\frac{\pi}{n}-\cos\frac{3\pi}{n}}{\left(\cos\frac{\pi}{n}-\cos\frac{3\pi}{2n}\right)^2}\right\} \tag{4.37}$$

where n is defined in equation (4.33), and the curves shown in Figs. 10 through 20 are based on this formula. The agreement between theory and experiment is remarkably good even down to values of ka of order unity. Since the exponential within the braces in (4.37) has a negative coefficient for all cone angles, the maxima in the cross section occur at

$$ka = (m + 5/8)\pi \ ,$$

$m = 0, 1, 2\ldots$, and the minima when

$$ka = (m + 9/8)\pi$$

(see, for example, Fig. 4 of Keller, 1960). The curve intersects that of the Rayleigh cross section at around ka = 1, and between them these two formulae are sufficient to indicate the variation of the nose-on return throughout the resonance region.

For angles of incidence away from nose-on an accurate determination of the back scattering cross section of a flat-backed cone is not so important for most purposes, and because of this the formulae have received less attention. In particular the geometrical theory of diffraction has only been taken as far as the first order

(high frequency) term, but it may be appropriate to summarize the formulae and give a few remarks about their applicability.

If the incidence is at an angle $\alpha \neq 0$ but within the backward cone the far field amplitude corresponding to (4.32) is

$$S = u(\alpha) + u(-\alpha) \tag{4.38}$$

(Keller, 1960) where[+]

$$u(\alpha) = \frac{1}{n} \cot \frac{\pi}{2n} \sqrt{\frac{a}{\lambda \sin\alpha}}\, e^{i\left\{\pi/4 - 2ka \operatorname{cosec} \theta_o \cos(\alpha - \theta_o)\right\}} \cdot \left\{1 \mp \frac{\cos\frac{\pi}{n} - 1}{\cos\frac{\pi}{n} - \cos\frac{3\pi - 2\alpha}{n}}\right\} . \tag{4.39}$$

with the upper sign for vertical polarization (or soft body) and the lower for horizontal polarization (hard body). We observe that $u(\alpha) \to \infty$ as $\alpha \to 0$: this is a consequence of the caustic which exists along the continuation of the cone's axis.

The above expression also holds in the aspect range $\pi/2 < \alpha < \pi$ providing the term $\cos\frac{3\pi + 2\alpha}{n}$ is replaced by $\cos\frac{2\alpha - \pi}{n}$, but is infinite at $\alpha = \pi$. This is again attributable to a caustic and to the differing wavelength dependence which then characterizes the solution. Physically the increasing value of S is associated with the specular lobe, and at $\alpha = \pi$ the contribution (4.23) is present and dominates the return through its lower wavelength dependence. Inasmuch as these are all first

[+] $\sqrt{\sin(-\alpha)}$ must be interpreted as $i\sqrt{\sin\alpha}$ in the formula for $u(-\alpha)$.

order results only, they give no information about the behavior of the field in the immediate vicinity of $\alpha = \pi$, and until such time as more detailed results are available, the only method for estimating the transition is to use the physical optics solution for a disc. We then have

$$S \simeq -\frac{ika}{2\tan\alpha} J_1(2ka\sin\alpha)\, e^{-2ika\cot(\pi - \theta_o)\cos\alpha} \tag{4.40}$$

(Crispin et al, 1959), which can be used for those angles α near to π at which the magnitude of (4.40) exceeds that of (4.38).

In the aspect range $\pi - \theta_o < \alpha < \pi/2$ the second diffracted wave does not appear, and the geometrical theory of diffraction then gives

$$S = u(\alpha) . \tag{4.41}$$

This is analogous to the physical optics result (4.23), and each can be written as

$$S = A(\alpha, \theta_o) \sqrt{\frac{a}{\lambda \sin\alpha}}\, e^{i\left\{\pi/4 - 2ka\cos(\alpha - \theta_o)\operatorname{cosec}\theta_o\right\}} \tag{4.42}$$

where A is a real quantity, but the values of A are quite distinct both in form and in magnitude. Unfortunately, a study of the experimental data does not provide a clear-cut indication of the formula which is preferable. Because of the inaccuracy associated with the physical optics prediction of the return from a shadow boundary (the base is part of the boundary at these aspects) it would seem that equation (4.41) should be more accurate, and certainly it does explain some of the dependence on polarization observable in the data (we shall later examine another source of a

polarization-dependent return not predicted by either theory). On the other hand, (4.41) is discontinuous[+] at $\alpha = \pi - \theta_o$ (cf equation 4.38), whereas the optics result is continuous, and it is also infinite at $\alpha = \theta_o - \pi/2$. This last is due to the specular return from the sides of the cone, and in a neighborhood of $\alpha = \theta_o - \pi/2$ we have no alternative but to use (4.29), replacing it by (4.41) when the magnitudes of the two contributions have become comparable.

In passing we note that the aspect range $\pi - \theta_o < \alpha < \pi/2$ is one for which a portion of the conical surface is in shadow, and it is now possible for a creeping wave contribution to appear. This is a polarization-dependent phenomenon and has been discussed by Goodrich et al (1958, 1959) in connection with the radiation pattern of slots on a cone. Its importance in the scattering problem has not yet been assessed, but it is unlikely to be significant.

Let us now consider the cone-sphere. The theory given by Keller (1960) predicts that for incidence within the backward cone the scattered field is composed of contributions from the tip and from the shadow boundary. The first of these can be obtained using physical optics, and is given in (4.26). The second is attributable to creeping waves which have traversed the back of the sphere, and since the separation between the cone-sphere join and the boundary increases with increasing frequency, it seems reasonable to estimate this return by reference to the known

[+] It is also discontinuous at $\alpha = \pi/2$.

sphere solution. Following Keller, the appropriate far field amplitude is then

$$S = -\frac{1}{4}(kb)^{4/3} e^{ikb\left\{\pi + 2\cos\alpha \operatorname{cosec}(\pi-\theta_o)\right\}} \left\{ G_H e^{-\tau_H (kb)^{1/3}} - G_S e^{-\tau_S (kb)^{1/3}} \right\} \tag{4.43}$$

where $b = a\sec(\pi-\theta_o)$ is the radius of the sphere and G_H, G_S, τ_S, τ_H are certain parameters which are defined in terms of Airy functions and their zeros. The second term is negligible in comparison with the first.

When the relative magnitudes of (4.26) and (4.43) are examined, it is found that for all except the very highest frequencies the latter is dominant in spite of its exponential decay. Thus, for example, when $\theta_o = 5\pi/6$ and $\alpha = 0$, equality between the two contributions is not reached until kb = 45.8 and consequently, as kb increases, the back scattering cross section σ/λ^2 should display an oscillation of increasing amplitude which reaches a maximum when kb = 45.8, and thereafter decreases. In particular, for kb less than (about) 15 the curve should be almost monotonic with the cross section given by the creeping waves alone; and for kb greater than (about) 80 the cross section should be effectively constant and equal to the tip contribution.

These results do not agree with experiment. Unfortunately the most reliable data is limited to narrow angle cones with kb < 14, and only a few isolated measurements have been made at higher frequencies or with cones of wider angle ($\theta_o < 5\pi/6$), but on this evidence equations (4.26) and (4.43) are inadequate. It is clearly unre-

alistic, of course, to expect that the formulae will be valid for kb of order unity (even the approximation to the creeping wave return is of insufficient accuracy for this purpose), but the magnitude and trends of the measured values are quite distinct from those indicated by the theory even for kb = O(10). Throughout the frequency range $5 < kb < 14$ the observed nose-on cross section oscillates in a relatively uniform manner with a period which is in good agreement with that implied by (4.26) and (4.43). The average level of the return, however, is much greater than predicted, as is the amplitude of oscillation. This amplitude shows no significant variation throughout the range, and certainly there is no evidence of the expected build-up towards the higher frequencies.

At nose-on incidence a considerable improvement in the theoretical predictions can be obtained by including a return from the cone-sphere join and by using a more complete representation for the creeping wave contribution. This is essentially what has been done by Kennaugh and Moffatt (1962) in the course of applying their "impulse approximation" technique (Kennaugh and Cosgriff, 1958). From the data available in the Radiation Laboratory it would appear that the first of these contributions can be estimated by physical optics with an error which is at most 20 percent for $kb \sim 10$. The far field amplitude associated with the tip and the join is then

$$S = -\frac{i}{4}\left\{\tan^2\theta_o - \sec^2\theta_o\, e^{2ikb\cos\theta_o\cot\theta_o}\right\} , \qquad (4.44)$$

which is believed to be the correct high frequency solution for a cone-sphere at nose-on incidence. For narrow angle cones the inclusion of the second term produces a large increase in S, and removes most of the discrepency between theory and experiment at the highest frequencies ($kb \sim 80$) for which data is available. At such frequencies the creeping wave contribution can be calculated with sufficient accuracy using (4.43), but the error increases with decreasing kb. For kb of order 10 the error is significant, and a more complete expression which is correct to within 1 percent for $kb \geqslant 5$ is

$$S = \left(\frac{kb}{2}\right)^{4/3} e^{ikb\left\{\pi+2\cos\alpha\,\mathrm{cosec}(\pi-\theta_o)\right\}+i\pi/3} \frac{1}{\beta\left\{Ai(-\beta)\right\}^2} \left\{1+e^{i\pi/3}\,\frac{8\beta}{15}\left(1+\frac{9}{32\beta^3}\right)\left(\frac{2}{kb}\right)^{2/3}\right\} \exp\left\{-e^{-i\pi/6}\,\beta\pi\left(\frac{kb}{2}\right)^{1/3} - e^{i\pi/6}\,\frac{\beta^2\pi}{60}\cdot\left(1-\frac{9}{\beta^3}\right)\left(\frac{2}{kb}\right)^{1/3}\right\} \qquad (4.45)$$

(Senior and Goodrich, 1963) where

$$\beta = 1.01879\ldots$$

and

$$Ai(-\beta) = 0.53565\ldots$$

At still lower frequencies even this becomes inadequate owing to the greater importance of the higher order waves which are neglected in (4.45), and no simple formula for the shadow boundary return is then available. On the other hand, numerical values can be obtained by subtracting the specular contribution (Logan, 1960) from

the complete far field amplitude computed from the Mie series. This has been done by Gent et al (1960) for selected values of kb and, implicitly, by Kennaugh and Moffatt (1962).

In spite of the improvement in the predictions of the nose-on behavior resulting from these modifications, there is still a systematic discrepancy between theory and experiment which is clearly evident for kb greater than (about) 4 and which probably persists until such time as the creeping wave contribution is negligible. As yet there is no theoretical method for calculating the additional return, though some of its properties can be determined by detailed analysis of experimental data.

For angles of incidence away from nose-on, the data available for the cone-sphere is less extensive; but on the basis of those patterns which have been taken, a few general comments about the back scattering cross section in the resonance region can be made. In the immediate vicinity of $\alpha = 0$ the behavior depends on the relative phases of (4.44) and (4.45). Since the polar diagram of the return from the join is peaked at nose-on and falls to zero in an angle comparable with the half cone angle $\pi-\theta_o$, σ/λ^2 has a maximum or minimum at $\alpha = 0$ if (4.44) and (4.45) are in phase or out of phase respectively, changing over to a minimum or maximum respectively at a value of α which is fractionally greater than $\pi-\theta_o$. As α increases beyond this, the cross section displays a marked dependence on polarization.

With vertical polarization σ/λ^2 oscillates with a relatively small amplitude about a level which is in good agreement with that determined by (4.45) alone, and

this continues until the side lobes of the specular flash are reached. The latter can be obtained from (4.29), and depending on the phase relationship between (4.29) and (4.45) there may be a few deep minima in the aspect range for which the two contributions are comparable in magnitude. The specular flash itself is in excellent agreement with the scattering amplitude shown in (4.30), but for the side lobes beyond $\alpha = \theta_o - \pi/2$ it is necessary to take into account the presence of the spherical cap in applying the physical optics method. The results obtained when this is done are reasonably accurate. For α greater than (about) 100^o the cross section is effectively constant out to 180^o, with a value which corresponds quite closely to the specular return from the sphere. The appropriate far field amplitude is therefore

$$S = -\frac{1}{2} kb\, e^{-2ikb \operatorname{cosec}\theta_o \left\{1 + \sin^2\theta_o - 2\sin\theta_o \cos\alpha\right\}^{1/2}} \left(1 - \frac{i}{2kb}\right) \qquad (4.46)$$

(Senior and Goodrich, 1963). Such discrepancies as are apparent may be due to the reflection of the creeping wave on the sphere at the join with the cone, but the resulting contribution should be small, and has not been observed in experimental data with $kb > 8$. We note in passing that Moffatt (1962) has proposed a modification of the physical optics integral for use in predicting the cross section at $\alpha = 180^o$. The agreement with experiment is probably within the experimental error. On the other hand, the data obtained by the Radiation Laboratory does not reveal the need for any modification (or addition) to (4.46).

With horizontal polarization the nose-on peak or trough is somewhat narrower than above, and beyond the turning point at $\alpha \sim \pi - \theta_o$, σ/λ^2 falls away rapidly. Apart from a few large but isolated peaks the cross section out to the side lobes of the specular flash is many db below that for vertical polarization, and this is explainable by the absence of the dominant creeping wave return (the cone sides prevent any such return from reaching the receiver without first undergoing a scattering at the tip). Because of the striking difference in behavior at the two polarizations it would not appear that the cylindrical current method (which is, in practice, independent of polarization) is applicable to this aspect range, though its use has been advocated by Moffatt (1962).

Through the region of the specular flash and its side lobes, the cross section shows little or no variation with polarization, and once again the physical optics method can be employed in its prediction, but beyond $\alpha = 100^o$ (approx.) an increasing oscillation sets in, and out to 180^o the behavior is quite distinct from that observed with vertical polarization. The average level is somewhat greater than that indicated by the sphere return alone, and the oscillation increases in amplitude reaching a maximum some few degrees short of rear-on. At $\alpha = 180^o$ the cross section varies from local maxima to local minima as a function of frequency and its value here is identical to that with vertical polarization.

It is believed that these oscillations are attributable to travelling waves excited on the surface of the body. Such waves can produce a significant contribution

to the back scattering cross section only with horizontal polarization, and the theory associated with them predicts an aspect-sensitive return which is similar to that found at near rear-on aspects with the cone-sphere, and in the aspect range between $\alpha = \pi - \theta_o$ and the side lobes of the specular flash for a cone with almost any termination.

When a long thin body is illuminated at near nose-on incidence the initial scattering is predominantly in the forward direction. A portion of the energy is guided along the surface, leading to a current distribution which is identifiable with a wave travelling down the body. When this reaches the further end a fraction of it is reflected back in the direction from which it came, and ultimately radiates in the back scattering direction. As a result the observed signal appears to originate at (or near) the rear of the body, and suggested to Peters (1958) and Belkina (1957) that this type of structure should act as a travelling wave antenna. By likening it to a long thin wire, Peters obtained an expression for the far field amplitude in the form

$$S = \gamma F(\theta) \qquad (4.47)$$

where γ is the (complex) current reflection coefficient and $F(\theta)$ is a pattern factor which is a function of the length of the wire in wavelengths and of the effective phase velocity along the surface.

It is obvious that the method is only as accurate as is the simulation by the wire, and is certainly limited in application to bodies whose length is large in comparison with both the wavelength and the width. Because of the basic model the

results are markedly dependent on the polarization, and the travelling waves provide a significant contribution to the cross section only at angles away from nose-on ($F \equiv 0$ for $\theta = 0$) with horizontal polarization. With any actual body having significant width, a small contribution with the other polarization is to be expected, but cannot be estimated using Peters' theory.

In spite of the inaccuracies inherent in the model, the method has proved extremely useful in practice. Applications to the finite cone have been given by Crispin et al (1959) and Dawson (1960b), and to the cone-sphere by Gent et al (1960), and for such purposes it is generally sufficient to assume that the phase velocity along the surface is the same as that in free space. The expression for $F(\theta)$ then reduces to

$$F(\theta) = \frac{\cot^2 \frac{\theta}{2}}{\ell n 2k\ell - 0.4228} \sin^2(k\ell \sin^2 \frac{\theta}{2}) \qquad (4.48)$$

where ℓ is the overall length of the body (or the distance from the nose to the reflection point, if this is different). The maximum in the pattern occurs at

$$\theta \sim 49.35(\lambda/\ell)^{1/2} \text{ degrees,} \qquad (4.49)$$

which decreases as $k\ell$ increases. In a neighborhood of this angle the pattern is similar to $(\sin x/x)^2$ in shape. The maximum value of S is

$$S_{max} = \frac{0.725\,\gamma k\ell}{\ell n 2k\ell - 0.4228} \qquad (4.50)$$

and the important role played by the reflection coefficient is now apparent. It is therefore unfortunate that no method is yet available for computing γ in terms of the shape parameters of the body. By analysing a large volume of experimental data, Dawson (1960a) has suggested that γ is proportional to $\sin^2\theta$, with a constant of proportionality which decreases from unity if the termination is sharp, to zero when the radii of curvature at the termination are several wavelengths or greater. There is no theoretical support for this suggestion and the dependence on θ appears questionable. Other (quite different) estimates of γ have been given by Siegel (1959), but even without a precise knowledge certain general statements can be made.

If the termination is sharp, γ is almost certainly independent of λ to the first order: σ_{max} then decreases with decreasing λ at an extremely slow rate, and in most practical cases (4.50) will be comparable in magnitude to the nose-on return from a flat base (equation 4.32). It will therefore be the dominant feature of the return in the aspect range between the nose-on and specular regions when the polarization is horizontal, and the large peaks which are observed are in approximately the positions predicted by the theory. It will also be significant at rear-on aspects for a cone-sphere, since the reflection point is now the apex.

If the rear of the body is smooth the reflection coefficient will be much smaller, and depending on the precise shape of the body the reflection may occur at some point where a higher derivative of the surface profile has a sharp discontinuity. This is believed to be the case with the cone-sphere, and the experimental data on

the scattering cross section at near nose-on aspects is suggestive of a reflection at the cone-sphere join, with γ proportional to λ (or possibly some higher power). Since the nose-on return also has this wavelength dependence, the relative importance of the travelling waves is unchanged.

V
EXPERIMENTAL DATA

The interest in cone-like structures has increased considerably during the last few years and a wealth of experimental data is now extant. Unfortunately a good deal of this still exists only in the files of the laboratories responsible and will doubtless remain so until some central organization can undertake (or delegate) the compilation task. Because of the needs of a particular laboratory at a given time, the data which they obtained may have been restricted to a few isolated cases and is in that sense "unpublishable", but when viewed in conjunction with comparable data obtained elsewhere it could be extremely valuable in filling in the "gaps" which exist.

The following listing is the result of a search through the open and classified literature, together with such unpublished data as the authors are personally aware of. It is certain that the list is not complete and it may even contain only a small fraction of the measurements which have been made. We would be grateful for information about any data which we have unintentionally omitted.

In almost every case the quantity which has been measured is the back scattered cross section, and attention will be confined to this; little is known about the phase or about the bistatic behavior. The flat backed cone is considered first, followed by the cone-sphere (referred to as the "carrot" in some British publications) and, in the third section, by a brief resumé of the data for cones with other types of terminations.

5.1 Flat-Backed Cone

Let a denote the radius of the base and $\pi-\theta_o$ the half cone angle.

Using cw equipment operating at 3.02, 3.8, 9.3 and 9.9 KMc, Brysk et al (1959) have measured the nose-on cross section in the following cases:

$\pi-\theta_o = 7.5^o$: ka = 0.118 to 3.0 (25 values)

$\pi-\theta_o = 9.6^o$: ka = 0.143 to 3.0 (21 values)

$\pi-\theta_o = 12^o$: ka = 0.165 to 3.0 (26 values)

$\pi-\theta_o = 45^o$: ka = 0.327 to 3.2 (20 values)

$\pi-\theta_o = 60^o$: ka = 0.490 to 4.8 (20 values)

Data was also obtained for

$\pi-\theta_o = 4^o$: ka = 0.187 to 1.05 (14 values)

using the same equipment at 8.465 and 9.9 KMc. The presentation is in the form of graphs, $\sigma/\pi a^2$ versus ka, on a log-log scale.

Keys and Primich (1959a) have used two cw systems operating at 8.75 and 35 KMc to obtain the nose-on cross section for cones of half angle $\pi-\theta_o = 4^o$, 20^o and 60^o with ka varying from 0.5 to 9.5 (approx.). The data is presented as graphs of σ/λ^2 versus $2a/\lambda$ on a log-log scale. The results for the widest angle cone are partially reproduced in Keys and Primich (1959b), and corresponding values for $\pi-\theta_o = 7.5^o$ and 30^o are also provided.

Probably the most complete set of data is that given in Keys and Primich (1959c and d). A pulsed system was used operating at 35 KMc with a pulse length of

10 millimicroseconds. The back scattering cross section σ/λ^2 is shown as a function of aspect, 0 to 360^o, for vertical and horizontal polarization and for the following values of ka:

$$ka = 0.933,\ 1.40,\ 1.86,\ 2.33,\ 3.08,\ 3.80,\ 4.18$$
$$4.56,\ 5.31,\ 6.06,\ 6.79,\ 7.45,\ 8.29,\ 9.02.$$

In the first of the above reports the cone angles treated have

$$\pi-\theta_o = 4^o,\ 7.5^o,\ 9.6^o,\ 12^o,\ 15^o \text{ and } 20^o$$

and in the second

$$\pi-\theta_o = 30^o,\ 37.5^o,\ 45^o,\ 52.5^o \text{ and } 60^o.$$

The overall accuracy is stated as $\pm$ 2 db.

If the nose-on cross sections are read off from these patterns and converted to values of $\sigma/\pi a^2$, the points shown in Figs. 10 through 20 are obtained. The curves have been calculated using equations (4.7) and (4.37) (Siegel's modified Rayleigh theory and Keller's second order theory), and are in good agreement with the data. Four typical aspect patterns are reproduced in Figs. 21 through 24 and in the following four figures the measured cross sections for the specular flash are plotted[+] as functions of ka for $\pi-\theta_o = 4^o,\ 15^o,\ 30^o$ and 60^o. The straight lines are the physical optics predictions (see equation 4.30). In most cases the discrepancy is no more than a factor 2 at most and because of the nature of the theoretical method the

[+]The values for the left and right flashes are both presented if they differ by more than 1 db.

agreement improves with increasing $\pi-\theta_o$ or ka. We note in passing that the cylindrical current prediction (also plotted in Figs. 25-28) is smaller than the physical optics by a factor $\sec^4\theta_o$ in the cross section. The factor increases from 1.0096 when $\pi-\theta_o = 4^o$ to 4 when $\pi-\theta_o = 60^o$ and on this basis it would appear that the "approximated form" of the cylindrical current method is somewhat inferior to physical optics.

For a cone of half angle $\pi-\theta_o = 7.5^o$ a series of measurements of the nose-on and base-on cross sections have been made by Olte and Silver (1959) using a cw ground plane system at 9.33 and 9.331 KMc. The base radius was changed by adding "discs" to one of several different basic cones, giving a coverage of the range

$$ka = 1.90 \text{ to } 6.20$$

with a total of 15 values shown for nose-on and 14 for base-on. The results are presented in the form of graphs of σ/σ_o (in db) versus L/λ on a linear scale, where L is the length of the cone and σ_o is the scattering cross section of a 6 in. diameter reference sphere.

The same equipment was earlier employed by Shostak and Angelakos (1957) to measure the scattering pattern as a function of aspect for a cone of half-angle 7.5^o. At that time, however, the accuracy of the system was poor and the experiments were later repeated by August and Angelakos (1960). For $\pi-\theta_o = 7.5^o$ and ka = 1.53, 3.14 and 6.18 the measured nose-on and base-on cross sections are

listed and in each case the aspect pattern, 0 to 180^{o}, for vertical polarization is shown. Measurements on these same models were also reported by Honda et al (1959).

Additional results for cones with $\pi-\theta_{o} = 7.5^{o}$ have been obtained by the Cornell Aeronautical Laboratory and Microwave Radiation Co., Inc., and the measured values of the nose-on cross sections were communicated to K. M. Siegel. No information about the equipment is available, but for ease of reference the data is listed below:

	σ/λ^2 (in db)		
ka	Hor. Pol.	Vert. Pol.	Organization
38.7	19.0	19.0	Cornell Aeronautical Lab.
23.7	13.4	13.4	
7.4	7.5	7.2	
26.4	21.9	17.3	Microwave Rad. Co., Inc.
6.6	1.2	2.1	
3.3	-6.0	-5.4	
1.64	-2.8	-3.1	

The only remaining measurement of which we are aware was carried out at the Royal Aircraft Establishment in England using a pulsed system at X band ($\lambda = 3.2$ cm). For $\pi-\theta_{o} = 15^{o}$ and ka = 9.016 the scattering pattern as a function of aspect, 0 to 120^{o} has been published by Dawson and Turner (1960). The results for both polarizations are given, and in Dawson (1960b) the aspect range is extended out to 180^{o}.

5.2 The Cone-Sphere

Much of the original data on the cone-sphere has appeared only in classified publications and this is true, for example, of the work carried out at the Royal Radar Establishment using a cw doppler system at 9.37 KMc (λ = 3.20 cm). Gent et al (1960) have reported measurements on 50 similar cone-sphere models with $\pi - \theta_o = 15^o$ and

$$b/\lambda = 1.00\ (0.01)\ 1.06,\ 1.08,\ 1.105,\ 1.125\ (0.025)\ 2.125$$

where b is the sphere radius. With each model the back scattered cross section was recorded for horizontal polarization at 1^o increments in the aspect angle in the range $\pm 5^o$ about the nominal nose-on position and from the symmetry of the resulting curves the precise value of the nose-on cross section was determined. In six cases (b/λ = 1.01, 1.08, 1.125, 1.925, 2.00 and 2.075) the patterns for $-2^o < \alpha < 20^o$ (or greater) are presented, together with the complete aspect pattern, 0 to 360^o, for the model having $b/\lambda = 1.02$.

During the past year, however, data on the cone-sphere has started appearing in the open literature. The first such release was by Kennaugh and Moffatt (1962) who used a cw X-band radar to measure the nose-on cross section of a series of cone-spheres having

$$\pi - \theta_o = 15^o \qquad \text{and} \qquad kb = 1 \text{ to } 7 \text{ (39 values)}.$$

The spacing of the points provides a reasonably complete coverage of this range in kb and serves to extend the data of Gent et al (1960) almost to the edge of the

Rayleigh region. The results are presented in the form of a graph of $\sigma/\pi b^2$ in db versus kb on a linear scale. A larger version of the graph has been provided by Moffatt (1962). These points have been renormalized and appear in Fig. 29.

The most extensive data so far obtained has recently been reported by Blore and Royer (1962). Using the 8.6 mm pulse equipment of the Defence Research Board in Canada the following nose-on cross sections have been measured:

$\pi-\theta_o = 7.5^o$	kb = 0.4 to 2.8	(30 values, approx.)
$\pi-\theta_o = 15^o$	kb = 0.2 to 9.6	(105 values, approx.)
$\pi-\theta_o = 20^o$	kb = 0.5 to 9.5	(80 values, approx.)
$\pi-\theta_o = 30^o$	kb = 0.2 to 9.6	(105 values, approx.)
$\pi-\theta_o = 37.5^o$	kb = 0.2 to 5.7	(85 values, approx.)

All values are the average of at least two measurements with both horizontal and vertical polarization, and are believed accurate to $\pm$ 0.5 db. The results are presented in the form of graphs of σ/λ^2 in db versus $26/\lambda$ on a linear scale, and in Figs. 29 and 30 we have reproduced the curves for two of the cone-spheres.

Isolated measurements on single models have also been carried out at the Royal Aircraft Establishment in England using an X-band pulse equipment, and the data is available in their reports. For the cone-sphere having $\pi-\theta_o = 15^o$ and kb = 44.9 Dawson and Turner (1960) give the aspect patterns (0^o to 80^o) for horizontal polarization, and the analogous results for kb = 6.28 have been presented by Dawson (1960b). With this same cone angle, but kb = 18.70, 43.89 and 89.77,

Turner (1960) has provided aspect patterns out to 70^{o} for vertical polarization, and also shows the results for a cone-sphere with $\pi-\theta_{o} = 25^{o}$ and ka = 30.0.

The above is a complete listing of the published data on the cone-sphere known to the present authors, but it is certain that many of the scattering measurements for this shape have not yet been reported in the literature. As an illustration of this fact, the following measurements on a cone-sphere having $\pi-\theta_{o} = 12.5^{o}$ and b = 4.5187 cm have been carried out by the Radiation Laboratory, and this is only one of the many cone-sphere models which have been investigated:

Aspect patterns 0^{o} to 360^{o}:

2.67 (0.10) 3.07 KMc, horizontal polarization
8.58 and 9.375 KMc, horizontal and vertical polarization
8.5, 9.3, 10.0 and 31.97 KMc, vertical polarization

Aspect patterns 0^{o} to 50^{o}:

7.98, 8.1, 8.34, 8.43, 8.58, 8.8, 8.93, 9.0,
9.15, 9.3, 9.6, 9.8, 9.954, 10.11, 10.43, 10.97,
and 11.97 KMc, vertical polarization.

At each of these frequencies 16 or more independent measurements of the nose-on cross section have been made to ensure the most accurate values possible over a complete cycle of the oscillation described in Section 4.3. All measurements were made with a cw system. It is hoped to publish at least some of this data in the near future.

5.3 Other Terminations

For terminations other than a flat back or a sphere with no discontinuity in the first derivative at the join, a comparison of the experimental data is more difficult owing to the variations in the structural features of the individual models. Nevertheless, it may be helpful to mention some of the data which is available for more general conical shapes.

For two flat-backed cones mounted base to base with $\pi-\theta_o = 20^o$, Blore and Royer (1962) have measured the nose-on cross section for

$$ka = 0.3 \text{ to } 9.3 \quad (60 \text{ values, approx.})$$

where a is the radius at the join. These same authors have also given data for doubly-rounded cones (the above shape, but with the junction of the two cones rounded off) with $\pi-\theta_o = 7.5^o$, 20^o and 37.5^o.

Four different rounded flat-backed cones have been investigated by Turner (1960) and for each the X-band aspect pattern, 0^o to 70^o, for vertical polarization is presented. If a denotes the maximum radius and δ is the radius of curvature at the join of the cone and the base, the models studied have the following specifications

$\pi-\theta_o = 15^o$	ka = 43.89	$\delta/\lambda = 3.17$
$\pi-\theta_o = 15^o$	ka = 44.89	$\delta/\lambda = 3.17$
$\pi-\theta_o = 15^o$	ka = 89.77	$\delta/\lambda = 3.17$
$\pi-\theta_o = 15^o$	ka = 89.77	$\delta/\lambda = 6.35$

The same type of shape has also been considered by Dawson (1960b), who gives the aspect pattern, 0^{o} to 60^{o}, with horizontal polarization for the following models:

$\pi-\theta_{o} = 15^{o}$ ka = 6.28 $\delta/\lambda = 0.319$

$\pi-\theta_{o} = 15^{o}$ ka = 6.28 $\delta/\lambda = 0.639$

$\pi-\theta_{o} = 15^{o}$ ka = 6.28 $\delta/\lambda = 1.435$

$\pi-\theta_{o} = 15^{o}$ ka = 18.84 $\delta/\lambda = 1.5$

For terminations which are even more complex, including the "cubic cap", reference should be made to Dawson (1960b), Kell (1960) and Melling (1960).

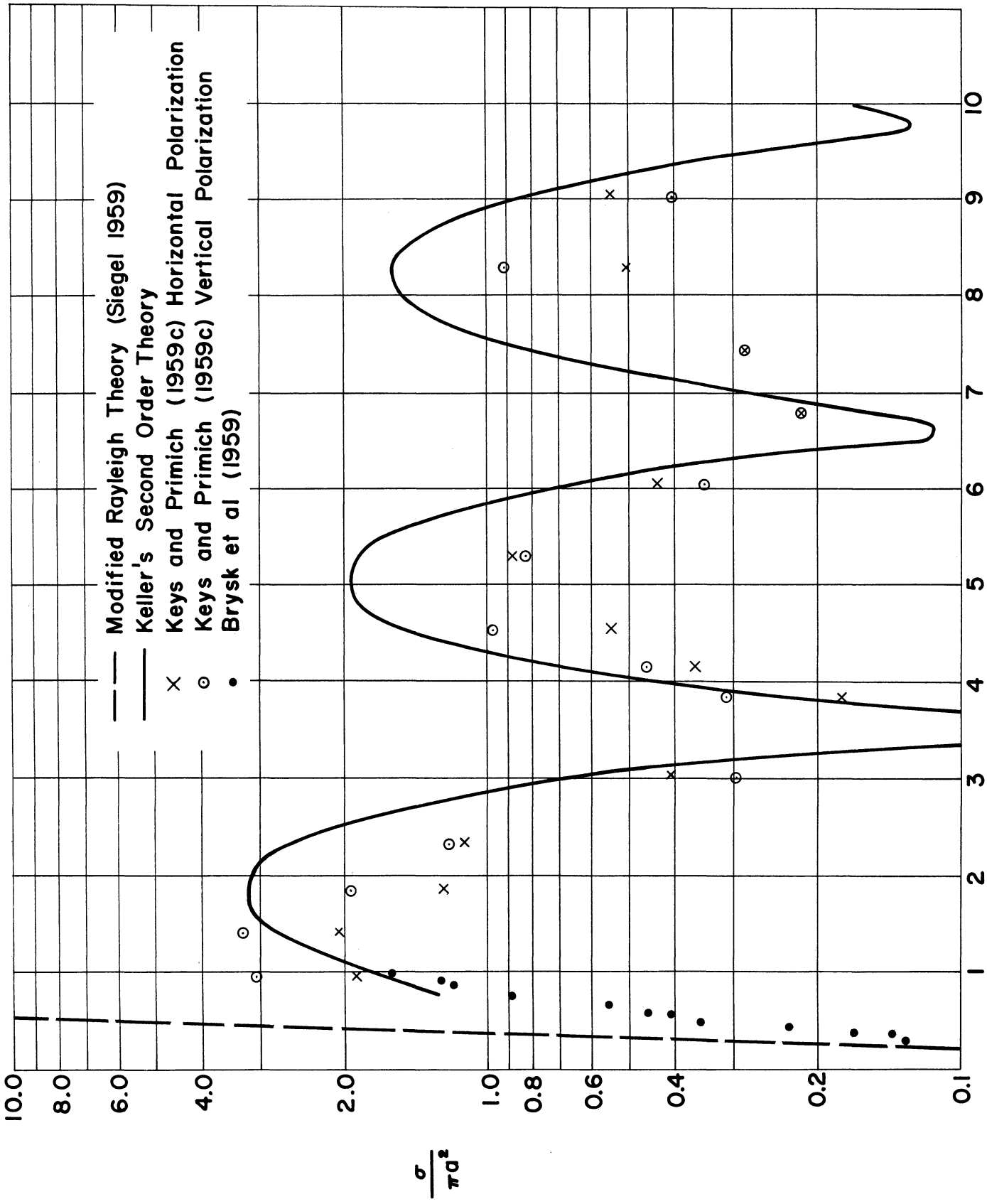

FIGURE 10: NOSE-ON RADAR CROSS SECTION OF FLAT BACKED CONE, $\pi - \theta_o = 4^o$

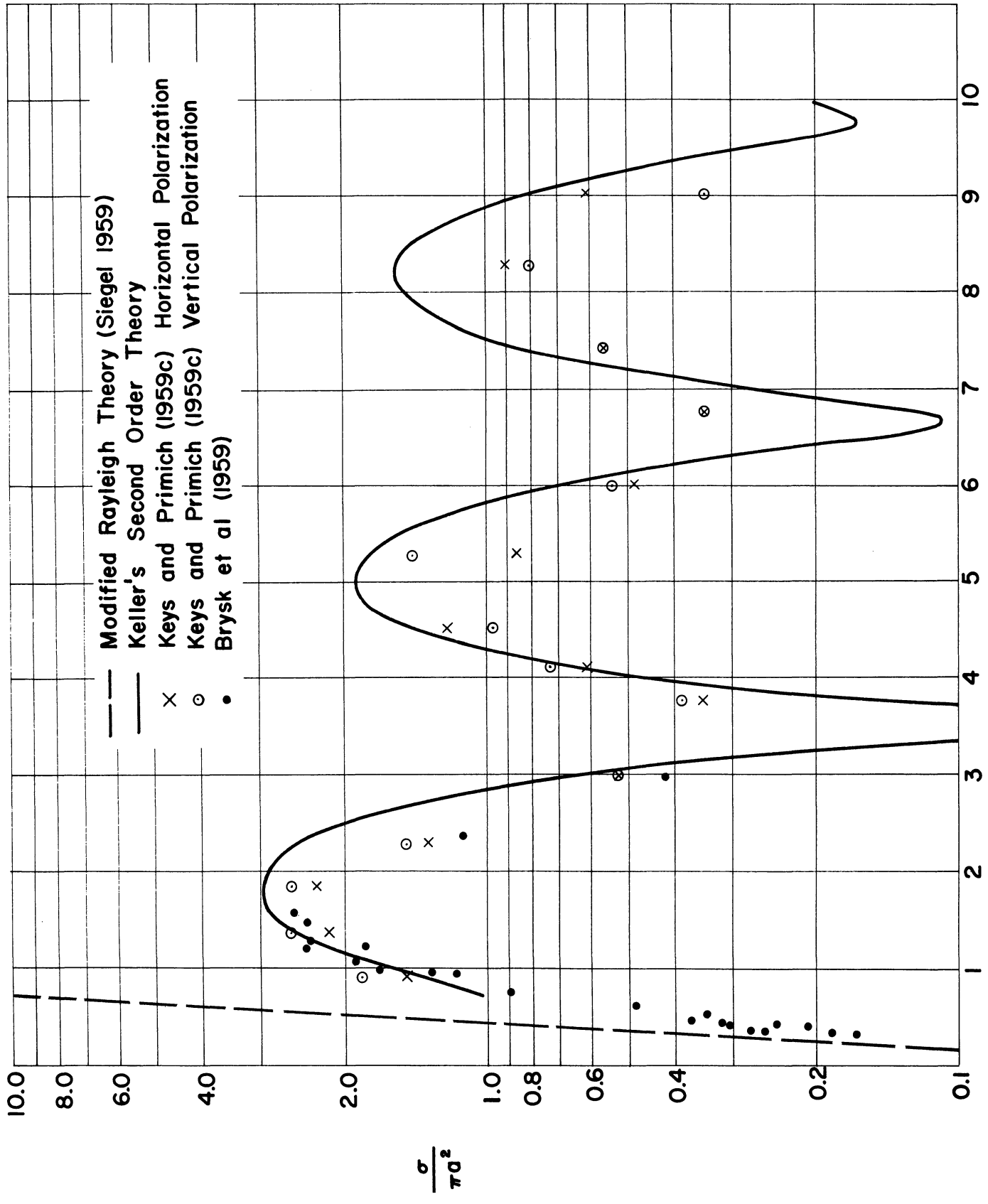

FIGURE 11. NOSE ON RADAR CROSS SECTION OF FLAT BACKED CONE, $\theta = 7.5^0$

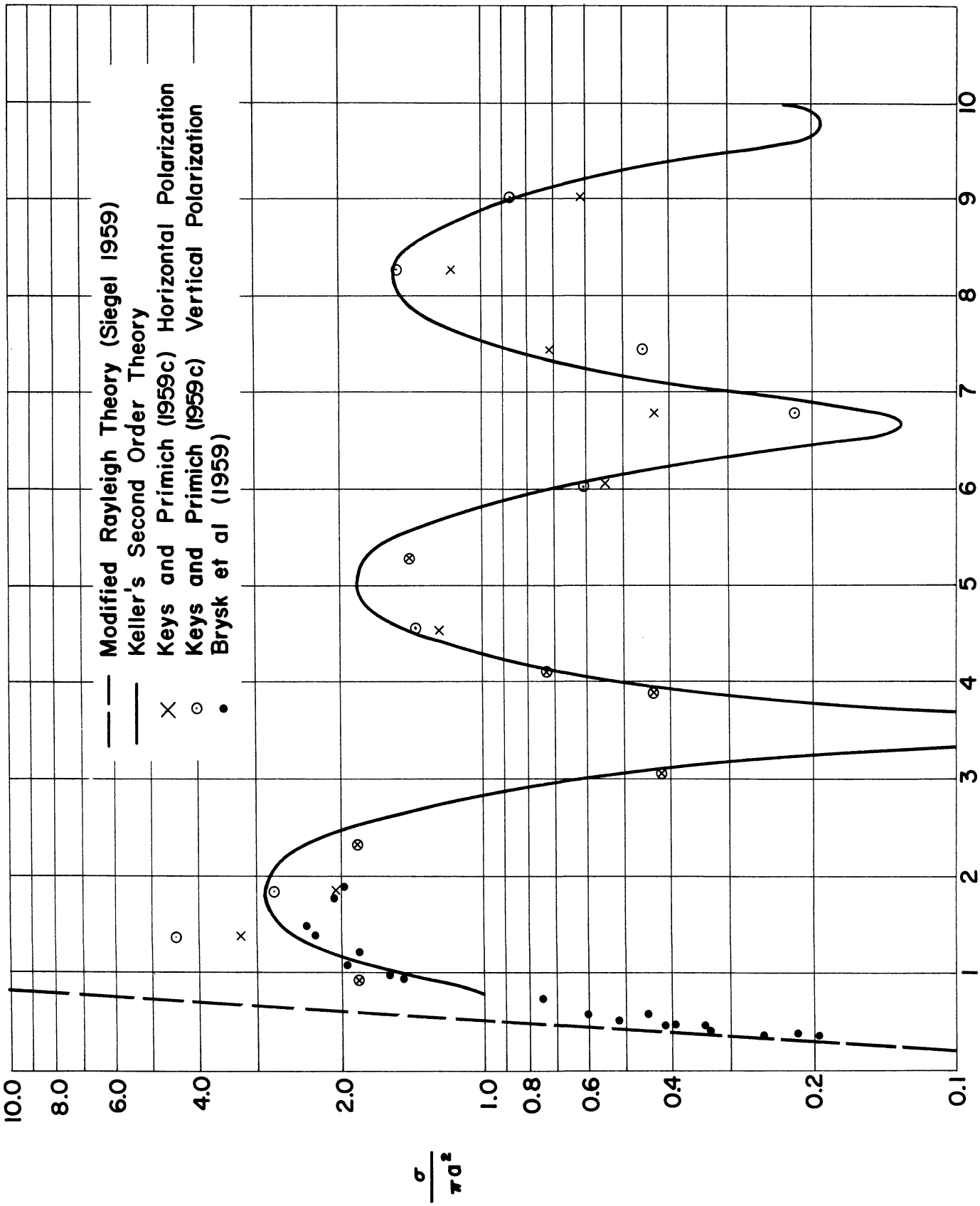

FIGURE 12: NOSE-ON RADAR CROSS SECTION OF FLAT BACKED CONE, $\pi - \theta_o = 9.6^o$

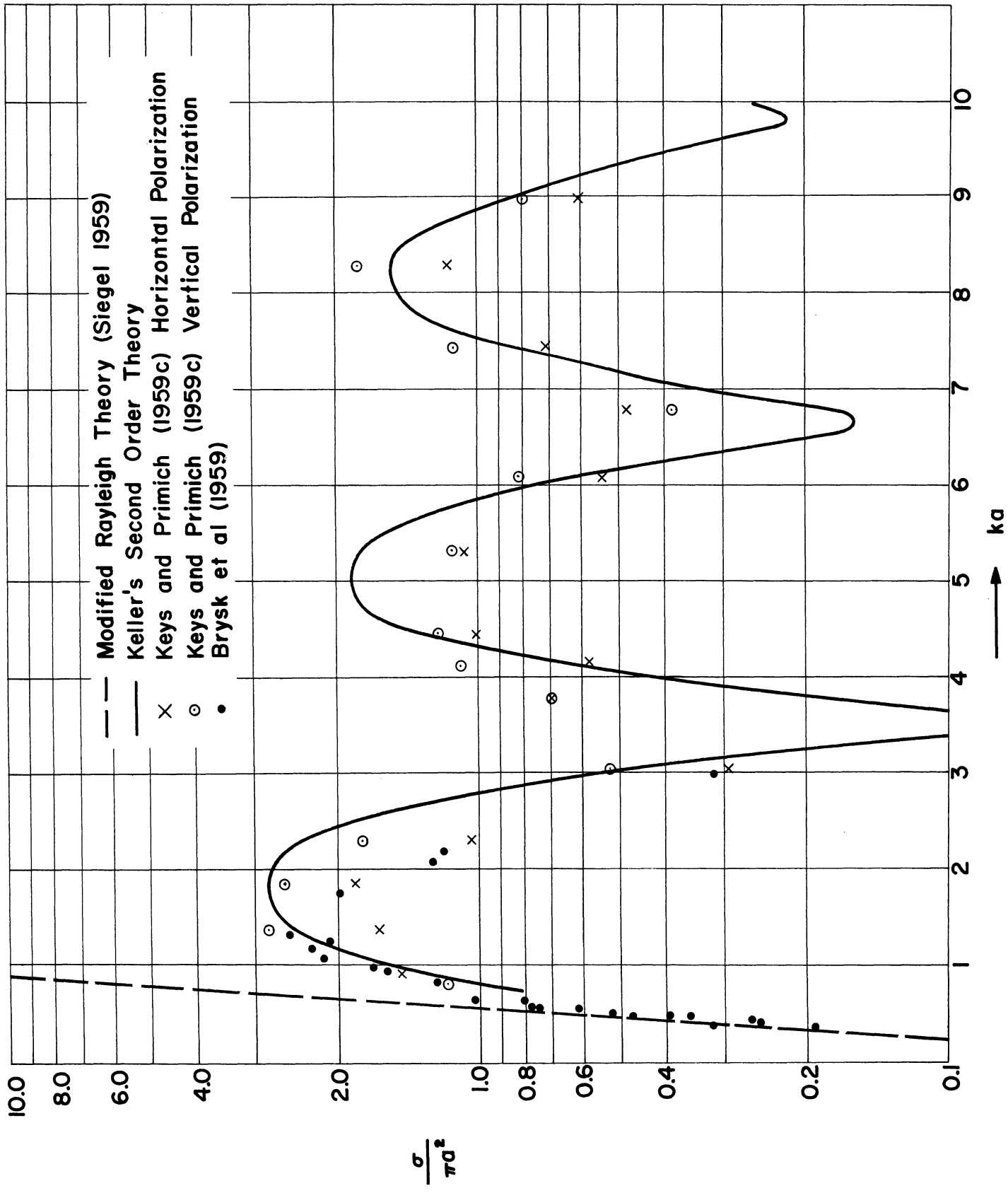
Modified Rayleigh Theory (Siegel 1959)
Keller's Second Order Theory
Keys and Primich (1959c) Horizontal Polarization
Keys and Primich (1959c) Vertical Polarization
Brysk et al (1959)
10.0
8.0
6.0
4.0
2.0
1.0
0.8
0.6
0.4
0.2
0.1
1
2
3
4
5
6
7
8
9
10
ka
σ/πa²

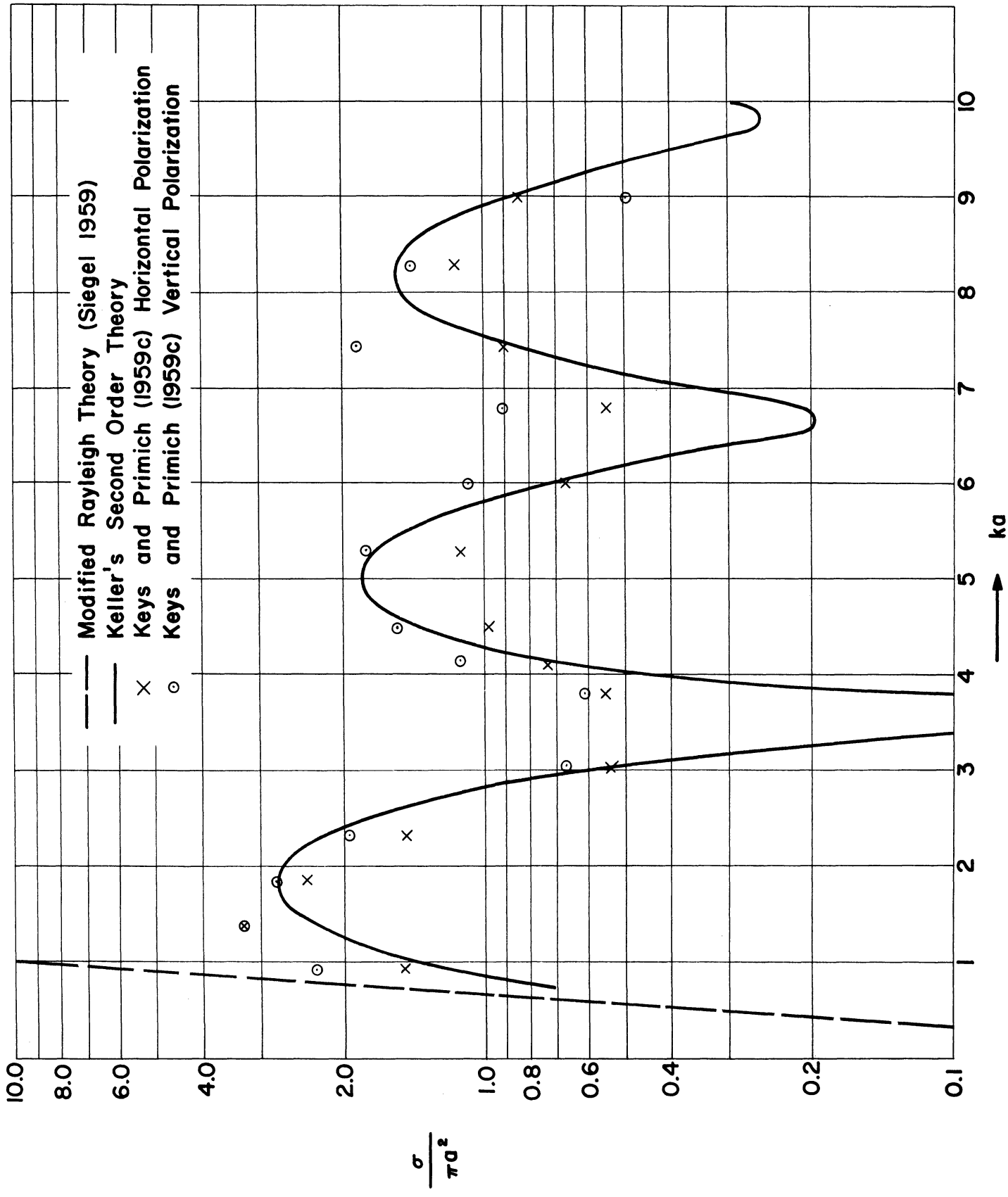

FIGURE 14: NOSE-ON RADAR CROSS SECTION OF FLAT BACKED CONE, $\pi - \theta_o = 15^o$

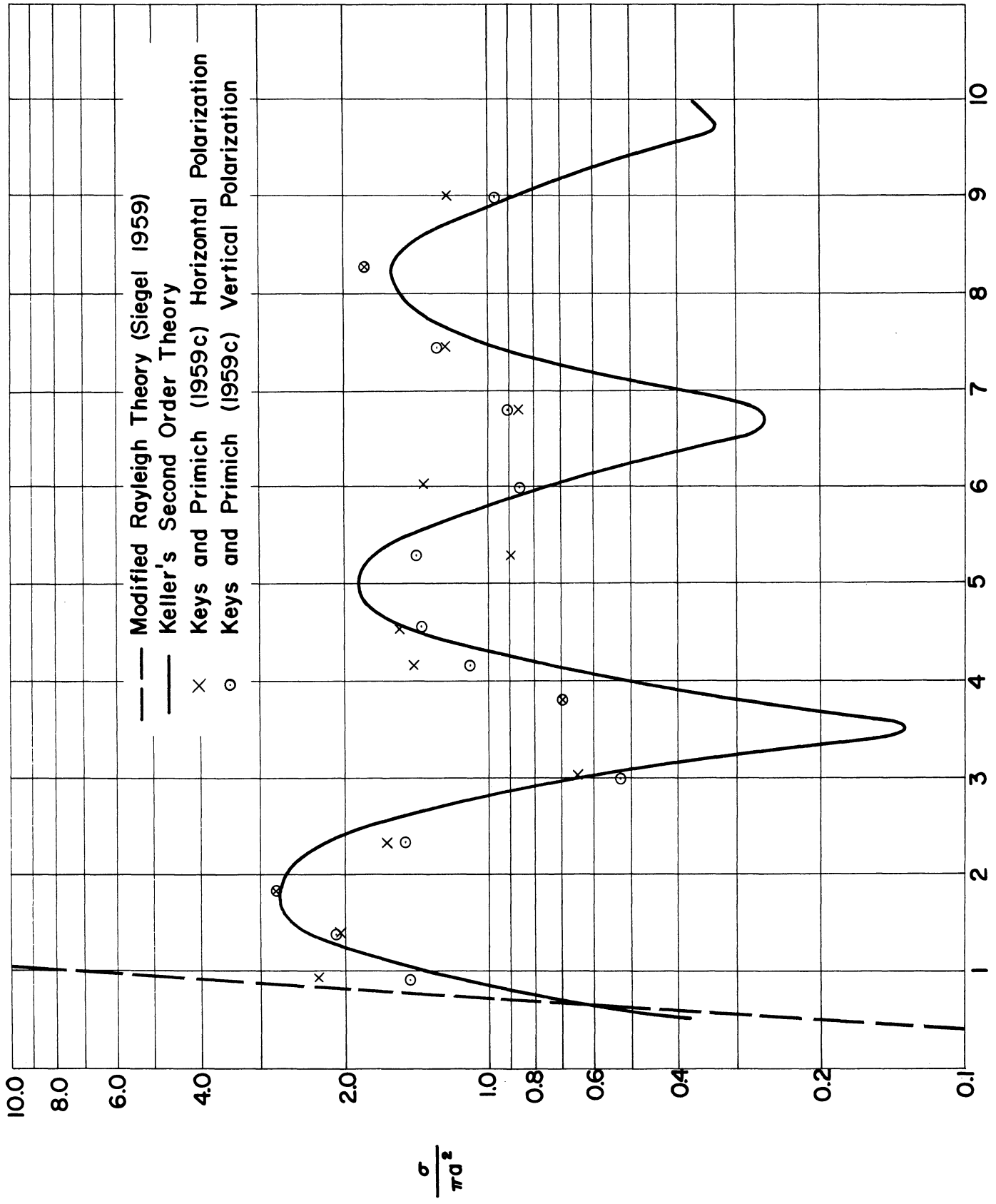

FIGURE 15. MODE ON RADAR CROSS SECTION OF FLAT BACKED CONE, $\alpha = 20^0$

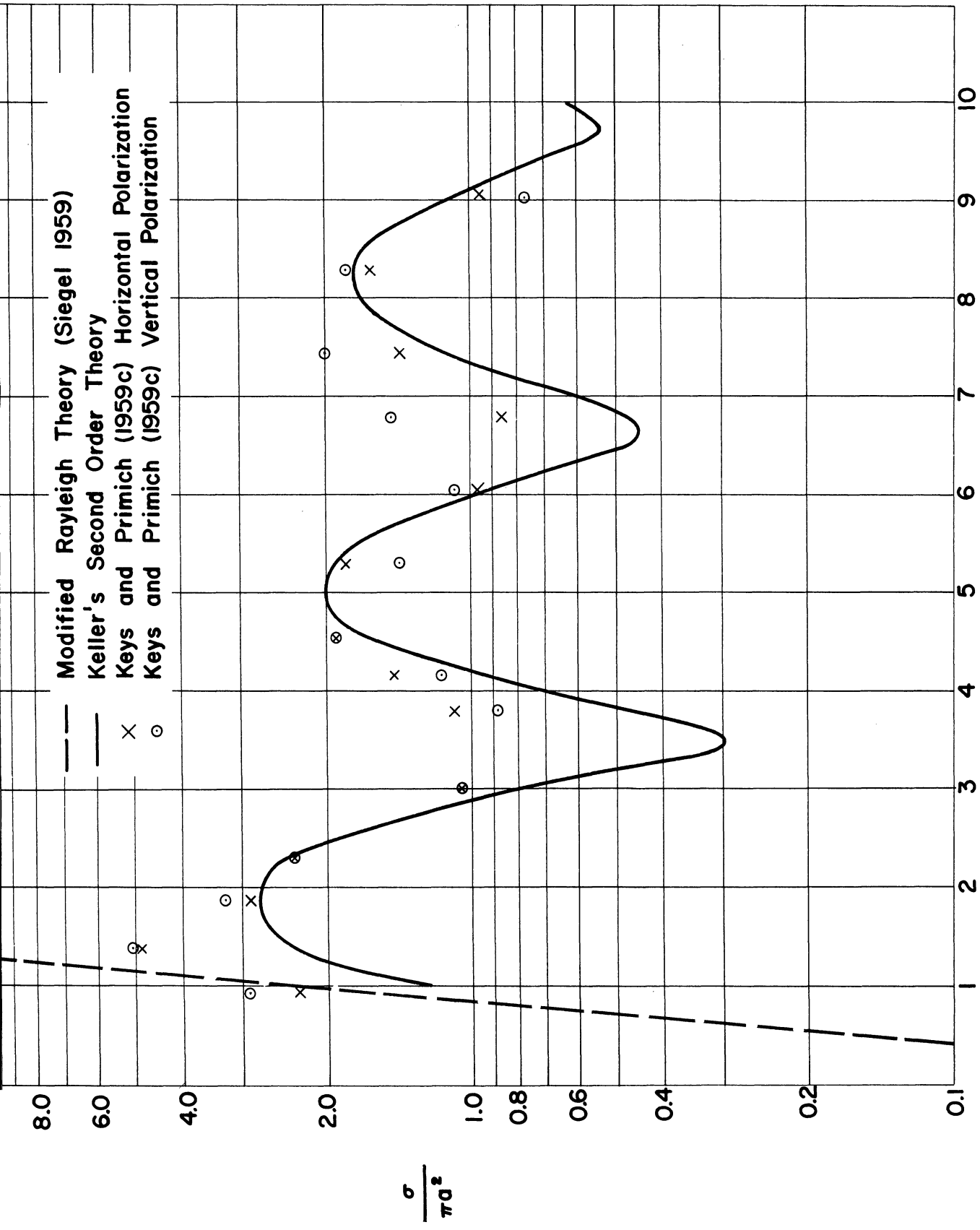

FIGURE 16: NOSE-ON RADAR CROSS SECTION OF FLAT BACKED CONE, $\pi - \theta_o = 30^o$

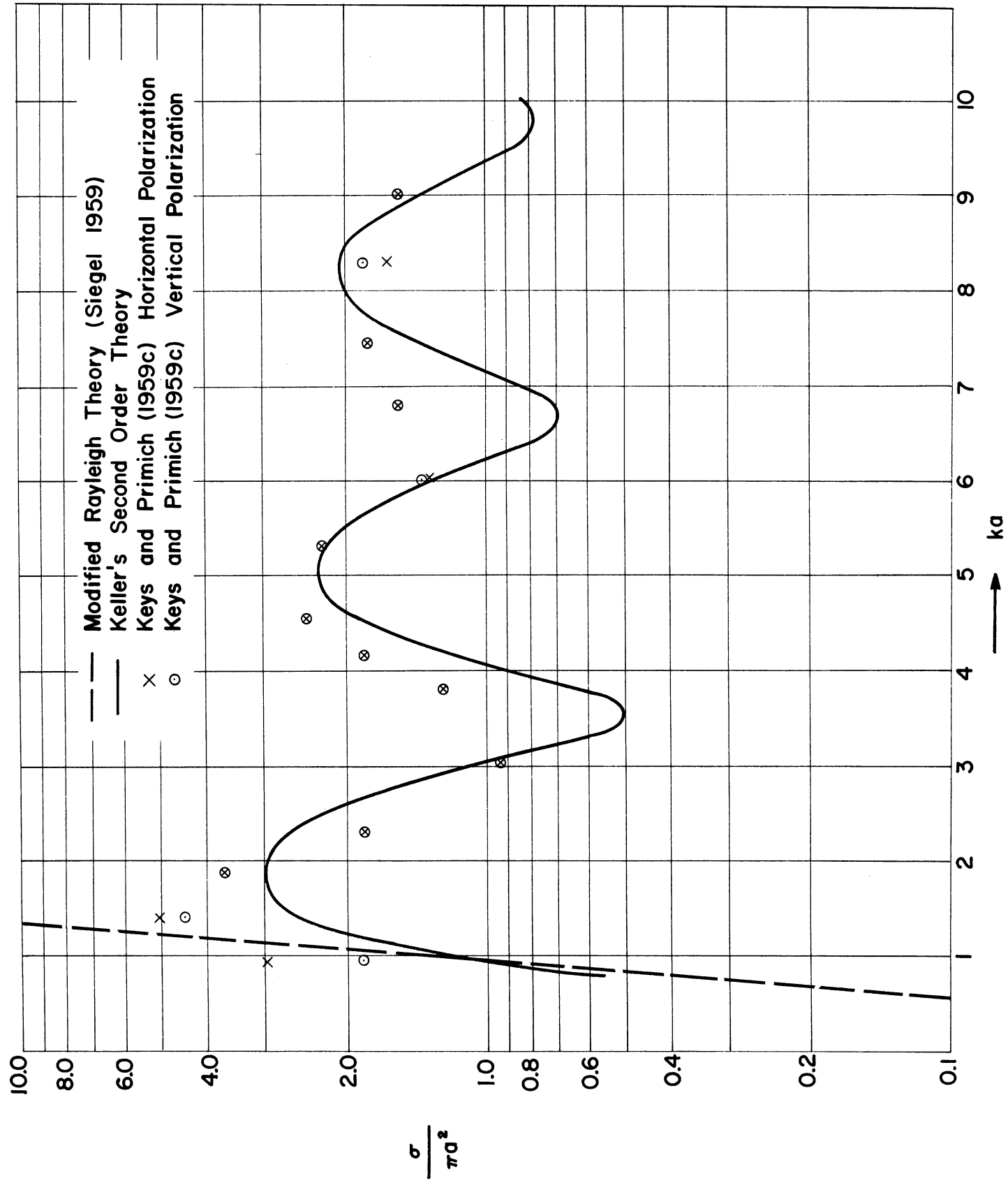
Modified Rayleigh Theory (Siegel 1959)
Keller's Second Order Theory
Keys and Primich (1959c) Horizontal Polarization
Keys and Primich (1959c) Vertical Polarization
10.0
8.0
6.0
4.0
2.0
1.0
0.8
0.6
0.4
0.2
0.1
1
2
3
4
5
6
7
8
9
10
ka
σ / πa²

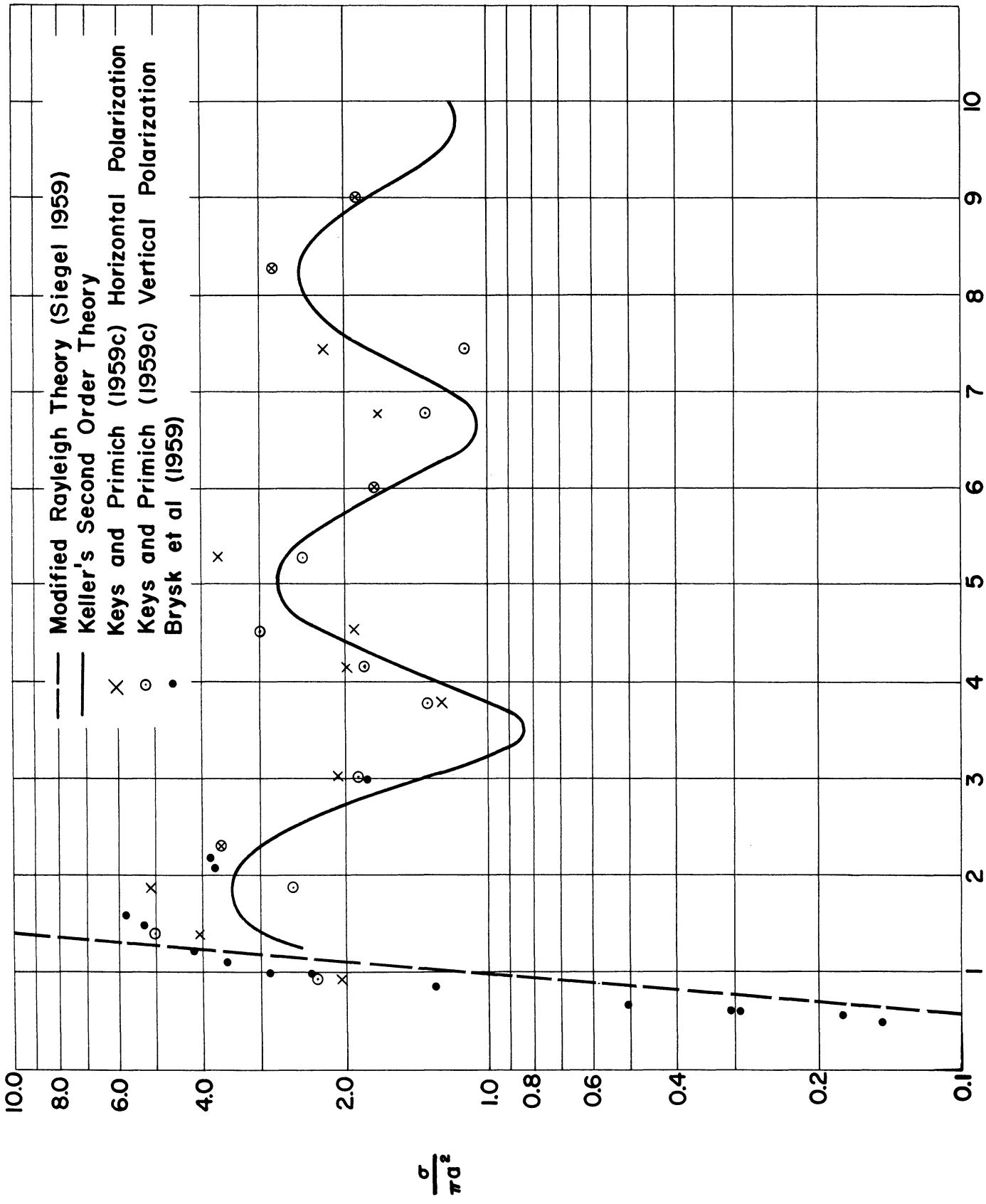

FIGURE 18: NOSE-ON RADAR CROSS SECTION OF FLAT BACKED CONE, $\pi - \theta_o = 45^o$

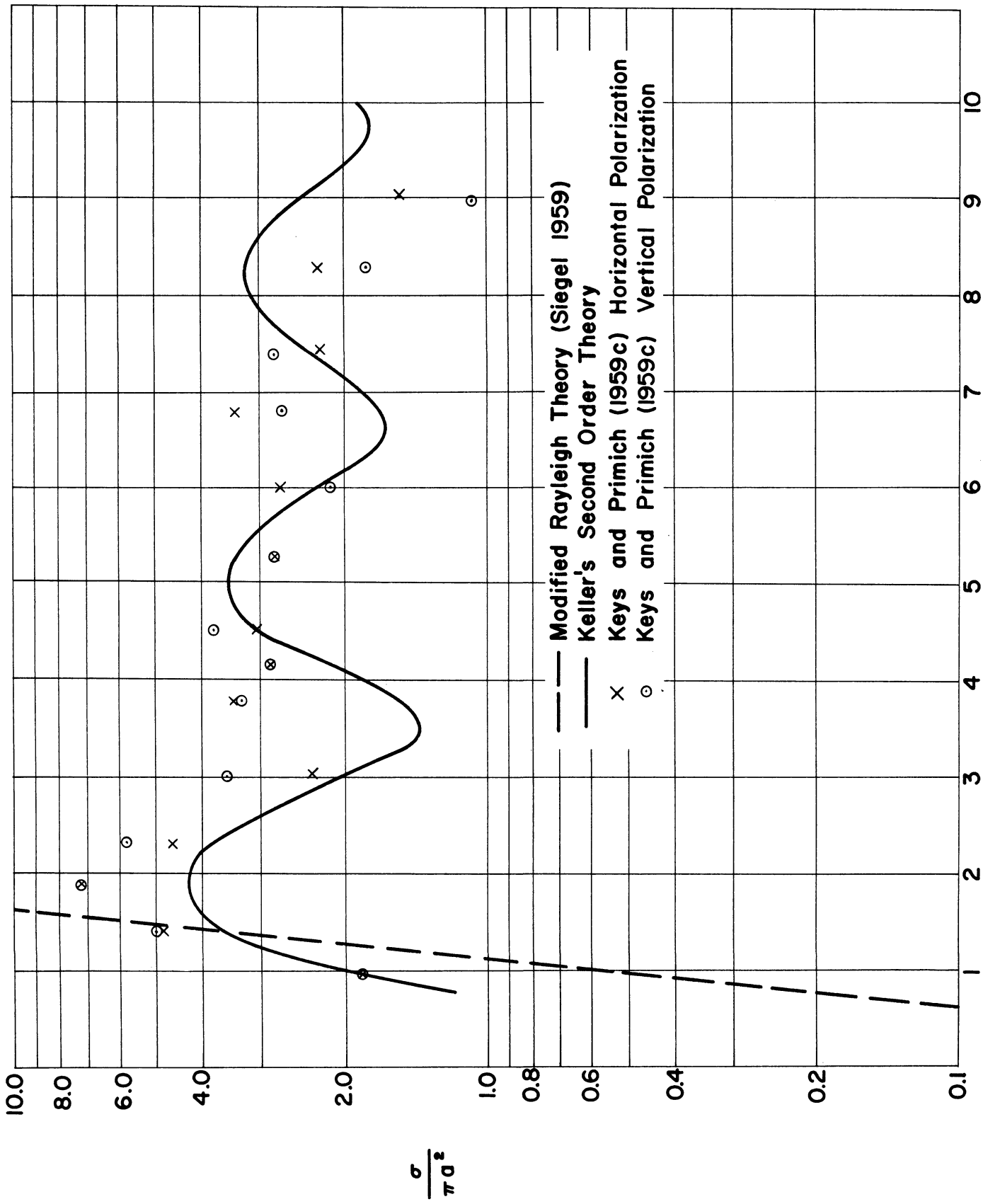

FIGURE 19: NOSE-ON RADAR CROSS SECTION OF FLAT BACKED CONE, $\pi - \theta_o = 52.5^o$

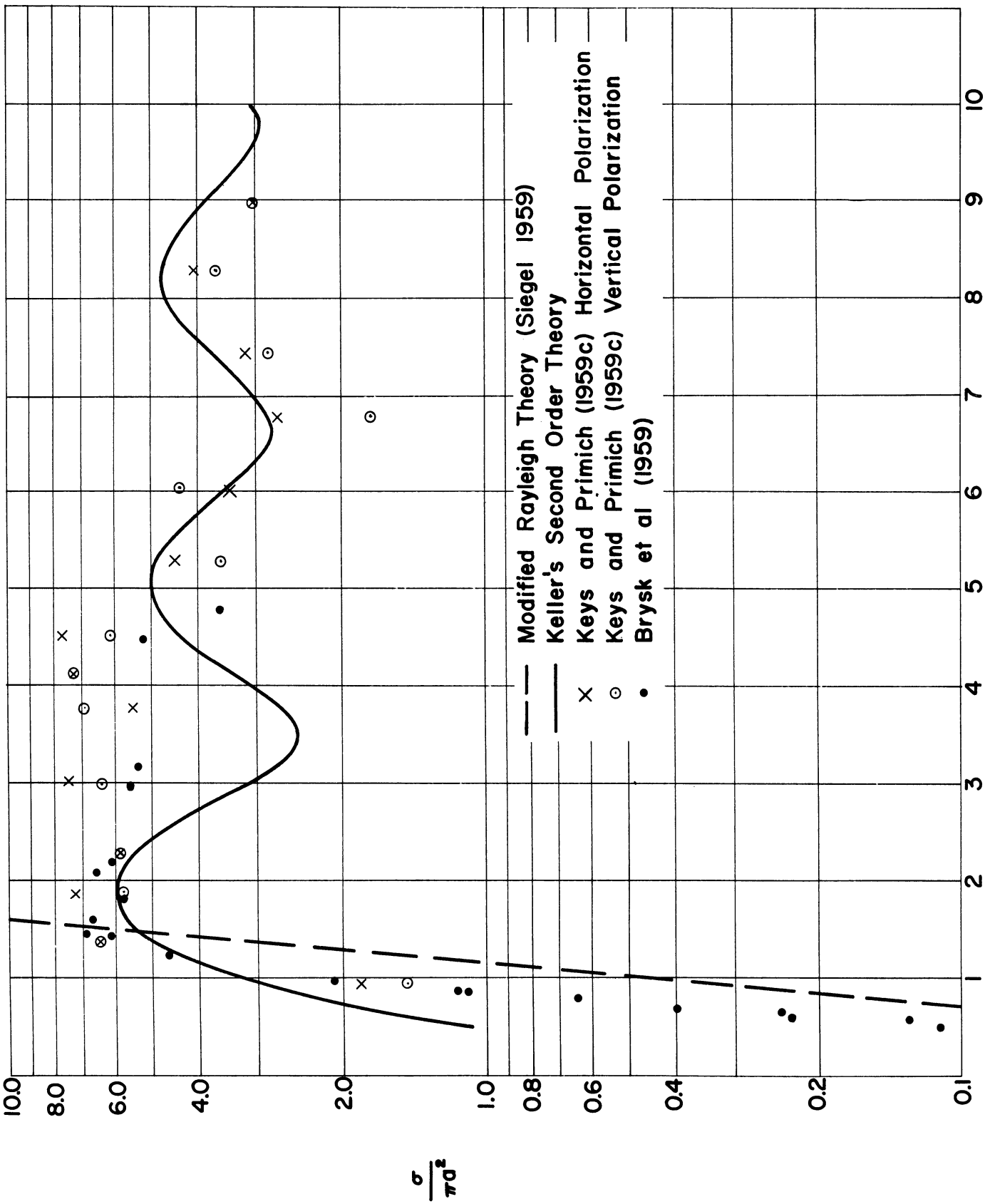

FIGURE 20: NOSE-ON RADAR CROSS SECTION OF FLAT BACKED CONE, $\pi - \theta_o = 60^o$

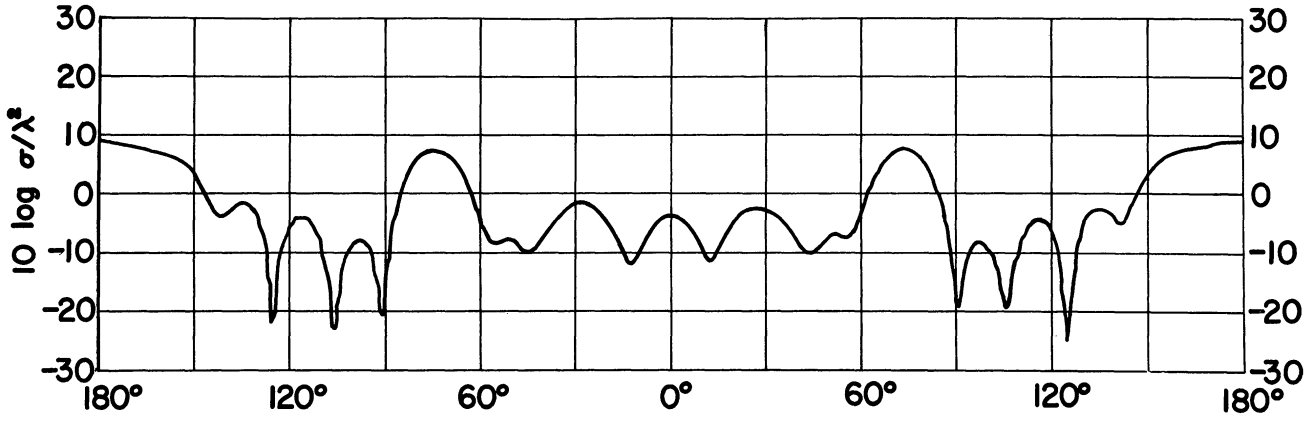

FIGURE 21: BACK SCATTERED RADAR CROSS SECTION OF FLAT BACKED CONE $\pi - \theta_o = 15^o$, ka = 3.08, Horizontal Polarization (Keys and Primich, 1959c)

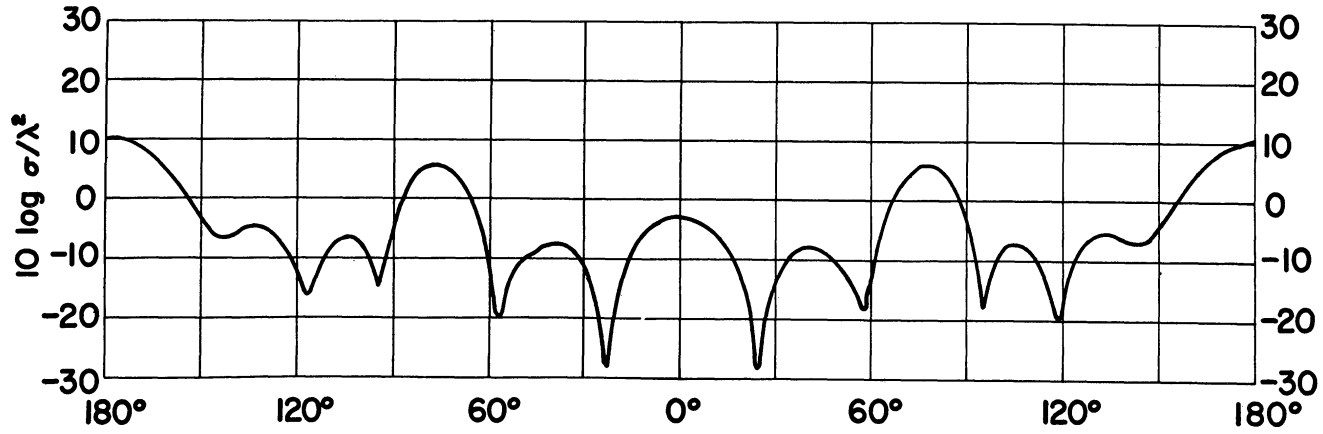

FIGURE 22: BACK SCATTERED RADAR CROSS SECTION OF FLAT BACKED CONE $\pi - \theta_o = 15^o$, ka = 3.08, Vertical Polarization (Keys and Primich, 1959c)

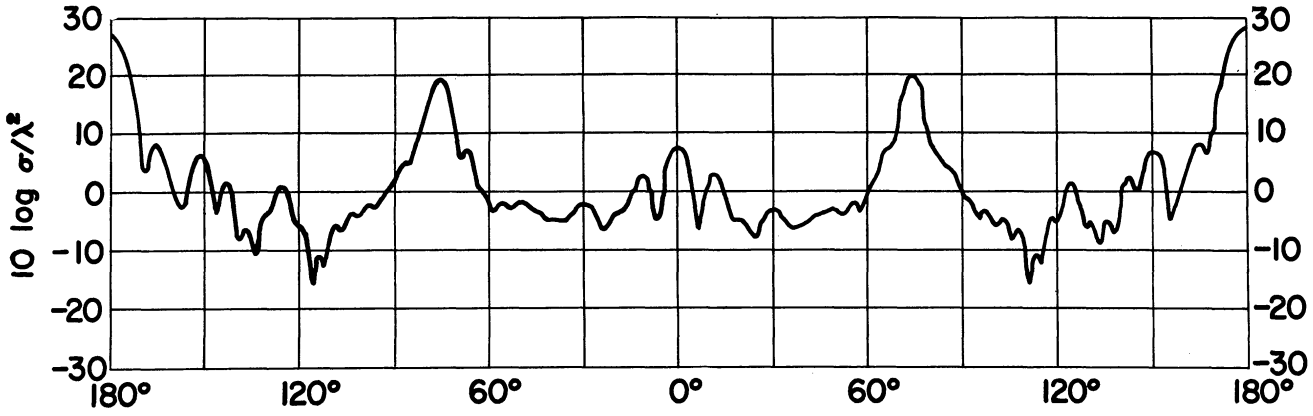

FIGURE 23: BACK SCATTERED RADAR CROSS SECTION OF FLAT BACKED CONE $\pi - \theta_o = 15^o$, ka = 9.02, Horizontal Polarization (Keys and Primich, 1959c)

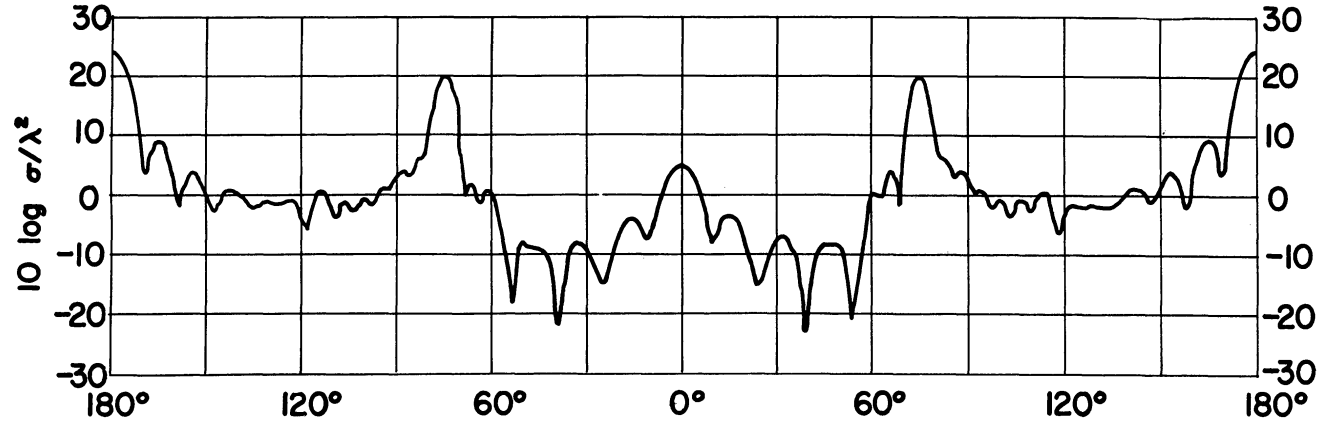

FIGURE 24: BACK SCATTERED RADAR CROSS SECTION OF FLAT BACKED CONE $\pi - \theta_o = 15^o$, ka = 9.02, Vertical Polarization (Keys and Primich, 1959c)

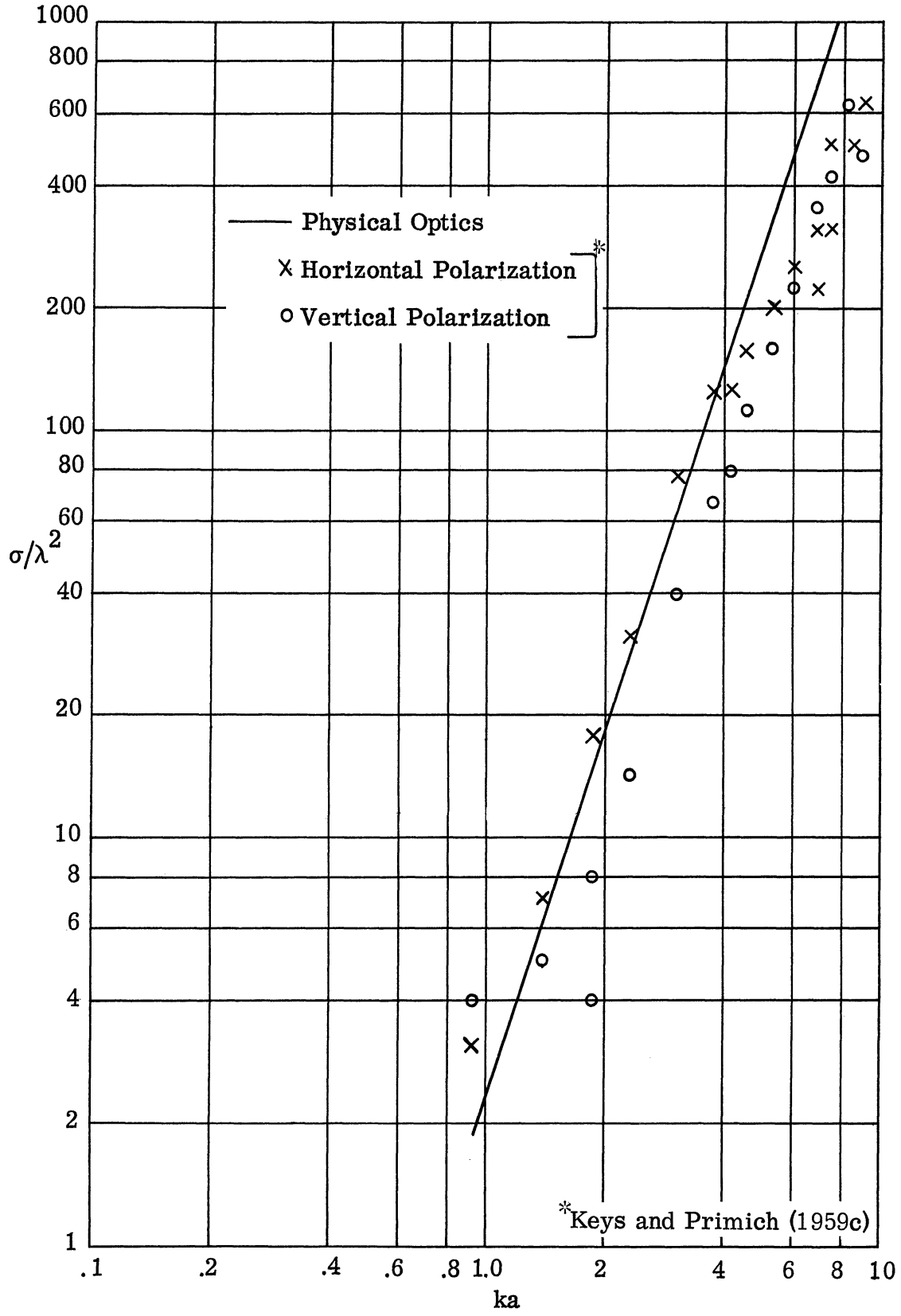

FIGURE 25: RADAR CROSS SECTION OF FLAT BACKED FINITE CONE - SPECULAR FLASH $\sigma(\theta_o - \pi/2)$, $\pi - \theta_o = 4^o$

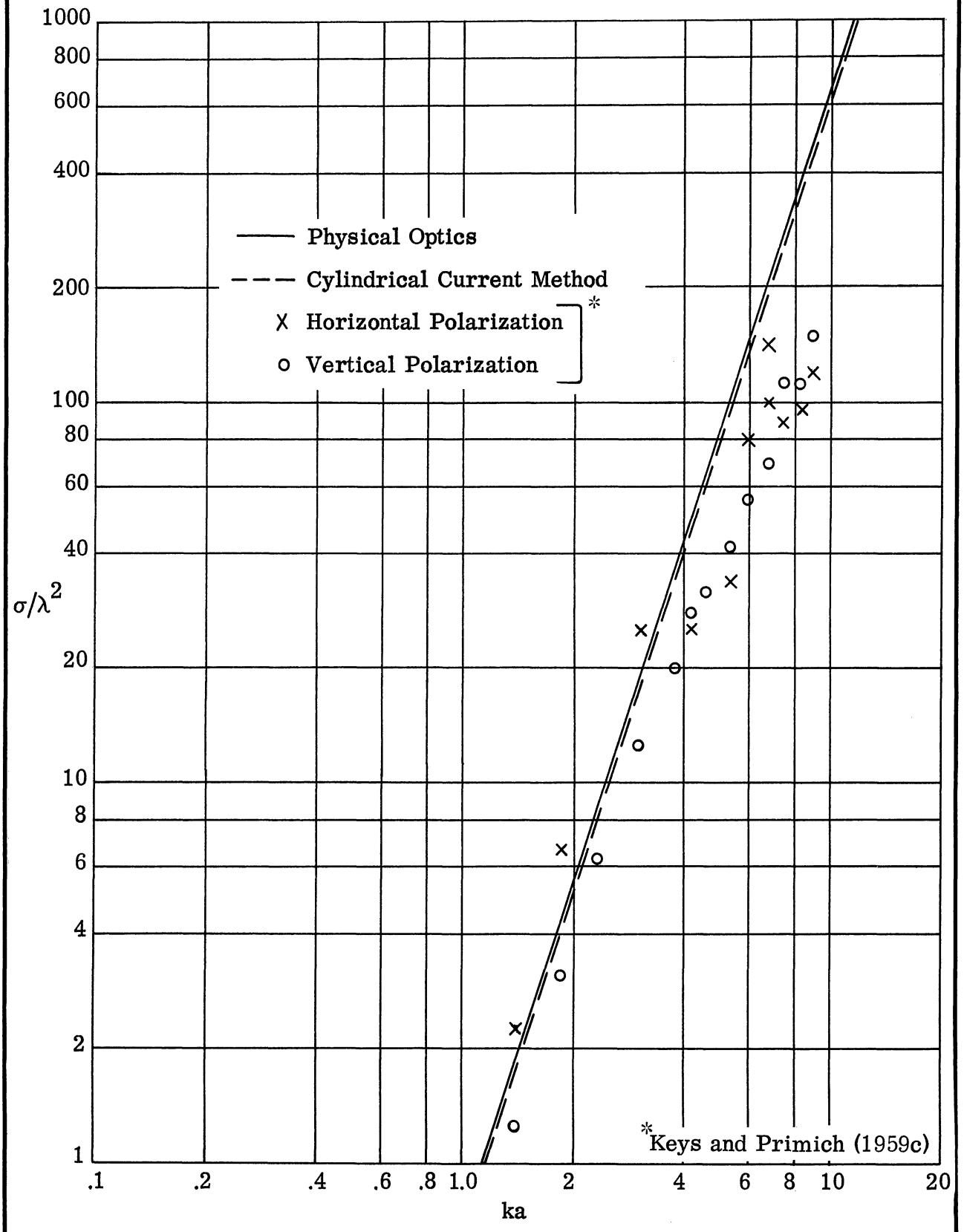

FIGURE 26: RADAR CROSS SECTION OF FLAT BACKED FINITE CONE - SPECULAR FLASH $\sigma(\theta_o - \pi/2)$, $\pi - \theta_o = 7.5^o$

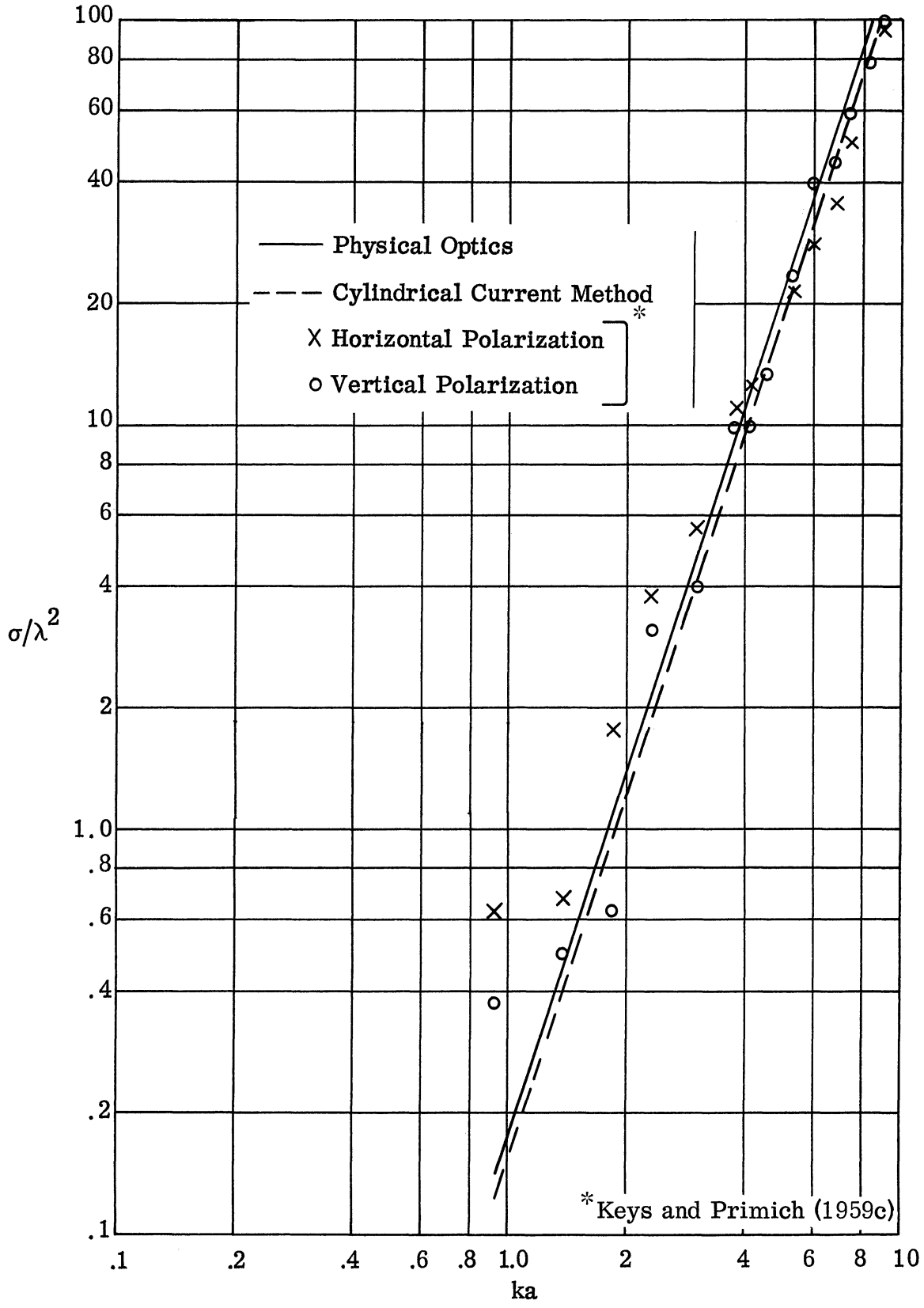

FIGURE 27: RADAR CROSS SECTION OF FLAT BACKED FINITE CONE - SPECULAR FLASH $\sigma(\theta_o - \pi/2)$, $\pi - \theta_o = 15^o$

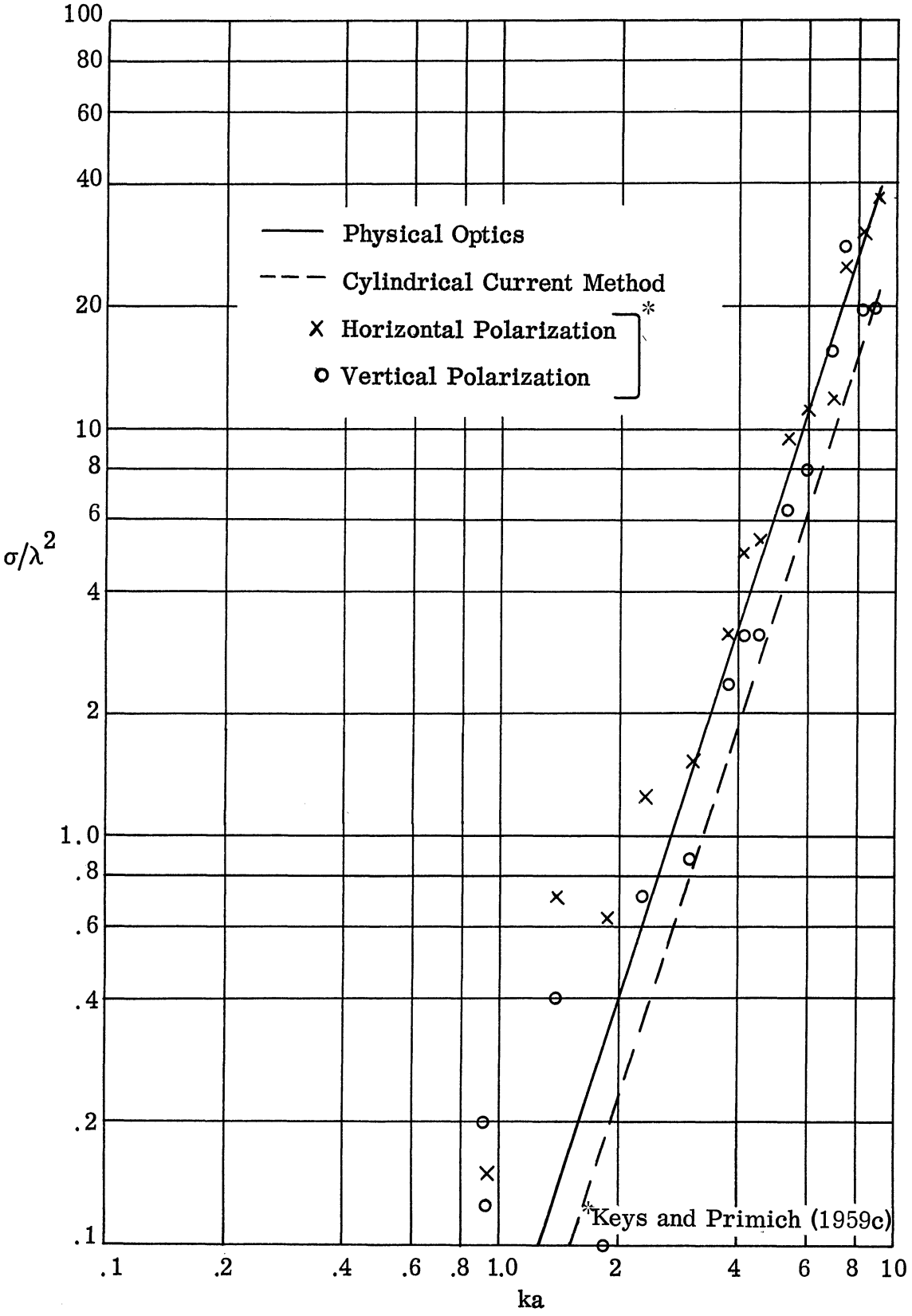

FIGURE 28: RADAR CROSS SECTION OF FLAT BACKED FINITE CONE - SPECULAR FLASH $\sigma(\theta_o - \pi/2)$, $\pi - \theta_o = 30^o$

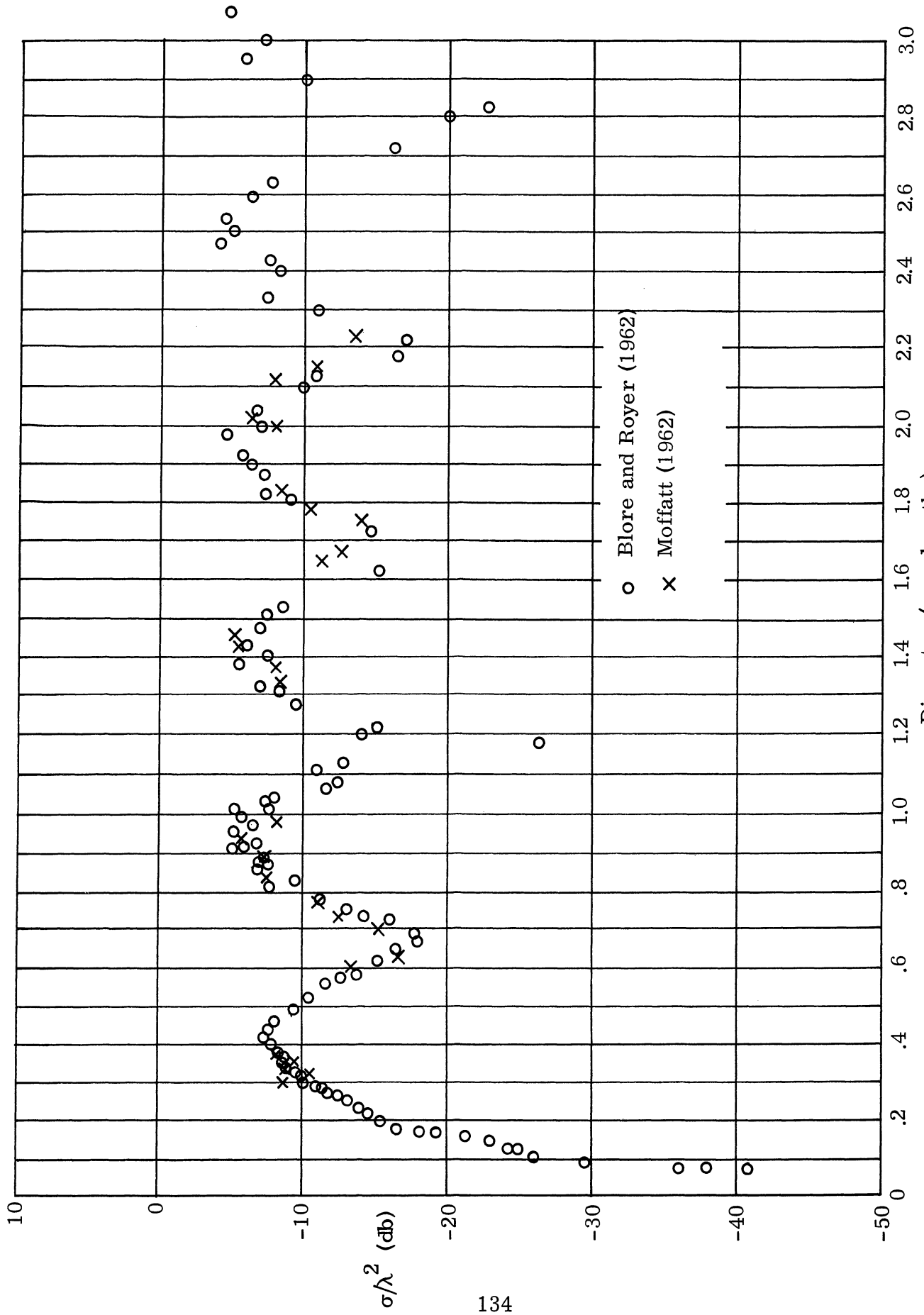

FIGURE 29: NOSE-ON RADAR CROSS SECTION OF CONE-SPHERE, $\pi - \theta_o = 15^o$

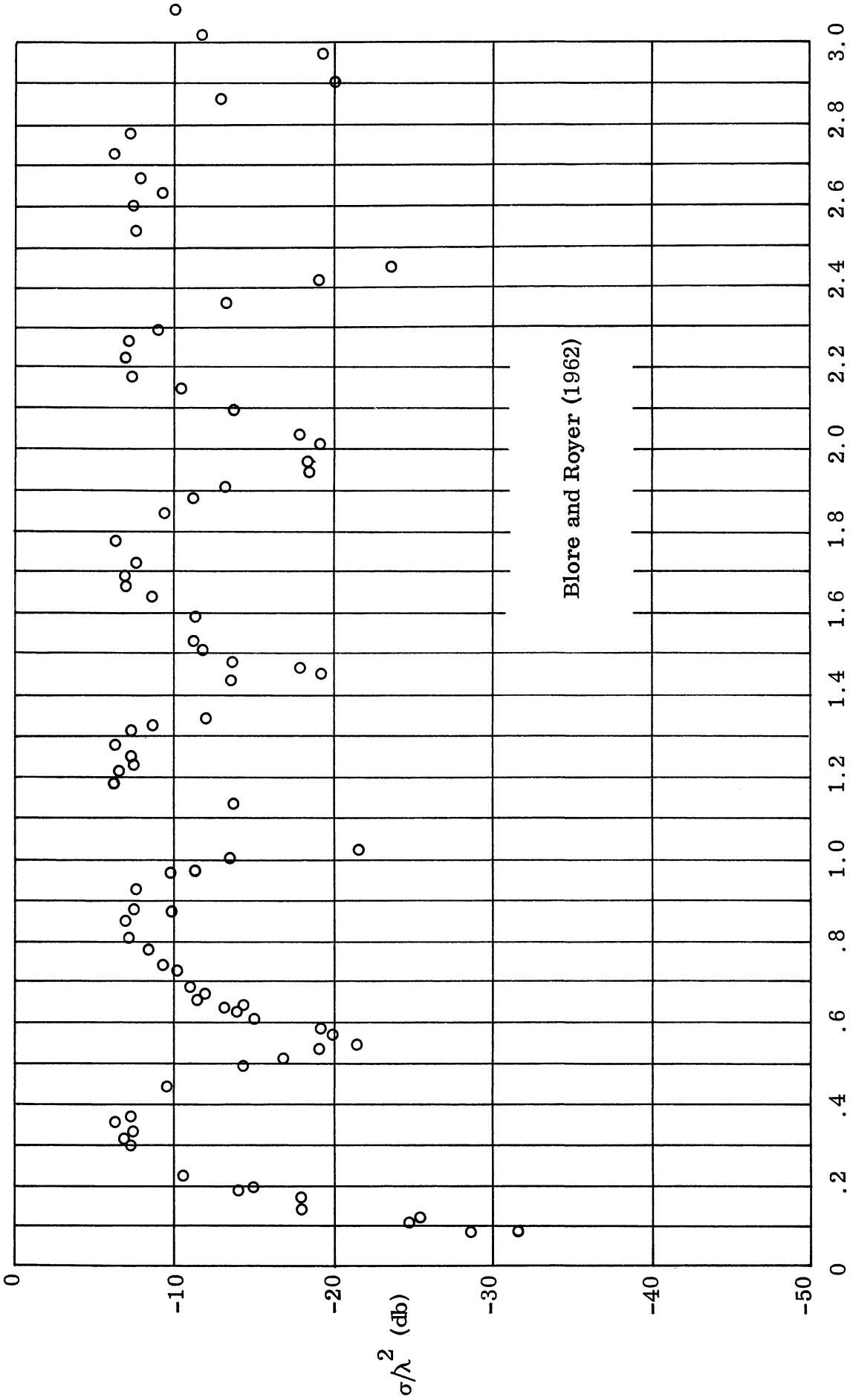

FIGURE 30: NOSE-ON RADAR CROSS SECTION OF CONE-SPHERE, $\pi - \theta_o = 30^o$

REFERENCES

Artmann, K. (1950) Z. Phys. 127, pp 468-494.

August, G. and D. J. Angelakos (1960) "Back Scattering from Cones", University of California, Electronics Research Laboratory, Rep. No. 252, Issue 60. (A shortened version of this is: Angelakos, D. J., and G. August, "Experimental Investigation of Back Scattering from Cones", presented at Symposium on the Echoing Properties of Missiles, Farnborough, England.) SECRET

Bailin, L. and S. Silver (1956) IRE Trans. AP-4, pp 5-16.

Belkina, M. G. (1957) "Radiation Characteristics of an Elongated Rotary Ellipsoid", appearing in Diffraction of Electromagnetic Waves by Certain Bodies of Revolution (Moscow).

Blore, W. E. and G. M. Royer (1962) "The Radar Cross Section of Bodies of Revolution" (private communication).

Born, M. and E. Wolf (1959) Principles of Optics (Pergamon Press, New York).

Bouwkamp, C. J. and H. B. G. Casimir (1954) Physica 20, pp 539-554.

Brysk, H., R. E. Hiatt, V. H. Weston and K. M. Siegel (1959) Can. J. Phys. 37, pp 675-679.

Brysk, H. (1960) Can. J. Phys. 38, pp 48-56.

Carrus, P. A. and C. G. Treuenfels (1951) J. Math. and Phys. 29, pp 292-299.

Carslaw, H. S. (1910) Phil. Mag. 6, pp 696-697.

Carslaw, H. S. (1914) Math. Ann. 75, pp 133-147.

Carslaw, H. S. (1916) Proc. London Math. Soc. 16, pp 84-93.

Crispin, J. W., Jr., R. F. Goodrich and K. M. Siegel (1959) "A Theoretical Method for the Calculation of the Radar Cross Sections of Aircraft and Missiles", The University of Michigan Radiation Laboratory Rep. No. 2591-1-H.

Crispin, J. W., Jr., K. M. Siegel and F. B. Sleator (1963) "The Resonance Region", Proc. Thirteenth General Assembly of URSI, London, 1960, to be published.

Darling, D. A. (1960) "Some Relations Between Potential Theory and the Wave Equation", The University of Michigan Radiation Laboratory Rep. No. 2871-5-T.

Dawson, T. W. G. (1960a) "Some Problems in the Theory of Radar Reflections from Missile Re-Entry Heads" presented at Symposium on the Echoing Properties of Missiles, Farnborough, England. SECRET

Dawson, T. W. G. (1960b) "The Design of Missile Re-Entry Heads Having Very Small Echoes and the Theory of Radar Reflections", Royal Aircraft Establishment, Farnborough, England, Rep. No. RAD 290. SECRET

Dawson, T. W. G., J. G. W. Miller and W. R. Turner (1960) "Radar Echoes from Bodies of Circular Cross Section Using Wedge Theory", Royal Aircraft Establishment, Farnborough, England, Tech. Note RAD 787.

Dawson, T. W. G. and W. R. Turner (1960) "Calculation of Radar Echoing Areas by the Cylindrical Current Method", Royal Aircraft Establishment, Farnborough, England, Tech. Note RAD 788.

Felsen, L. B. (1953) "Back Scattering from Wide Angle and Narrow Angle Cones", presented at McGill Symposium on Microwave Optics. Air Force Cambridge Research Center Rep. No. TR-59-118 (II). (1959)

Felsen, L. B. (1955) J. Appl. Phys. 26, pp 138-151.

Felsen, L. B. (1957a) IRE Trans. AP-5, pp 109-121.

Felsen, L. B. (1957b) IRE Trans. AP-5, pp 121-129.

Felsen, L. B. (1957c) "Radiation from Source Distributions on Cones and Wedges", Polytechnic Institute of Brooklyn Microwave Research Institute Research Rep. No. R-574-57 PIB-512.

Felsen, L. B. (1957d) IRE Trans. AP-5, pp 402-404

Felsen, L. B. (1958) "Back Scattering from a Semi-Infinite Cone", Polytechnic Institute of Brooklyn Microwave Research Institute Memo. No. 43-R675-58 PIB-603.

Felsen, L. B. (1959) IRE Trans. AP-7, pp 168-180.

Gent, H., J. S. Hey and P. G. Smith (1960) "The Echoing Area of 15^{o} Semi-Angle Cone-Spheres with Sphere Radii Between One and Two Wavelengths", presented at Symposium on the Echoing Properties of Missiles, Farnborough, England. SECRET

Goodrich, R. F., R. E. Kleinman, A. L. Maffett, N. E. Reitlinger, C. E. Schensted and K. M. Siegel (1958) L'Onde Elect. 1, pp 49-57.

Goodrich, R. F., R. E. Kleinman, A. L. Maffett, C. E. Schensted, K. M. Siegel, M. G. Chernin, H. E. Shanks and R. E. Plummer (1959) IRE Trans. AP-7, pp 213-222.

Goodrich, R. F., B. A. Harrison, R. E. Kleinman and T. B. A. Senior (1961) "Studies in Radar Cross Sections XLVII - Diffraction and Scattering by Regular Bodies - I: the Sphere", The University of Michigan Radiation Laboratory Rep. No. 3648-1-T.

Goryanov, A. S. (1961) Radio Engineering and Electronics, 6, pp 65-81.

Green, G. (1828) "Essay on Electricity and Magnetism" see Mathematical Papers (MacMillan Co., New York) 1871.

Hansen, W. W. and L. I. Schiff (1948) "Theoretical Study of Electromagnetic Waves Scattered from Shaped Metal Surfaces", Stanford University Microwave Laboratory Quart. Rep. 1 to 4.

Heine, H. E. (1878) Handbuch der Kugelfunctionen: Theorie und Anwendungen (Berlin) Second Edition.

Hobson, E. W. (1889) Trans. Cambridge Phil. Soc. 14, pp 211-236.

Hobson, E. W. (1931) The Theory of Spherical and Ellipsoidal Harmonics (Cambridge University Press, Cambridge).

Honda, J. S., S. Silver and F. D. Clapp (1959) "Scattering of Microwaves by Figures of Revolution", University of California Electronics Research Laboratory Rep. No. 232, Issue 60.

Jahnke, E. and F. Emde (1945) Tables of Functions with Formulas and Curves (Dover Publications, New York).

Kell, R. E. (1960) "Radar Cross Section of Ballistic Missile Nose Cones", presented at Symposium on the Echoing Properties of Missiles, Farnborough, England. SECRET

Keller, J. B. (1957) J. Appl. Phys. 28, pp 426-444.

Keller, J. B. (1958) "A Geometrical Theory of Diffraction" Proc. Symp. Appl. Math., 8 (McGraw-Hill, New York). pp 27-52.

Keller, J. B. (1959) "Back Scattering from a Finite Cone", New York University Institute of Mathematical Sciences Rep. No. EM-127; but see IRE Trans. AP-8, pp 175-182 (1960).

Keller, J. B. (1961) IRE Trans. AP-9, pp 411-412.

Kennaugh, E. M. and R. L. Cosgriff (1958) "The Use of Impulse Response in Electromagnetic Scattering Problems", IRE Nat. Conv. Record 6, Part 1, pp 72-77.

Kennaugh, E. M. and D. L. Moffatt (1962) Proc. IRE 50, p. 199.

Kerr, D. (1951) Propagation of Short Radio Waves (McGraw-Hill, New York).

Keys, J. E. and R. I. Primich (1959a) Can. J. Phys. 37, pp 521-522.

Keys, J. E. and R. I. Primich (1959b) "The Experimental Determination of the Far-Field Scattering from Simple Shapes", presented at URSI Symposium on Electromagnetic Theory, Toronto, Canada; published in abstract form in IRE Trans. AP-7, p. 577.

Keys, J. E. and R. I. Primich (1959c) "The Radar Cross Section of Right Circular Metal Cones: I", Defense Research Telecommunications Establishment Rep. No. 1010.

Keys, J. E. and R. I. Primich (1959d) "The Radar Cross Section of Right Circular Metal Cones: II" Defense Research Telecommunications Establishment Rep. No. 1023.

Kraus, L. and L. Levine (1961) Comm. Pure Appl. Math. 14, pp 49-68.

Logan, N. A. (1960) Proc. IRE 10, p. 1782.

Macdonald, H. M. (1900a) Trans. Cambridge Phil. Soc. 18, pp 292-297.

Macdonald, H. M. (1900b) Proc. London Math. Soc. 31, pp 264-278.

Macdonald, H. M. (1902) Electric Waves (Cambridge University Press, Cambridge).

Macdonald, H. M. (1915) Proc. London Math. Soc. 14, pp 410-427.

Magnus, W. and F. Oberhettinger (1949) Formulas and Theorems for the Special Functions of Mathematical Physics (Chelsea, New York).

Mehler, F. G. (1870) Elbing Jahresbericht; but see Math. Ann. 18 pp 161-194 (1881)

Melling, W. P. (1960) "Bistatic Radar Cross Section Measurements of Nose Cones and Decoys", presented at Symposium on the Echoing Properties of Missiles, Farnborough, England. SECRET

Mentzer, J. R. (1955) Scattering and Diffraction of Radio Waves (Pergamon Press, London and New York).

Moffatt, D. L. (1962) "Low Radar Cross Sections, the Cone-Sphere", The Ohio State University Antenna Laboratory Rep. No. 1223-5.

Nisbet, A. (1955) Proc. Roy. Soc. (A) 231, pp 250-263.

Northover, F. H. (1962) Quart. J. Mech. Appl. Math. 15, pp 1-9.

Olte, A. and S. Silver (1959) IRE Trans. AP-7, pp 561-567.

Pal, B. (1918) Bull. Calcutta Math. Soc. 9, pp 83-95.

Pal, B. (1919) Bull. Calcutta Math. Soc. 10, pp 187-194.

Peters, L., Jr. (1958) IRE Trans. AP-6, pp 133-139.

Plonus, M. A. (1961) "A Study of the Biconical Antenna", The University of Michigan Radiation Laboratory Rep. No. 3620-1-F.

Plonus, M. A. (1962) "Application of Selective Mode Coupling in the Solution to Biconical Antennas" presented at URSI Symposium on Electromagnetic Theory and Antennas, Copenhagen, Denmark.

Lord Rayleigh (1897) Phil. Mag. 44, pp 28-52.

Rogers, C. C., J. K. Schindler and F. V. Schultz (1962) "The Scattering of a Plane Electromagnetic Wave by a Finite Cone", presented at URSI Symposium on Electromagnetic Theory and Antennas, Copenhagen, Denmark.

Schensted, C. E. (1953) "Application of Summation Techniques to the Radar Cross Section of a Cone", presented at McGill Symposium on Microwave Optics. Air Force Cambridge Research Center Rep. No. TR-59-118 (II). (1959)

Senior, T. B. A. (1960) Can. J. Phys. 38, pp 1702-1705.

Senior, T. B. A. and D. A. Darling (1963) "Low Frequency Expansions for Scattering by Separable and Non-Separable Bodies", to be published.

Senior, T. B. A. and R. F. Goodrich (1963) "Scattering by a Sphere", to be published.

Shostak, A and D. Angelakos (1957) "Back Scatter from a Right Circular Cone", University of California Electronics Research Laboratory Rep. No. 191, Issue 60.

Siegel, K. M., D. M. Brown, H. E. Hunter, H. A. Alperin and C. W. Quillen (1951) "The Zeros of the Associated Legendre Functions $P_n^m(\mu')$ of Non-Integral Degree", The University of Michigan Willow Run Research Center Rep. No. UMM-82.

Siegel, K. M. and H. A. Alperin (1952) "Scattering by a Semi-Infinite Cone", The University of Michigan Willow Run Research Center Rep. No. UMM-87.

Siegel, K. M., J. W. Crispin, Jr., R. E. Kleinman and H. E. Hunter (1952) J. Math. and Phys. 31, pp 170-179.

Siegel, K. M., H. A. Alperin, J. W. Crispin, Jr., H. E. Hunter, R. E. Kleinman, W. C. Orthwein and C. E. Schensted (1953a) "Studies in Radar Cross Sections IV - Comparison Between Theory and Experiment of the Cross Section of a Cone", The University of Michigan Willow Run Research Center Rep. No. UMM-92.

Siegel, K. M., J. W. Crispin, Jr., R. E. Kleinman and H. E. Hunter (1953b) J. Math. and Phys. 32, pp 193-196.

Siegel, K. M., H. A. Alperin, R. R. Bonkowski, J. W. Crispin, Jr., A. L. Maffett, C. E. Schensted and I. V. Schensted (1955a) J. Appl. Phys. 26, pp 297-305.

Siegel, K. M. J. W. Crispin, Jr., and C. E. Schensted (1955b) J. Appl. Phys. 26, pp 309-313.

Siegel, K. M. (1959) Appl. Sci. Res. B 7, pp 293-328.

Siegel, K. M., R. F. Goodrich and V. H. Weston (1959) Appl. Sci. Res. B 8, pp 8-12.

Siegel, K. M. (1962) "The Quasi-Static Radar Cross Sections of Complex Bodies of Revolution" appearing in Electromagnetic Waves, ed. R. E. Langer (University of Wisconsin Press, Madison).

Siegel, K. M. (1963) Proc. IEEE 51, pp 232-233.

Sletten, C. J. (1952) "Electromagnetic Scattering From Wedges and Cones", Air Force Cambridge Research Center Rep. No. E5090.

Sommerfeld, A. (1935) "Electromagnetische Schwengungen" appearing in Die Differential und Integralgleichung en der Mechanik and Physic - II (Vieweg und Sohn, Braunschweig).

Spencer, R. C. (1951) "Back Scattering from Conducting Surfaces", Air Force Cambridge Research Center Rep. No. E5070.

Stratton, J. A. (1941) Electromagnetic Theory (McGraw-Hill, New York).

Turner, W. R. and T. W. G. Dawson (1960) "Calculation of Head-On Radar Echoes from Bodies of Circular Cross-Section by the Physical Optics Method", Royal Aircraft Establishment, Farnborough, England, Tech. Note RAD 786.

Turner, W. R. (1960) "Further Calculations of Radar Echoing Areas by the Cylindrical Current Method", Royal Aircraft Establishment, Farnborough, England, Tech. Note RAD 792.

Wilcox, C. H. (1957) J. Math. Mech. 6, pp 167-201.